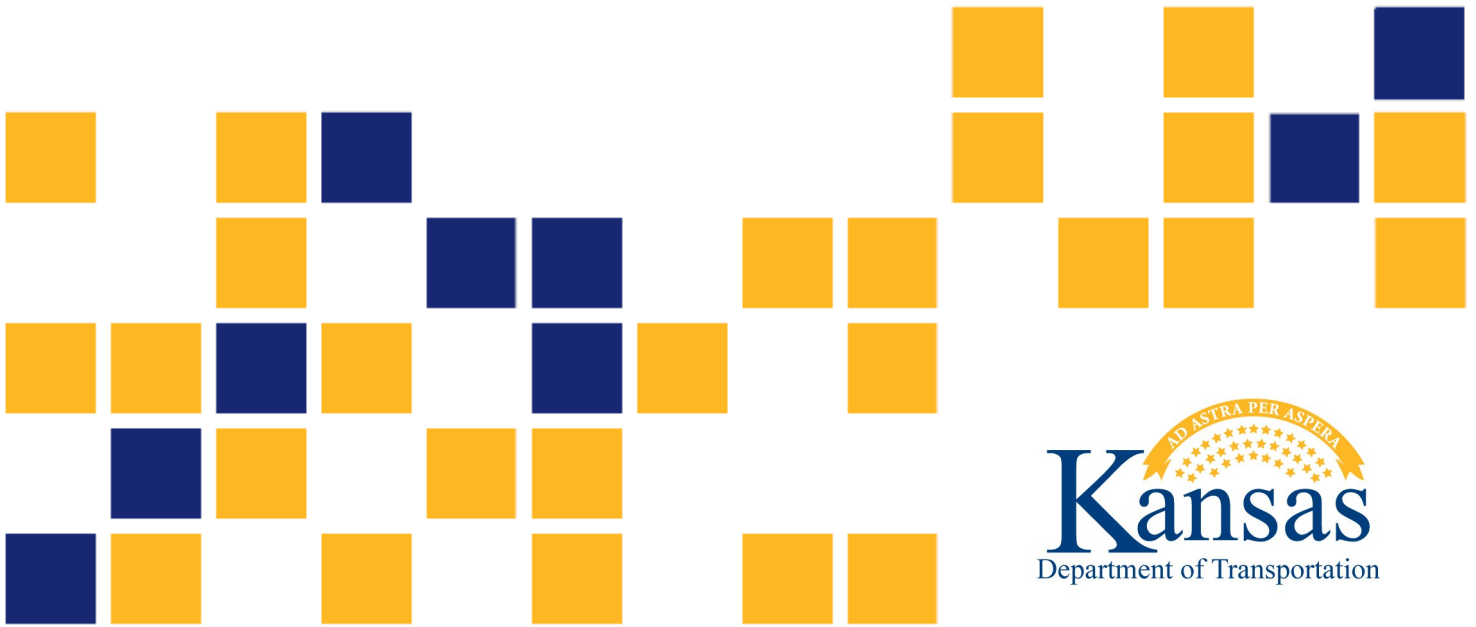


# Evaluation of Cement-Modified Soil (CMS) with Microcracking

George A. Tannoury, P.E.  
Mahdi Al-Naddaf, Ph.D.  
Jie Han, Ph.D., P.E.  
Robert L. Parsons, Ph.D., P.E.  
Chi Zhang, Ph.D.

*The University of Kansas*





<b>1 Report No.</b> K-TRAN: KU-18-6		<b>2 Government Accession No.</b>		<b>3 Recipient Catalog No.</b>	
<b>4 Title and Subtitle</b> Evaluation of Cement-Modified Soil (CMS) with Microcracking				<b>5 Report Date</b> August 2020	
				<b>6 Performing Organization Code</b>	
<b>7 Author(s)</b> George A. Tannoury, P.E. Mahdi Al-Naddaf, Ph.D. Jie Han, Ph.D., P.E. Robert L. Parsons, Ph.D., P.E. Chi Zhang, Ph.D.				<b>8 Performing Organization Report No.</b>	
<b>9 Performing Organization Name and Address</b> The University of Kansas Department of Civil, Environmental & Architectural Engineering 1530 West 15th St Lawrence, Kansas 66045-7609				<b>10 Work Unit No. (TRAIS)</b>	
				<b>11 Contract or Grant No.</b> C2111	
<b>12 Sponsoring Agency Name and Address</b> Kansas Department of Transportation Bureau of Research 2300 SW Van Buren Topeka, Kansas 66611-1195				<b>13 Type of Report and Period Covered</b> Final Report July 2017–June 2019	
				<b>14 Sponsoring Agency Code</b> RE-0739-01	
<b>15 Supplementary Notes</b> For more information write to address in block 9.					
<b>16 Abstract</b> <p>Cement modification of subgrade has been widely practiced for the past few decades. Recently, cement has become a more economical binder to modify in-situ subgrade soil since other binders, such as fly ash, have become less available and therefore their prices have increased significantly. In addition, a much higher percentage of fly ash needs be used, when compared with cement to achieve the same subgrade strength and stiffness. In general, cement-modified subgrade is prone to develop shrinkage cracking, which can eventually reflect through asphalt pavement layers to the surface after construction. For some subgrade soils, a high cement content is needed to meet the unconfined compressive strength requirement without jeopardizing durability. A higher cement content will result in higher shrinkage cracking potential. To overcome this problem, a microcracking technology has been developed and adopted in the field. This technology involves re-compaction of cement-modified soil (CMS) with a roller, 24 to 48 hours after initial compaction, to induce microcracks in the CMS and minimize the potential for large shrinkage cracks. Microcracking of CMS is not expected to significantly reduce the strength and stiffness of CMS, but it is expected to increase its hydraulic conductivity and reduce the potential for large shrinkage cracks. Unfortunately, the procedure to simulate microcracking of CMS in the laboratory and to evaluate its effect on properties of CMS has not been established yet. This report documents the development of such a procedure and discusses the effect of microcracking on the properties (strength and modulus) of CMS specimens. The developed procedure utilized unconfined compression (UC) tests to generate microcracks in specimens. To generate microcracks, the loading stress level was found to be equal to the unconfined compressive strength of the CMS specimen. The laboratory results showed that microcracking increased the hydraulic conductivity of the specimen and reduced its electrical resistivity when the specimen was saturated. The Light Weight Deflectometer (LWD) tests conducted in the field showed that adding cement increased the subgrade modulus. However, after applying three passes of roller compaction to generate the microcracks in the CMS in the field, the subgrade modulus dropped to approximately 40% of its original value on average.</p>					
<b>17 Key Words</b> Soil Cement Tests, Subgrade, Microcracking, Compression Tests, Deflectometers			<b>18 Distribution Statement</b> No restrictions. This document is available to the public through the National Technical Information Service <a href="http://www.ntis.gov">www.ntis.gov</a> .		
<b>19 Security Classification (of this report)</b> Unclassified	<b>20 Security Classification (of this page)</b> Unclassified	<b>21 No. of pages</b> 107	<b>22 Price</b>		

Form DOT F 1700.7 (8-72)

This page intentionally left blank.

# **Evaluation of Cement-Modified Soil (CMS) with Microcracking**

Final Report

Prepared By

George A. Tannoury, P.E.  
Mahdi Al-Naddaf, Ph.D.  
Jie Han, Ph.D., P.E.  
Robert L. Parsons, Ph.D., P.E.  
Chi Zhang, Ph.D.

The University of Kansas

A Report on Research Sponsored by

THE KANSAS DEPARTMENT OF TRANSPORTATION  
TOPEKA, KANSAS

and

THE UNIVERSITY OF KANSAS  
LAWRENCE, KANSAS

August 2020

© Copyright 2020, **Kansas Department of Transportation**

## **PREFACE**

The Kansas Department of Transportation's (KDOT) Kansas Transportation Research and New-Developments (K-TRAN) Research Program funded this research project. It is an ongoing, cooperative and comprehensive research program addressing transportation needs of the state of Kansas utilizing academic and research resources from KDOT, Kansas State University and the University of Kansas. Transportation professionals in KDOT and the universities jointly develop the projects included in the research program.

## **NOTICE**

The authors and the state of Kansas do not endorse products or manufacturers. Trade and manufacturers names appear herein solely because they are considered essential to the object of this report.

This information is available in alternative accessible formats. To obtain an alternative format, contact the Office of Public Affairs, Kansas Department of Transportation, 700 SW Harrison, 2<sup>nd</sup> Floor – West Wing, Topeka, Kansas 66603-3745 or phone (785) 296-3585 (Voice) (TDD).

## **DISCLAIMER**

The contents of this report reflect the views of the authors who are responsible for the facts and accuracy of the data presented herein. The contents do not necessarily reflect the views or the policies of the state of Kansas. This report does not constitute a standard, specification or regulation.

## Abstract

Cement modification of subgrade has been widely practiced for the past few decades. Recently, cement has become a more economical binder to modify in-situ subgrade soil since other binders, such as fly ash, have become less available and therefore their prices have increased significantly. In addition, a much higher percentage of fly ash needs be used, when compared with cement to achieve the same subgrade strength and stiffness. In general, cement-modified subgrade is prone to develop shrinkage cracking, which can eventually reflect through asphalt pavement layers to the surface after construction. For some subgrade soils, a high cement content is needed to meet the unconfined compressive strength requirement without jeopardizing durability. A higher cement content will result in higher shrinkage cracking potential. To overcome this problem, a microcracking technology has been developed and adopted in the field. This technology involves re-compaction of cement-modified soil (CMS) with a roller, 24 to 48 hours after initial compaction, to induce microcracks in the CMS and minimize the potential for large shrinkage cracks. Microcracking of CMS is not expected to significantly reduce the strength and stiffness of CMS, but it is expected to increase its hydraulic conductivity and reduce the potential for large shrinkage cracks. Unfortunately, the procedure to simulate microcracking of CMS in the laboratory and to evaluate its effect on properties of CMS has not been established yet. This report documents the development of such a procedure and discusses the effect of microcracking on the properties (strength and modulus) of CMS specimens. The developed procedure utilized unconfined compression (UC) tests to generate microcracks in specimens. To generate microcracks, the loading stress level was found to be equal to the unconfined compressive strength of the CMS specimen. The laboratory results showed that microcracking increased the hydraulic conductivity of the specimen and reduced its electrical resistivity when the specimen was saturated. The Light Weight Deflectometer (LWD) tests conducted in the field showed that adding cement increased the subgrade modulus. However, after applying three passes of roller compaction to generate the microcracks in the CMS in the field, the subgrade modulus dropped to approximately 40% of its original value on average.

## **Acknowledgements**

This research project was financially sponsored by the Kansas Department of Transportation (KDOT) and Terracon Consultants, Inc. Mr. Isaac Ferguson, the Geotechnical Specialist at the Kansas DOT, is the project monitor. The laboratory manager, Mr. David Woody, and technician, Mr. Kent Dye, in the Department of Civil, Environmental, and Architectural Engineering (CEAE) at the University of Kansas (KU) provided their support in laboratory testing. The research team also would like to thank Mr. Luke Metheny with KDOT for his support in facilitating the field work and Mr. Matt Catlin and Mr. Scott Randle at Terracon for their support for this research.



# Table of Contents

Abstract.....	v
Acknowledgements.....	vi
Table of Contents.....	vii
List of Tables.....	ix
List of Figures.....	xi
Chapter 1: Introduction.....	1
Chapter 2: Literature Review.....	3
2.1 Introduction.....	3
2.2 Stabilization Additives.....	3
2.3 Cement in Soil Stabilization.....	5
2.3.1 Cation Exchange.....	6
2.3.2 Particle Restructuring.....	6
2.3.3 Cementitious Hydration.....	6
2.3.4 Pozzolanic Reaction.....	6
2.4 Shrinkage Cracking of Cement-Modified Soil.....	7
2.5 Background of Microcracking Technology.....	8
Chapter 3: Materials and Laboratory Tests.....	10
3.1 Introduction.....	10
3.2 Materials.....	10
3.2.1 Soil Selection.....	10
3.2.2 Additives.....	11
3.3 Laboratory Testing.....	12
3.3.1 Sample Preparation.....	12
3.3.2 Soil Classification.....	12
3.3.3 Soil Compaction Characteristics.....	14
3.3.4 Unconfined Compressive Strength.....	17
3.3.5 Wet-Dry Cycles.....	17
3.3.6 Hydraulic and Electrical Conductivity.....	18
3.3.7 Resilient Modulus Testing.....	19

Chapter 4: Microcracking Simulation in Laboratory.....	22
4.1 Cement Modified Soil.....	22
4.1.1 Marion County Soil.....	22
4.1.2 Sedgwick County Soil.....	23
4.2 Microcracking.....	25
4.2.1 Marion County Soil.....	25
4.2.2 Sedgwick County Soil.....	37
Chapter 5: Field Study .....	42
5.1 Electrical Resistivity .....	42
5.2 Light Weight Deflectometer Test Results .....	44
5.3 Falling Weight Deflectometer (FWD) Field Testing.....	49
5.3.1 FWD Analysis.....	51
5.4 Resilient Modulus Results .....	57
5.4.1 Laboratory Reconstituted Specimens.....	57
5.4.2 Field Core Specimens .....	57
5.4.3 Effect of Microcracking on Resilient Modulus.....	59
Chapter 6: Conclusions and Recommendations .....	63
6.1 Conclusions.....	63
6.2 Recommendations.....	64
References.....	65
Appendix A: Properties of Cement.....	69
Appendix B: Additional Figures Related to Chapter 4.....	71
Appendix C: Data Related to Chapter 5 .....	77

## List of Tables

Table 3.1:	Atterbeg limits of soils from Marion and Sedgwick Counties .....	14
Table 3.2:	Compaction Characteristics of Soils from Marion and Sedgwick Counties .....	17
Table 3.3:	Testing sequence for CMS specimens.....	21
Table 4.1:	Unconfined compressive strength of CMS after cured for 7 days – Marion County .....	23
Table 4.2:	Unconfined compressive strength of CMS after cured for 7 days – Sedgwick County .....	24
Table 4.3:	Unconfined compressive strength of CMS with 5.0% cement content after 48-hour curing.....	26
Table 4.4:	The UC test results for the CMS specimens with 5.0% cement during and after preloading .....	29
Table 4.5:	Unconfined compressive strengths and moduli of failed CMS specimens for the Marion County soil subjected to second loading .....	30
Table 4.6:	UC strengths of CMS specimens before and after microcracking for the Marion County soil.....	32
Table 4.7:	Effects of microcracks in CMS specimens on the UC strength and modulus ( $E_{50}$ ) at 7-day curing for the Marion County soil .....	33
Table 4.8:	Unconfined compressive strength of CMS at 5.5% cement after 48-hour curing....	37
Table 4.9:	Unconfined compressive strengths and moduli of failed CMS specimens for the Sedgwick County soil subjected to second loading .....	38
Table 4.10:	UC strengths of CMS specimens before and after microcracking for the Sedgwick County soil.....	41
Table 4.11:	Effects of microcracks in CMS specimens on the UC strength and modulus ( $E_{50}$ ) at 7-day curing for the Sedgwick County soil .....	41
Table 5.1:	Field electrical resistivity before and after microcracking on the Sedgwick County site.....	43
Table 5.2:	Field electrical resistivity before and after microcracking on the Hutchinson site ..	44
Table 5.3:	Stress distribution factors for different types of soil .....	46
Table 5.4:	Resilient Modulus of Cracked CMS Specimen No. 1 Cored from Marion County ....	57

Table 5.5: Resilient Modulus of Cracked CMS Specimen No. 2 Cored from Marion County ....	58
Table 5.6: Resilient Modulus of Cracked CMS Specimen No. 4 Cored from Marion County ....	58
Table 5.7: Resilient Modulus of Cracked CMS Specimen No. 6 Cored from Marion County ....	59
Table 5.8: Resilient Modulus Test Characteristics .....	60
Table C.1: GPS coordinated for the FWD testing.....	77
Table C.2: Back-calculated modulus versus station location at 87 <sup>th</sup> Street EB lane in Sedgwick County.....	79
Table C.3: Back-calculated modulus versus station location at 87 <sup>th</sup> Street WB lane in Sedgwick County.....	81
Table C.4: Back-calculated modulus versus station location at 330 <sup>th</sup> Avenue EB lane in Marion County.....	83
Table C.5: Back-calculated modulus versus station location at 330 <sup>th</sup> Avenue WB lane in Marion County.....	85
Table C.6: Resilient Modulus of the Uncracked CMS Specimen No. 1 for the Sedgwick County Soil.....	87
Table C.7: Resilient Modulus of the Uncracked CMS Specimen No. 4 for the Sedgwick County Soil.....	87
Table C.8: Resilient Modulus of the Uncracked CMS Specimen No. 1 for the Marion County Soil.....	88
Table C.9: Resilient Modulus of the Uncracked CMS Specimen No. 2 for the Marion County Soil.....	88
Table C.10: Resilient Modulus of the Cracked CMS Specimen No. 2 for the Sedgwick County Soil.....	89
Table C.11: Resilient Modulus of the Cracked CMS Specimen No. 3 for the Sedgwick County Soil.....	89
Table C.12: Resilient Modulus of the Cracked CMS Specimen No. 3 for the Marion County Soil.....	90
Table C.13: Resilient Modulus of the Cracked CMS Specimen No. 4 for the Marion County Soil.....	90

## List of Figures

Figure 2.1: Physical State versus Moisture Contents of Clay Materials .....	4
Figure 3.1: Google Maps for the collected soil locations of: (a) clayey sand with gravel (SC), and (b) fat clay with sand (CH).....	11
Figure 3.2: Grain size distribution curves of the native soils from: (a) Marion County and (b) Sedgwick County (1 inch = 25 mm).....	13
Figure 3.3: Compaction characteristics of the native soil from Marion County: (a) compaction curves and (b) effect of moisture content on CBR .....	15
Figure 3.4: Compaction characteristics of the native soil from Sedgwick County: (a) compaction curves and (b) effect of moisture content on CBR .....	16
Figure 3.5: Electrical conductivity test setup of the CMS specimen connected to the PSIP unit.....	18
Figure 3.6: Typical triaxial chamber with external LVDTs and a load cell .....	19
Figure 4.1: Unconfined compressive strength of CMS versus cement content after cured for 7 days for the Marion County soil.....	23
Figure 4.2: Unconfined compressive strength of CMS versus cement content after cured for 7 days for the Sedgwick County soil.....	25
Figure 4.3: Stress-strain curves of CMS with 5.0% cement after 48-hour curing for the Marion County soil.....	26
Figure 4.4: Stress-strain curves of CMS with 5.0% cement after 48-hour curing: (a) loaded to the preloading stress level, and (b) after preloading .....	28
Figure 4.5: Stress-strain curves before and after microcracking of CMS specimens in Trial 3 for the Marion County soil.....	29
Figure 4.6: Stress-strain curves of CMS specimens at 5% cement in Trial 4 for the Marion County soil: (a) during the microcracking process after 2-day curing, and (b) after the microcracking process after 7-day curing .....	31
Figure 4.7: CMS specimen No. 3 of Trial 4 for the Marion County soil: (a) before microcracking, (b) after microcracking at 48-hour curing, and (c) after UC testing at 7-day curing.....	32

Figure 4.8: Volume change during the wet-dry test cycle based on: (a) wet condition and (b) dry condition .....	34
Figure 4.9: Mass loss for the brushed specimen calculated after a complete wet-dry cycle for all cycles .....	35
Figure 4.10: Hydraulic conductivity variation with different effective pressure .....	36
Figure 4.11: Resistivity variation with degree of saturation and age of CMS specimens for the Marion County soil.....	36
Figure 4.12: Stress-strain curves of CMS at 5.5% cement after 48-hour curing for the Sedgwick County soil.....	37
Figure 4.13: Stress-strain curves before and after microcracking of CMS specimens in Group 1 for the Sedgwick County soil.....	38
Figure 4.14: Stress-strain curves of CMS specimens at 5.5% cement in Group 2 for the Sedgwick County soil: (a) during the microcracking process after 2-day curing, and (b) after the microcracking process after 7-day curing.....	40
Figure 4.15: CMS Specimen 4 of Group 2 for the Sedgwick County soil: (a) before microcracking, (b) after microcracking at 48-hour curing, and (c) after UC testing at 7-day curing.....	41
Figure 5.1: Typical Wenner 4-Pin Setup .....	42
Figure 5.2: The Zorn LWD device: (a) photo and (b) schematics of the LWD and subgrade system (two DOF).....	45
Figure 5.3: LWD tests conducted for the Marion County project: (a) testing locations and (b) effect of microcracking.....	47
Figure 5.4: LWD tests conducted for the Sedgwick County project: (a) testing locations, (b) effect of cement, and (c) effect of microcracking .....	48
Figure 5.5: Schematic of FWD and deflection basin.....	50
Figure 5.6: Measured deflections and inputs: (a) EB lane, (b) WB lane, and (c) input layer modulus and Poisson's ratio values for back-calculation of the 87 <sup>th</sup> Street pavement in Sedgwick County.....	53
Figure 5.7: Measured deflections and inputs: (a) EB lane, (b) WB lane, and (c) input layer modulus and Poisson's ratio values for back-calculation of the 330 <sup>th</sup> Avenue pavement in Marion County.....	54

Figure 5.8: Back-calculated modulus versus station locations along 87 <sup>th</sup> Street in Sedgwick County: (a) EB lane and (b) WB lane .....	55
Figure 5.9: Back-calculated modulus versus station locations along 330 <sup>th</sup> Avenue (Marion County): (a) EB lane and (b) WB lane .....	56
Figure 5.10: $k_1$ Values .....	61
Figure 5.11: $k_2$ Values .....	61
Figure 5.12: $k_3$ Values .....	62
Figure 5.13: Resilient Moduli of the Remolded CMS Specimens for Sedgwick County and Marion County Soils .....	62
Figure A.1: Cement properties used in Marion County .....	69
Figure B.1: Stress-strain curves of CMS specimens of Marion County after 7-day curing at cement contents: (a) 3.5%, (b) 5.0%, and (c) 6.5%.....	71
Figure B.2: Stress-strain curves of CMS specimens of Sedgwick County after 7-day curing at cement contents: (a) 4.0%, (b) 5.5%, and (c) 7.0%.....	73
Figure B.3: Density variation during the wet-dry cycles (a) total density after wet cycles and (b) dry density after dry cycles.....	75
Figure B.4: Moisture variation after wet cycles .....	76

This page intentionally left blank.



# Chapter 1: Introduction

Performance of pavement structures highly depends on the quality of aggregate materials used in the construction and the competency of subgrade support. The aggregate used in roadway construction projects located in the western half of the State of Kansas is typically imported from quarries located in southeast Kansas or from the State of Oklahoma, thus increasing construction cost. Chemical modification/stabilization of subgrade has been used for several decades to improve its inferior engineering properties and provide a stable working platform during construction. The chemical modification/stabilization of the subgrade relies heavily on the use of lime, fly ash, and cement. Cement modification of subgrade was widely practiced during the 1940s and the 1950s. In the last couple of decades, fly ash, a by-product of energy generation from coal-fired power stations, has dominated the chemical stabilization industry and was considered the most cost-effective stabilizer. But more recently, new regulations from the United States Environmental Protection Agency (EPA) have impacted the availability and price of fly ash for use by state Departments of Transportation and other public entities. Furthermore, current trends suggest fly ash supplies may continue to decrease while its price increases.

Recently, cement has become a more economical binder to modify in-situ subgrade soil since a much higher percentage of fly ash needs be used, when compared with cement, to achieve the same subgrade strength and stiffness. In general, cement-modified subgrade is prone to develop shrinkage cracking, which can eventually reflect through asphalt pavement layers to the surface after construction. These reflective cracks will serve as an easy pathway for surface water to infiltrate the cohesive subgrade, which will exhibit a significant drop in its strength and stiffness and will result in premature failures of the pavement. Research has shown that shrinkage cracking of soil-cement first decreases with cement content, then reaches a minimum amount, and thereafter increases with the cement content. Generally, the optimum cement content resulting in the least amount of shrinkage is lower than the cement content required to achieve durable soil-cement. Also, for some subgrade soils, a high cement content is needed to meet the unconfined compressive strength and stiffness requirement without jeopardizing the long-term durability. The required high cement content will result in higher shrinkage cracking potential. To overcome this problem, a

microcracking technology has been developed and adopted in the field. This technology involves re-compaction of cement-modified soil (CMS) with a roller, 24 to 72 hours after initial compaction, to induce microcracks in the CMS and minimize the potential for large shrinkage cracks. Microcracking of CMS is not expected to significantly reduce the strength and stiffness of CMS, but it is expected to increase its hydraulic conductivity and reduce the potential for large shrinkage cracks. Unfortunately, the procedure to simulate microcracking of CMS in the laboratory and to evaluate its effect on the properties of CMS has not been established yet. This report documents the development of such a procedure and discusses the effect of microcracking on the properties (mainly strength and modulus) of CMS specimens.

The overall objective of this study was to evaluate laboratory and field performance of CMS after microcracking and its benefits for pavement applications. Although the previous research confirmed the applicability and effectiveness of this construction method in the field, no literature was found describing a procedure or method to simulate the microcracking process in the laboratory. This study proposes a laboratory method that can be used to simulate the microcracking process on CMS in the field using unconfined compression (UC) tests. The UC specimens were used to evaluate the properties of CMS with and without microcracking, including their strength and stiffness.

More details concerning CMS and its observed performance are described in the following chapters. Chapter 2 consists of a literature review describing the composition and mechanisms of CMS and the research on its use for soil stabilization, including microcracking. Chapter 3 describes the materials and laboratory tests adopted in this study. Chapters 4 and 5 discuss the laboratory results and the field work, respectively. Chapter 6 provides the conclusions and recommendations from this study.

# Chapter 2: Literature Review

## 2.1 Introduction

This chapter presents a brief description of the additives that can be used to modify/stabilize subgrade soil and their chemical reactions with moist soil, cement in soil stabilization, the causes for shrinkage cracking of cement-modified soil (CMS), and the background of the microcracking technology.

## 2.2 Stabilization Additives

In-place stabilization is an economically feasible solution that could significantly reduce the construction cost, reduce the maintenance cost throughout the life of the pavement, and extend the pavement life. For the projects where the on-site soils have strength deficiencies or have problematic behavior (i.e., shrink/swell), the design will typically require high-quality materials that are often expensive or not readily available near the project. Costs associated with hauling suitable materials to the site will result in a significant increase in total construction cost. Most of the time, to maintain a long-lasting pavement for these projects where the on-site native soils may not meet the specification of the project, a stabilized subgrade soil is often essential. The stabilization can help improve the engineering properties of these inferior soils.

The bearing capacity of a soil depends on internal friction and cohesion. The internal friction angle of a soil is related to its soil gradation, particle angularity, and degree of compaction. Soil cohesion results from the adherence of particles due to surface tension, physical-chemical forces, and cementation between them. The hygroscopic water surrounding the soil particles is important for soil compaction to reach an optimum condition and a maximum density.

Typically, clay materials can behave like a solid, semisolid, plastic, or liquid, depending on its moisture content (see Figure 2.1). The cohesive properties of soil are dependent on the amount and nature of expansive clay particles. Standard Test Method ASTM D4318 (2017) is used to determine liquid limit, plastic limit, and plasticity index of soils. The plasticity index (PI) is the difference between the liquid limit and the plastic limit of the soil. A greater PI value for a soil is an indication that there is a larger proportion of expansive clay (e.g., montmorillonite) and a substantial potential of volume changes during wetting and drying.

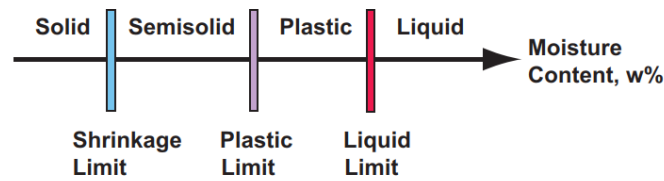


**Figure 2.1: Physical State versus Moisture Contents of Clay Materials**

Also, the chemical additive may fill or partially fill the voids between soil particles thus reducing the hydraulic conductivity of the soil. The reduction of the voids may also affect volumetric change behavior within a soil, shifting from a contractive to a dilative condition. It is the function of a chemical additive to bond soil particles, promote cohesive shear strength, and increase the difficulty of particle movement under loads. The stabilizing agent can affect the soil fabric typically by flocculation upon mixing and cementation over longer periods (NCHRP, 2004).

Lime, fly ash, cement kiln dust (CKD), and portland cement are the most known types of chemicals used in subgrade stabilization. The availability of these chemicals varies from one area to another. Selecting a stabilizer or additive is based on the type of soil that needs to be stabilized, the reason behind the utilization of the stabilized layer, the desired enhancement of the soil properties, the stabilized soil layer strength and durability requirement, and the condition of the environment and overall cost (US Department of the Army, 1992).

Lime is made from calcium carbonate ( $\text{CaCO}_3$ ) found in limestone, chalk, or seashells. There are two common types of lime: quicklime (i.e., calcium oxide ( $\text{CaO}$ )), and hydrated lime or slaked lime (i.e., chemically represented as calcium hydroxide,  $\text{Ca}(\text{OH})_2$ ). Lime is obtained by heating the raw material to a temperature between  $800^\circ\text{C}$  and  $1100^\circ\text{C}$ . When heated to these temperatures, the chalk breaks down by giving off carbon dioxide ( $\text{CO}_2$ ) and leaving calcium oxide ( $\text{CaO}$ ) that is known as quicklime. When exposed to water, the quicklime ( $\text{CaO}$ ) chemically reacts with the  $\text{H}_2\text{O}$  molecules and transforms to hydrated lime  $\text{Ca}(\text{OH})_2$ . This reaction is exothermic. The hydrated lime can react again when exposed to the atmosphere by absorbing carbon dioxide ( $\text{CO}_2$ ) to become calcium carbonate ( $\text{CaCO}_3$ ) once again.

Fly ash is a chemical byproduct of the coal fire in power plants. The fly ash is considered a pozzolanic material and contains substances such as  $\text{SiO}_2$ ,  $\text{TiO}_2$ ,  $\text{Al}_2\text{O}_3$ ,  $\text{Fe}_2\text{O}_3$ ,  $\text{MnO}$ ,  $\text{MgO}$ ,  $\text{CaO}$ ,  $\text{Na}_2\text{O}$ ,  $\text{K}_2\text{O}$ ,  $\text{P}_2\text{O}_5$ ,  $\text{SO}_3$ , and organic carbons (Das, 1990). The classification of fly ash is based on the chemical composition, and Class C and Class F are the two types of fly ash used in construction. Class C contains a significant quantity of free lime and can produce pozzolanic and cementitious reactions with water. A high content of calcium oxide results in lighter color fly ash, while a high content of organics results in darker color fly ash. Class F is the least commonly used fly ash due to its lack of self-cementitious properties and its requirement for an activator to react. Fly ash can improve engineering properties of soil. However, the properties of fly ash vary between production plants and depend on the chemical compound of the coal and combustion technology used at each plant (Muhunthan & Sariosseiri, 2008).

Cement kiln dust (CKD) is a by-product of the portland cement manufacturing process. The dust is a particulate mixture of partially calcined and unreacted raw feed, clinker dust and ash, enriched with alkali sulfates, halides, and other volatiles. Several factors influence the chemical and physical properties of CKD. Because plant operations differ considerably with respect to raw feed, type of operation, dust collection facility, and type of fuel used, the use of the terms for typical or average CKD when comparing different plants can be misleading. CKD is not only cost effective, but also has several desired properties and therefore has become, over the years, a popular stabilization agent.

### **2.3 Cement in Soil Stabilization**

The main purpose of using soil stabilizer(s) is to provide calcium ions ( $\text{Ca}^{2+}$ ) in sufficient amount so that the monovalent cations, like sodium  $\text{Na}^+$  (typically available on the surfaces of clay particles), are exchanged to lower the plasticity and improve the workability of the soil. Portland cement can supply this necessary ingredient and, when used properly, can effectively modify the properties of clayey soils/aggregates. The four basic reactions occurring in cement stabilization are cation exchange, particle restructuring, cementitious hydration, and pozzolanic reaction.

### *2.3.1 Cation Exchange*

When lime or cement is mixed with soil, it traps moisture and allows for a process of ionization and production of calcium cations to take place. These cations exchange with the clay lattice to substitute the monovalent ions, like sodium  $\text{Na}^+$  with calcium ions ( $\text{Ca}^{2+}$ ). The method for chemical stabilizer(s) used to exchange ions is the same as applied by calcium cation with clay structures, specifically with the sodium and potassium of the structure. A key requirement for attaining the benefits of this type of stabilization is to have sufficient mixing. The clay structure is broken down and excess water is released due to the strong ionization energy of calcium that bonds together the clay particles within hours after the clay is mixed with cement.

### *2.3.2 Particle Restructuring*

This phenomenon involves the change of the texture of the clay material from a plastic to a more friable material. It is also known as the flocculation and agglomeration of the clay particles that result in an increase of the internal friction angle of the clay. The restructuring of the clay occurs within several hours after the clay is mixed with cement.

### *2.3.3 Cementitious Hydration*

This phenomenon involves a series of chemical reactions which occur with the introduction of water to calcium and silica present in cement. This reaction will result in the formation of calcium-silicate-hydrate (C-S-H), calcium aluminum hydrate (C-A-H), and excess calcium hydroxide  $\text{Ca}(\text{OH})_2$ . The C-S-H and C-A-H are what bond the clay particles together to form a solid matrix. This process starts one day to one month after mixing.

### *2.3.4 Pozzolanic Reaction*

Subsequent to the hydration reaction, a slower pozzolanic reaction involves the excess calcium hydroxide  $\text{Ca}(\text{OH})_2$  from the hydration reaction combined with water and silica or alumina dissolved from the clay particles to form additional C-S-H or C-A-H, respectively. This reaction occurs over months and years and can further strengthen the soil-cement structure.

## 2.4 Shrinkage Cracking of Cement-Modified Soil

Cement is commonly used in practice to modify/improve engineering properties of inferior soils. Cement-modified soil (CMS) often has a shrinkage potential. Shrinkage that is associated with cement-modified soil can be divided into two categories: autogenous shrinkage (resulting from hydration of cement) and drying shrinkage (resulting from loss of moisture). George (1968a, 1968b) and Bofinger, Hassan, and Williams (1978) studied the shrinkage cracking phenomenon extensively and concluded that drying is the major cause for shrinkage. The degree of shrinkage cracking depends on several influence factors: tensile strength of the modified soil (George, 1969; Bofinger et al., 1978); restraint by friction between the modified soil layer and its underlying layer (Bofinger, 1971; George, 1973); creep characteristics of the modified soil (George, 1969; Bofinger et al., 1978); temperature (Bofinger, 1971; George, 1973); amount and type of clay in the modified soil (George, 1968a, 1968b); and moisture content and degree of compaction (Bofinger et al., 1978).

In general, the loss of moisture in the soil-cement mixture is the primary reason for shrinkage that eventually will crack the stabilized layer. Another factor that could also lead to shrinkage of chemically stabilized layers is the change in temperature. A study comparing the time rate of shrinkage of kaolinite soil-cement and montmorillonite soil-cement showed that kaolinite soil-cement shrank faster due to the large particle size of the kaolin clay, implying that most of the soil water is not absorbed to the surface and can be evaporated. Also, complete hydration of cement would require over 40 percent of water by weight. The same study showed that the drying effect of cement on specimens coated with wax will result in some shrinkage without loss of moisture. This study proves that hydration of cement would steal the moisture of the soil matrix.

Past studies have well documented the factors that cause shrinkage in CMS; however, recent efforts have focused on understanding design and construction practices that can minimize the shrinkage cracking problem. George (2001) conducted a soil stabilization field trial in Mississippi and concluded that pre-cracking of a stabilized base by roller compaction at 24 hours after placement minimized its shrinkage cracking. The Portland Cement Association (PCA, 2003) recommends 7-day unconfined compressive strengths of CMS should be within the range of 300–400 pound force per square inch (psi) in the design phase. During construction, PCA (2003)

recommends compaction of CMS at or slightly below its optimum moisture content with moist curing until a moisture barrier is placed.

## **2.5 Background of Microcracking Technology**

Although most early methods for reducing shrinkage cracking in CMS focused on controlling desiccation using moist-curing or asphalt-curing membranes, more recent techniques explored the use of stress relief layers, such as chip seals, geosynthetics, or thin unbound granular base layers, to reduce reflective cracking. These techniques can reduce the likelihood of reflective cracking, but require additional steps in the construction process that will increase construction cost. An innovative concept has been developed in Austria which involves the use of a vibratory smooth drum roller to create a microcracked CMS layer during the early curing stage (Litzka & Haslehner, 1995). The study reported that this microcracking process prevented the development of large stress cracks in the asphalt overlay. According to Litzka & Haslehner, microcracking is typically performed by three passes of a roller 24 to 48 hours after compaction (Sebesta, 2005). Brandl (1999) reported that the microcracking technique was most suitable among the available options for minimizing cracking on the Austrian–Hungarian Highway. The objective of microcracking is to induce hundreds of tiny cracks to accommodate the need for shrinkage without impacting the final pavement stiffness. These cracks will substitute the natural large individual cracks that have the potential to reflect up into flexible surface layers and influence the structural performance. After the initial successful microcracking work in Austria, this construction technique was tried again in Texas as early as 2000 to evaluate this microcracking concept. Scullion (2002) described these efforts, including the test sites on residential streets, and presented a specification for the microcracking process in the field. This study showed favorable results using the microcracking procedure. While the microcracking treatment applied on some soil-cement sections showed apparent effectiveness demonstrated using field deflection testing and comparison of the back calculated in-situ moduli with the design moduli, other microcracked soil-cement sites did not perform as predicted and did exhibit some cracking. The cracking developed in microcracked sections is likely related to the type of soil, the cement content, the means to



control the degree of microcracking in the field, the mixing temperature, and the age after mixing at which the microcracking is applied.

Although the previous research confirmed the applicability of this construction method in the field, no literature was found describing a procedure or method to simulate the microcracking process in the laboratory. This research proposes a laboratory method that can be used to simulate the microcracking process on CMS in the field using unconfined compression (UC) specimens. The UC specimens were used to evaluate the properties of CMS with and without microcracking, including their strength and stiffness.

# Chapter 3: Materials and Laboratory Tests

## 3.1 Introduction

In this study, laboratory test procedures were used to examine the native and cement-modified soils for subgrade stabilization in two project sites in Kansas. Before the development of the procedure to generate microcracking of CMS specimens in the laboratory, several test methods were adopted in the laboratory to characterize the properties of native soil and CMS and are discussed in this chapter.

## 3.2 Materials

### *3.2.1 Soil Selection*

Two different soils from ongoing projects in Marion County and Sedgwick County were selected and evaluated in this research. These soils were classified as clayey sand with gravel (SC) and fat clay with sand (CH), respectively according to the Unified Soil Classification System (USCS) described in ASTM D2487 (2017). The Marion County soil (bulk) was collected from a project located along 330<sup>th</sup> Street, between K-15 and the Marion-McPherson county line, west of Tampa, Kansas. The existing roadway was previously paved with a two-inch thick hot mix asphalt (HMA) layer that exhibited severe distresses (longitudinal, transverse, and fatigue cracking). The bulk soil was excavated at depths of approximately 1 foot along a 1-mile road segment of the 8-mile roadway that was planned to be built on a 1-foot-thick soil-cement subgrade overlaid by a 3-inch-thick HMA layer. In addition, the bulk soil from depths of approximately 1 to 3 feet below the existing grades was sampled by Terracon, on May 8, 2017, prior to initiation of construction activities for this project.

The Sedgwick County bulk soil was retrieved from a project located on East 87<sup>th</sup> Street South, between S 95<sup>th</sup> Street and Greenwich Road, about 4 miles southeast of Derby, Kansas. The existing roadway was previously surfaced with a river sand and gravel layer of approximately 6 inches thick. The soil samples were collected from the existing roadway surface down to a depth of approximately 10 inches along the proposed project alignment. The pavement section for this project comprised of 10 inches of CMS overlaid by a 2-inch-thick HMA layer. Also, bulk subgrade

soil samples from depths of approximately 1 to 3 feet below the existing grades were sampled by Terracon on May 10, 2018, prior to starting construction activities for this project. Figure 3.1 shows the locations of these two sites on the Google Map.



(a)



(b)

**Figure 3.1: Google Maps for the collected soil locations of: (a) clayey sand with gravel (SC), and (b) fat clay with sand (CH)**

### 3.2.2 Additives

The additive of interest for this study, portland cement (hydraulic cement) Type I/II, was selected to modify the native soil and improve its properties. The chemical properties of this additive are presented in Appendix A.

### **3.3 Laboratory Testing**

#### *3.3.1 Sample Preparation*

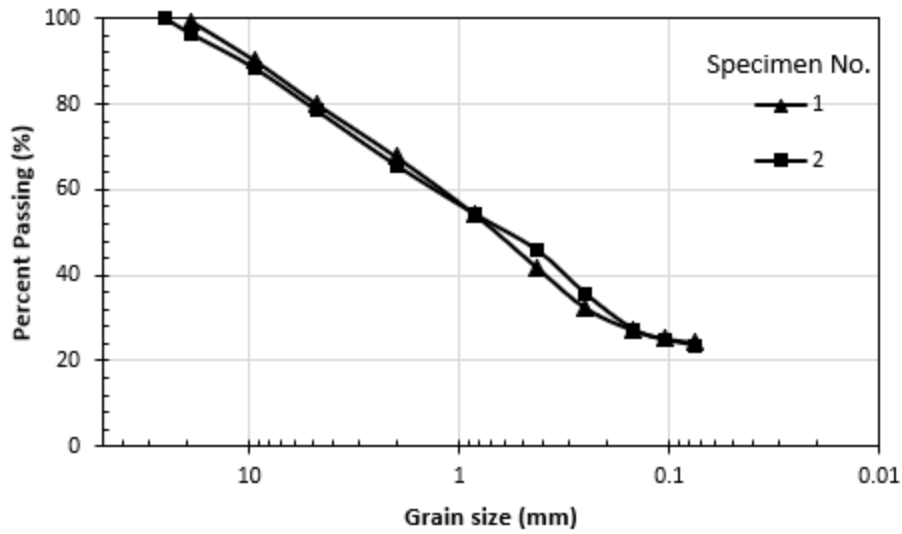
The bulk soil samples collected from these projects at depths of approximately zero to 1 foot below the existing pavement subgrade in Marion County and depths of approximately zero to 10 inches below the granular surface in Sedgwick County were first mixed thoroughly, and a portion of the mixed soil was dried for 24 hours at 60°C in a large oven. To determine the Atterberg limits of each soil, the dry soil was washed through a No. 40 (0.425 mm) sieve using water in accordance with ASTM D4318. The portion of the soil that passed the No. 40 sieve was dried again for 24 hours at 60°C and then crushed using a mortar and pestle. The compaction characteristics of these soils were determined to prepare reconstituted soil specimens mixed with cement. To evaluate the unconfined compressive strengths of the reconstituted specimens mixed with cement at different cement contents, the dry soil was crushed, pulverized, and passed through the 3/4-in (19-mm) sieve.

#### *3.3.2 Soil Classification*

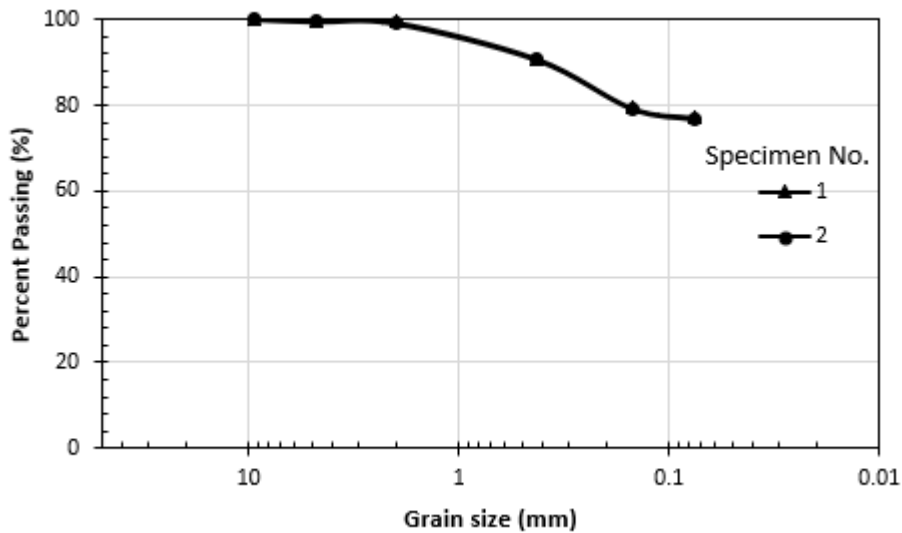
The grain size distribution, the Atterberg limits, the standard Proctor compaction curves, and the laboratory California bearing ratios (CBR) were determined for these two soils. Sieve analyses were performed using a wet sieve method in accordance with ASTM D422 (2007) to obtain the grain size distribution of the native soil. Two specimens for each material source (approximately 2.9 pounds [1300 g] of oven-dried soil each) were washed through a No. 200 sieve (0.075 mm). The portions of the soils retained on and passing the sieve were dried and weighed. Based on the percent of soil passing the No. 200 (0.075 mm) sieve, the Marion County soil within a depth of approximately 12 inches from the subgrade surface was classified as a coarse-grained soil. On the other hand, the Sedgwick County soil was classified as a fine-grained soil. Figures 3.2(a) and 3.2(b) present the grain size distribution curves of the Marion County and Sedgwick County soils, respectively.

The liquid limits, plastic limits, and plasticity indices of the native soils were determined according to ASTM D4318. The liquid limits were determined using the multipoint liquid limit method (Method A) described in ASTM D4318. Based on the Atterberg limits, the soils from

Marion County were classified as a clayey sand with gravel (SC) and lean clay (CL) of the fine portion according to the Unified Soil Classification System (USCS) described in ASTM D2487. On the other hand, the soil from Sedgwick County was classified as fat clay with sand (CH) according to the USCS described in ASTM D2487. Table 3.1 presents the Atterberg limits of the soils from both projects.



(a)



(b)

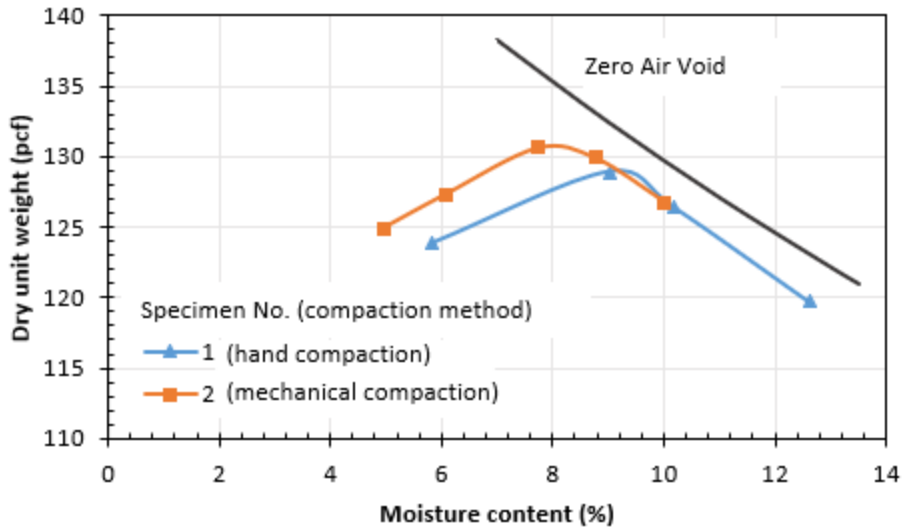
**Figure 3.2: Grain size distribution curves of the native soils from: (a) Marion County and (b) Sedgwick County (1 inch = 25 mm)**

**Table 3.1: Atterbeg limits of soils from Marion and Sedgwick Counties**

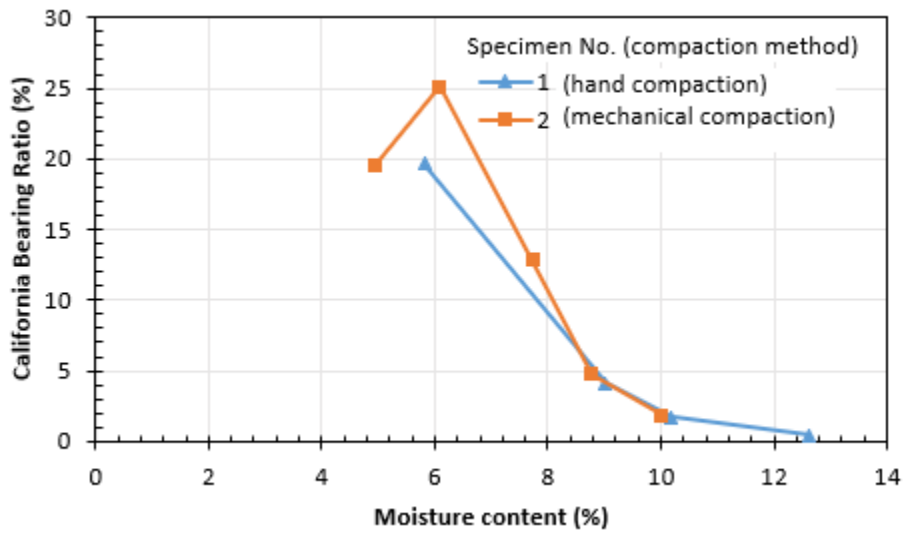
<b>Project Location</b>	<b>Marion county</b>	<b>Sedgwick county</b>
<b>Properties</b>	<b>SC soil</b>	<b>CH soil</b>
Liquid limit (LL)	30	50
Plastic limit (PL)	15	21
Plastic index (PI)	15	29

### *3.3.3 Soil Compaction Characteristics*

The native soils were tested to determine their optimum moisture contents and maximum dry densities using the standard Proctor compaction method described in ASTM D698 (2012). Method C was utilized to determine the moisture content-maximum dry density curves presented in Figures 3.3(a) and 3.4(a). After the compaction tests, the same specimens were tested for their California bearing ratios (CBR) following the procedure described in ASTM D1883 (2016). Figures 3.3(b) and 3.4(b) present the effect of the moisture content on the California bearing ratio, indicating the susceptibility of the subgrade strength to moisture content. For each project, two specimens were compacted with two different methods (hand and mechanical compaction) and then tested for the maximum dry unit weight and CBR. Since the mechanical compaction generates more uniform distribution of compaction energy than hand compaction, a lower optimum moisture content and a higher maximum dry density were obtained for soil samples using mechanical compaction. However, the curves generated by hand compaction were used in this research since subsequent work was mostly performed by hand. The optimum moisture content, the maximum dry density, and the CBR at the optimum moisture content for each native soil are presented in Table 3.2.

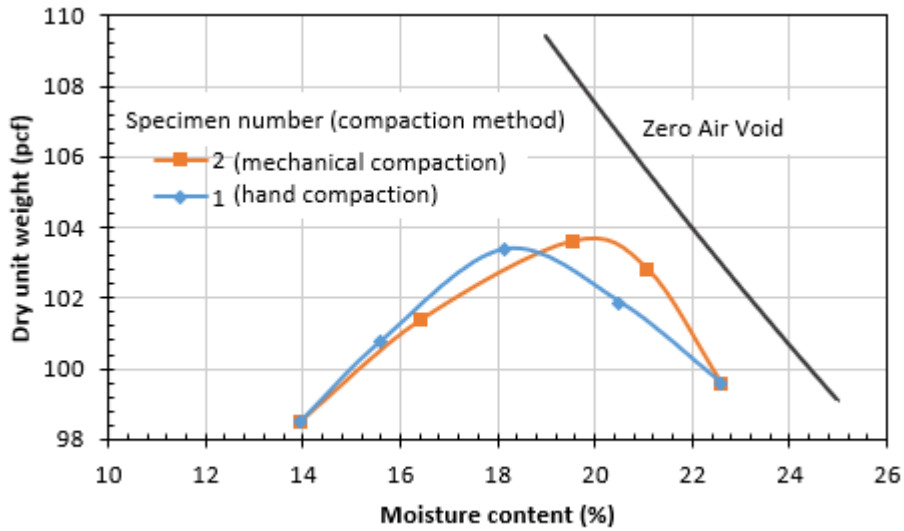


(a)

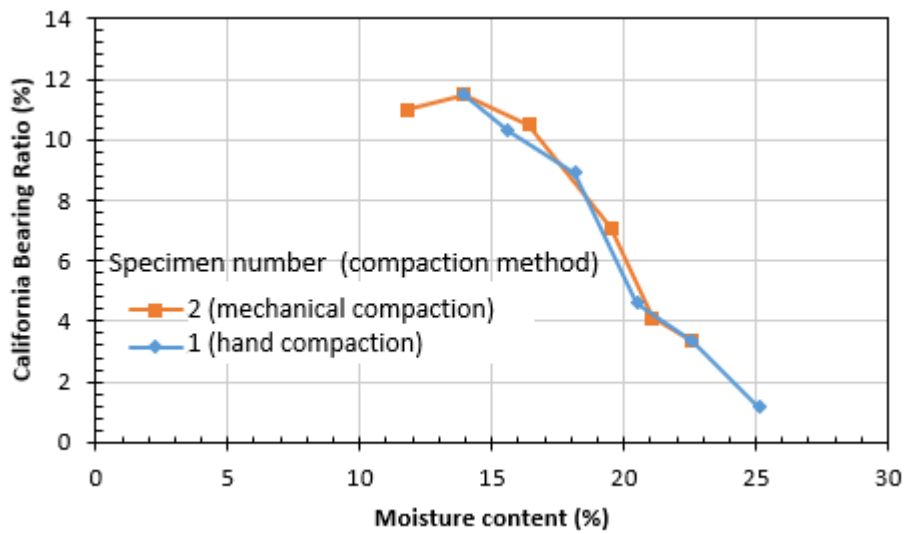


(b)

Figure 3.3: Compaction characteristics of the native soil from Marion County: (a) compaction curves and (b) effect of moisture content on CBR



(a)



(b)

Figure 3.4: Compaction characteristics of the native soil from Sedgwick County: (a) compaction curves and (b) effect of moisture content on CBR



**Table 3.2: Compaction Characteristics of Soils from Marion and Sedgwick Counties**

<b>Project Location</b>	<b>Marion County</b>	<b>Sedgwick County</b>
<b>Properties</b>	<b>SC soil</b>	<b>CH soil</b>
Optimum moisture content, $w_{opt}$ (%)	9.2	19.0
Maximum dry unit weight, $\gamma_d$ (pcf)	129	103
California Bearing Ratio (CBR) at $w_{opt}$ (%)	4.0	7.6

### *3.3.4 Unconfined Compressive Strength*

The specimen preparation procedure consisted of adding a specific percentage of portland cement to the native soil and then mixing them by hand. The amount of portland cement was calculated as a percentage by dry weight of the soil. Specimens were prepared for unconfined compressive strength (UC) testing in accordance with ASTM D1632 (2017) and tested for unconfined compressive strengths following ASTM D1633 (2017). The specimens were prepared with different cement contents and at the optimum moisture content or +2% of the optimum moisture content as determined for the native soil from each county. Unconfined compressive strength tests were performed on both un-cracked and microcracked specimens after various curing periods. The curing process took place in a moisture room at approximately 100% relative humidity and  $23 \pm 2^\circ\text{C}$  room temperature. The UC test results are presented in Chapter 4.

### *3.3.5 Wet-Dry Cycles*

Wet-dry cycle tests were performed according to ASTM D559 (2015). Two identical un-cracked specimens and one microcracked specimen of the Marion County CMS were prepared at the desired cement content and the optimum moisture content following the UC specimen preparation procedure. The specimens were cured for 7 days in a moisture room and subjected to wet-dry cycles. Each wet-dry cycle consisted of submerging three CMS specimens in water for 5 hours and then placing them in a  $71^\circ\text{C}$  oven for 42 hours. After completing each cycle, one un-cracked specimen was brushed and weighed to determine the mass loss of soil. The other specimens were measured for volumetric change and weighed to determine any change in moisture content. The test continued until 12 wet-dry cycles were completed or until the specimen failed. The wet-dry cycle test results are presented in Chapter 4.

### 3.3.6 Hydraulic and Electrical Conductivity

Hydraulic conductivity tests were performed according to ASTM D5084 (2016). Both un-cracked and microcracked specimens of the Marion County CMS were prepared at the desired cement content and the optimum moisture content following the UC specimen preparation procedure. The specimens were cured for 7 days in a moisture room and then subjected to saturation in a permeability test chamber before testing for hydraulic conductivity. On average, the saturation stage took approximately 8 days in order to reach saturation. After completing the saturation, both un-cracked and microcracked specimens were tested for hydraulic conductivity at three different confining pressures. Before and after the saturation stage of each specimen, the specimen electrical conductivity was measured using the portable field/laboratory spectral induced polarization (SIP) unit (PSIP) as shown in Figure 3.5. The PSIP is a high-performance multi-channel geophysical instrument optimized for laboratory and in-situ near surface SIP, conventional resistivity, time-domain induced polarization, and self-potential measurements. The hydraulic and electrical conductivity test results are presented in Chapter 4.

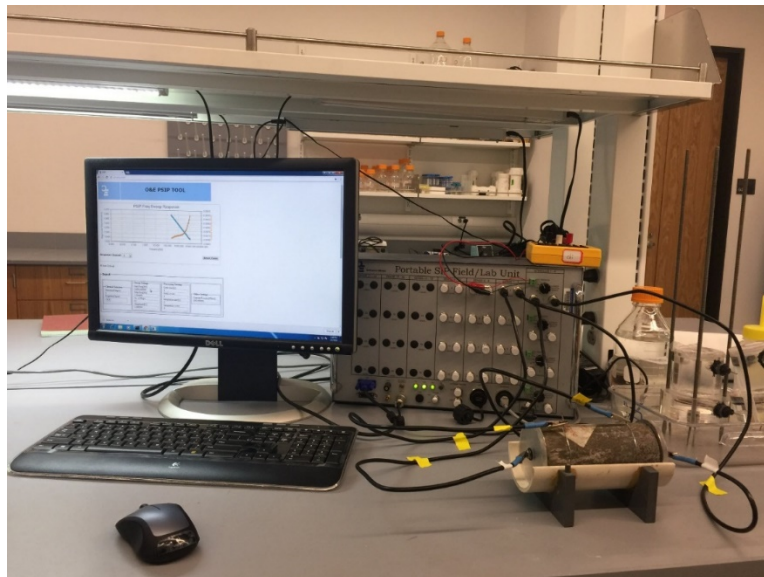
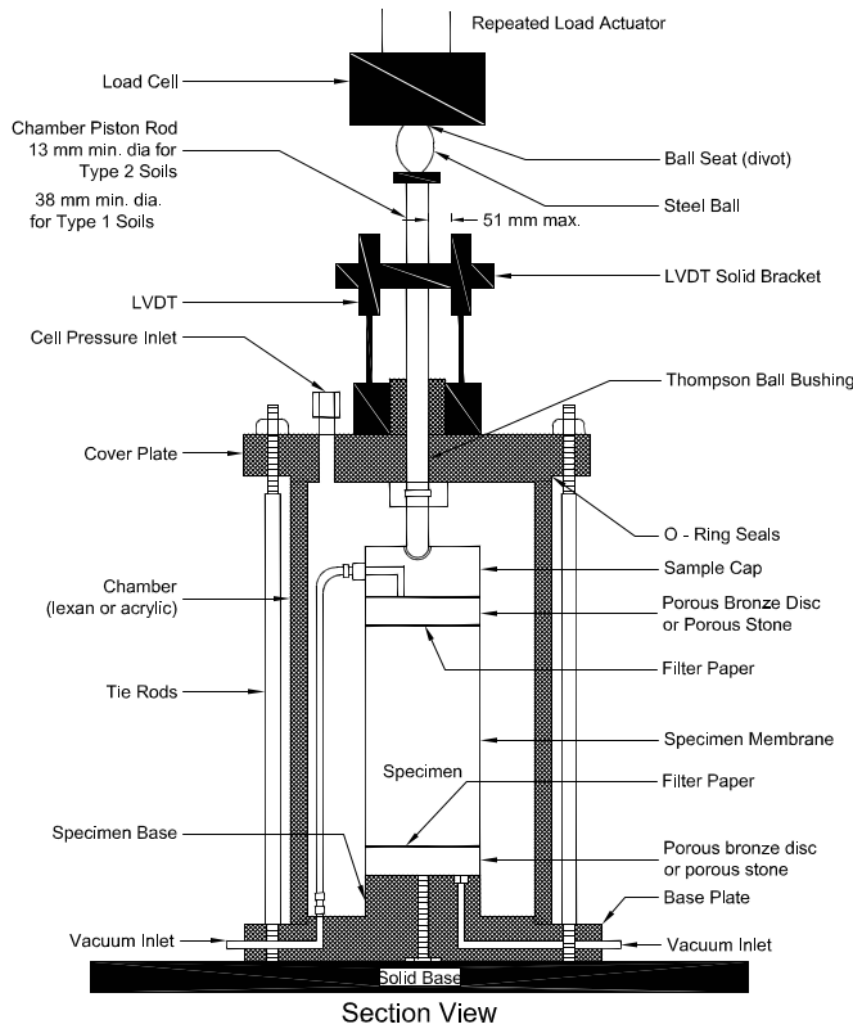


**Figure 3.5: Electrical conductivity test setup of the CMS specimen connected to the PSIP unit**

### 3.3.7 Resilient Modulus Testing

Resilient modulus ( $M_R$ ), a measure of stiffness, is a fundamental material property for bound and unbound pavement materials. This property for a subgrade or base material is an important input for the Mechanistic-Empirical Pavement Design Guide (MEPDG). The resilient modulus for an individual soil can significantly vary with its density, moisture content, gradation, plasticity index, and stress level (Vanapalli, Fredlund, & Pufahl, 1999). Figure 3.6 shows the typical triaxial chamber with external LVDTs and a load cell.



Note: LVDT tips shall rest on the triaxial cell itself or on a plate/bracket that is rigidly attached to the triaxial cell.

**Figure 3.6: Typical triaxial chamber with external LVDTs and a load cell**  
Source: Simpson, Schmalzer, and Rada (2007)

The resilient modulus test using the cyclic triaxial test equipment is designed to simulate traffic wheel loading on a soil by applying a sequence of repeated or cyclic loading on the specimen. In this research, the standard test method for determining the resilient modulus of soils and aggregate materials (AASHTO Designation T 307, 1999) was employed. The stress levels are selected to represent overburden pressures of specimens in the subgrade. The axial deviatoric stress is composed of two components: cyclic stress, which is the applied deviatoric stress, and a constant stress, which typically represents a seating load on the soil specimen. It should be noted that the constant stress is typically equivalent to 10% of the overall maximum axial stress.

A haversine-shaped wave load pulse with a frequency of 1 Hz was applied as the traffic wheel loading on the soil. A loading period of 0.1 sec and a relaxation period of 0.9 sec were used in the testing. The testing sequence employed in this test procedure is presented in Table 3.3.

The resilient modulus test was conducted on cement-modified soil specimens collected from the field after microcracking using the coring technique. Also, resilient modulus tests were conducted on un-cracked and microcracked specimens that were mixed with cement at the desired cement contents and reconstituted in the lab using the soils collected from Marion County and Sedgwick County.

**Table 3.3: Testing sequence for CMS specimens**

Sequence No.	Confining Pressure, $\sigma_3$		Max. Axial Stress, $\sigma_{max}$		Cyclic Stress, $\sigma_{cyclic}$		Constant Stress, $0.1\sigma_{max}$		No. of Load Applications
	kPa	psi	kPa	psi	kPa	psi	kPa	psi	
0	41.4	6.0	27.6	4	24.8	3.6	2.8	0.4	500-1000
1	41.4	6.0	13.8	2	12.4	1.8	1.4	0.2	100
2	41.4	6.0	27.6	4	24.8	3.6	2.8	0.4	100
3	41.4	6.0	41.4	6	37.3	5.4	4.1	0.6	100
4	41.4	6.0	55.2	8	49.7	7.2	5.5	0.8	100
5	41.4	6.0	68.9	10	62.0	9.0	6.9	1.0	100
6	27.6	4.0	13.8	2	12.4	1.8	1.4	0.2	100
7	27.6	4.0	27.6	4	24.8	3.6	2.8	0.4	100
8	27.6	4.0	41.4	6	37.3	5.4	4.1	0.6	100
9	27.6	4.0	55.2	8	49.7	7.2	5.5	0.8	100
10	27.6	4.0	68.9	10	62.0	9.0	6.9	1.0	100
11	13.8	2.0	13.8	2	12.4	1.8	1.4	0.2	100
12	13.8	2.0	27.6	4	24.8	3.6	2.8	0.4	100
13	13.8	2.0	41.4	6	37.3	5.4	4.1	0.6	100
14	13.8	2.0	55.2	8	49.7	7.2	5.5	0.8	100
15	13.8	2.0	68.9	10	62.0	9.0	6.9	1.0	100

## Chapter 4: Microcracking Simulation in Laboratory

### 4.1 Cement Modified Soil

#### 4.1.1 Marion County Soil

Portland cement (hydraulic cement) Type I/II was selected to modify the native soil and improve its engineering properties. To design the soil-cement mix, a strength criterion based on unconfined compressive (UC) strength of soil-cement specimens cured for 7 days in the moisture room was adopted. Since this study involved field and laboratory evaluations of the cement modified soil, and the actual CMS mixture was designed and constructed in the field to achieve a 7-day UC strength of 300 psi, the selected 7-day UC strength in this study for Marion County was 300 psi. To find the appropriate cement content, the soil was mixed with cement at three different cement contents, 3.5%, 5.0%, and 6.5%. For each cement content, five specimens were prepared in accordance with ASTM D1632 and tested for their unconfined compressive strengths following ASTM D1633. Soil and cement were mixed at  $\pm 0.5\%$  of the optimum moisture content as determined for the native soil. The soil-cement mix was placed and compacted in a mold, cured in the mold in a temperature-controlled moist-curing room for 12 to 18 hours, and then removed from the mold using a UC specimen extruder. The specimen was returned to the moisture room for continuous curing and protected from dripping water.

After 7 days of the moist curing period, unconfined compression tests were performed on CMS specimens in the moist condition directly after their removal from the moisture room. Table 4.1 summarizes the unconfined compressive strengths for all specimens of the three mixes with the cement contents of 3.5%, 5.0%, and 6.5%. Figure 4.1 shows the effect of the cement content on the UC strength of CMS. At the target UC strength, the cement content was determined as 5.0%. The 5.0% cement content was used in the following laboratory evaluation performed for this project and represented the cement content used in the field for the construction of this project. The stress-strain curves of the CMS specimens after 7-day curing are presented in Appendix B Figure B.1.

**Table 4.1: Unconfined compressive strength of CMS after cured for 7 days – Marion County**

Mix No.	Specimen No.	Cement content (%)	Compressive strength (psi)	Average strength (psi)
1	1	3.5	205	206
	2		212	
	3		262	
	4		208	
	5		144	
2	1	5.0	290	305
	2		306	
	3		349	
	4		337	
	5		242	
3	1	6.5	433	417
	2		394	
	3		397	
	4		443	
	5		420	

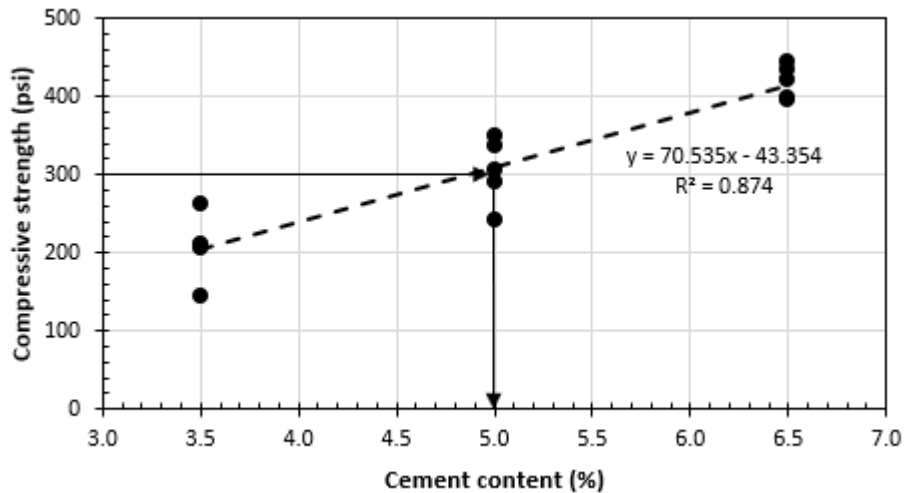


**Figure 4.1: Unconfined compressive strength of CMS versus cement content after cured for 7 days for the Marion County soil**

#### 4.1.2 Sedgwick County Soil

Similar to the procedure followed for the Marion County project, portland cement Type I/II was also used to modify the native soil from Sedgwick County. In this project, a strength criterion based on the unconfined compressive (UC) strength of 210 psi for soil-cement specimens

cured for 7 days in the moisture room was considered for the design of the soil-cement mix. This 7-day UC strength was selected to simulate the field condition based on the project requirement. To find the appropriate cement content, the native soil was mixed with cement at three different cement contents, 4.0%, 5.5%, and 7.0%. For each cement content, three specimens were prepared in accordance with ASTM D1632 and tested for their unconfined compressive strengths following ASTM D1633. Soil and cement were mixed at +2.0% of the optimum moisture content as determined for the native soil. The soil-cement mix was placed and compacted in a mold, cured in the mold in a temperature-controlled moisture room for 12 to 18 hours, and then removed from the mold using a UC specimen extruder. The specimen was returned to the moisture room for continuous curing and protected from dripping water. After 7 days of the moist curing period, unconfined compression tests were performed on CMS specimens in the moist condition directly after their removal from the moisture room. Table 4.2 provides the unconfined compression test results of the three mixes from Sedgwick County with the cement contents of 4.0%, 5.5%, and 7.0%. Figure 4.2 shows the effect of the cement content on the UC strength of CMS. At the target UC strength, the cement content was determined as 5.5%. This cement content was used in the following laboratory evaluation and represents the cement content used in the field for the construction of the project. Figure B.2 in Appendix B presents the original stress-strain curves of the CMS specimens after 7-day curing.

**Table 4.2: Unconfined compressive strength of CMS after cured for 7 days – Sedgwick County**

Mix No.	Specimen No.	Cement content (%)	Compressive strength (psi)	Average strength (psi)
1	1	4.0	138	133
	2		132	
	3		130	
2	1	5.5	194	202
	2		200	
	3		211	
3	1	7	291	301
	2		298	
	3		315	



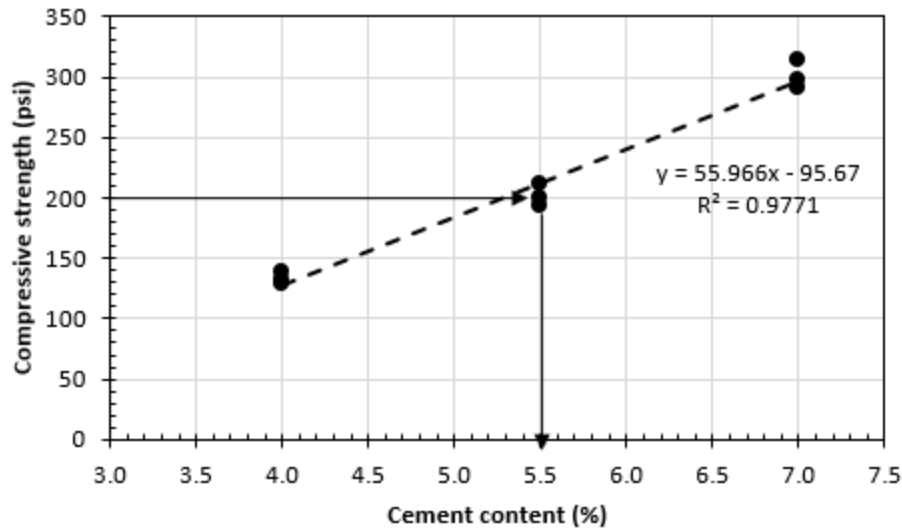


**Figure 4.2: Unconfined compressive strength of CMS versus cement content after cured for 7 days for the Sedgwick County soil**

## 4.2 Microcracking

### 4.2.1 Marion County Soil

The simulation of the microcracking process in the laboratory was intended to replicate the procedure adopted in the field during construction. As mentioned earlier, microcracks in a CMS layer are induced in the field by re-compacting the CMS layer with a roller after the initial compaction and a partial curing time of 24 to 48 hours. In other words, the microcracks are generated by preloading the CMS surface of the treated layer and inducing a network of fine cracks. This process will prevent the formation of major and wide shrinkage cracks that typically develop in soils mixed with cement. In practice, unconfined compression tests are conducted in the laboratory to determine the cement content for a CMS mix. In this research, microcracking of the specimens prepared in the laboratory was simulated using the unconfined compression testing machine. The specimens were subjected to axial loading until yielding was identified.

Before development and verification of the microcracking process, the UC strength of CMS specimens was determined after being moist-cured for a period of 48 hours. Six UC specimens of CMS at the desired cement content of 5.0% were prepared and tested after 48-hour

moist curing. Table 4.3 provides the UC test results of the specimens using the soil from Marion County. The average UC strength of CMS after 48-hour curing was 228 psi, or 75% of the 7-day strength. Figure 4.3 presents the stress-strain curves of the UC tests of the CMS specimens mixed at 5.0% cement content with the Marion County soil after 48-hour curing. This figure shows that the CMS material had a brittle behavior (i.e., the stress sharply dropped after the peak).

**Table 4.3: Unconfined compressive strength of CMS with 5.0% cement content after 48-hour curing**

Specimen No.	Compressive strength (psi)	Average strength (psi)
1	234	228
2	197	
3	226	
4	238	
5	233	
6	240	

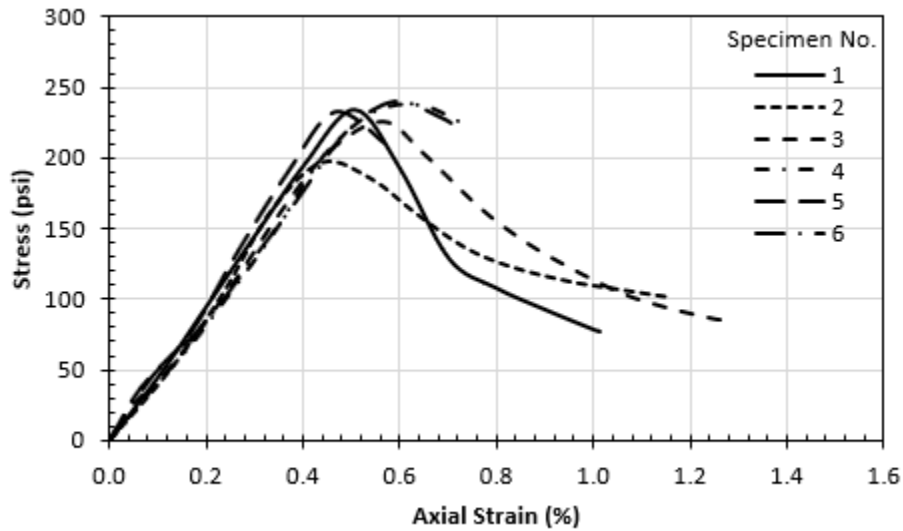
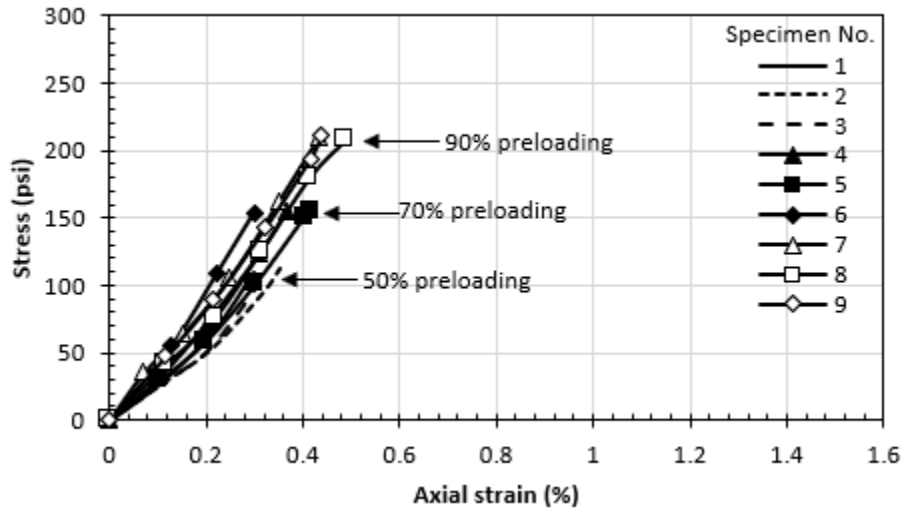


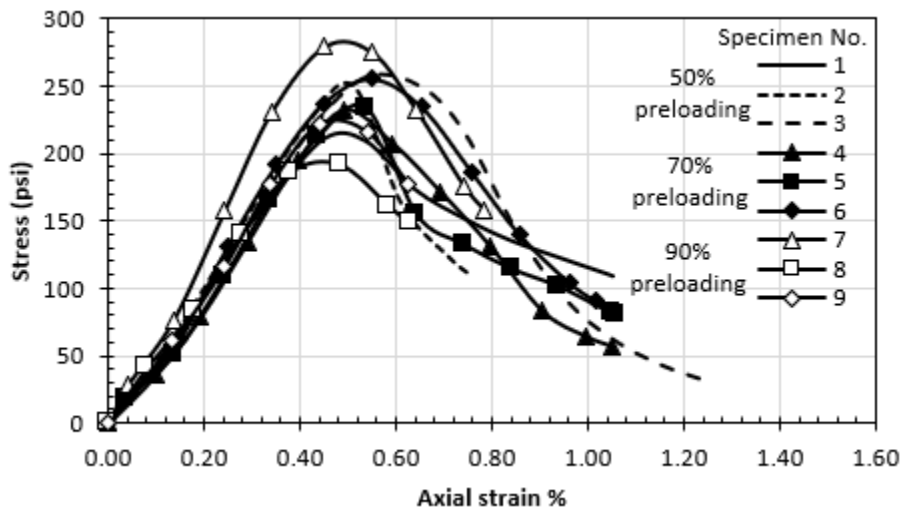
**Figure 4.3: Stress-strain curves of CMS with 5.0% cement after 48-hour curing for the Marion County soil**

To simulate the microcracking process in the laboratory by preloading the CMS specimen after a short curing period, three trials were made. In these trials, three stress levels of preloading were applied to the UC specimens after the 48-hour curing period: approximately 50%, 70%, and 90% of the ultimate UC strength of the specimens. Figure 4.4(a) depicts the stress-strain curves of the UC specimens during preloading. For each preloading level, three CMS specimens were prepared and loaded. After the preloading stage, no sign of any cracks was observed on the UC specimens for all preloading levels. This phenomenon was also confirmed when the preloaded specimens were tested to failure after 2-hour waiting time, showing no strength reduction. In fact, the UC strengths of the preloaded specimens were slightly higher than those cured for 48 hours. Figure 4.4(b) shows the stress-strain curves of the UC specimens after preloading. Table 4.4 summarizes the results of the UC tests for all preloading levels.

The specimens of Trial 3 were preloaded to 90% of the ultimate UC strength and then tested for the UC strength after a 2-hour waiting period. These failed or microcracked specimens from Trial 3 were loaded again in the UC tests, which showed strength and modulus ( $E_{50}$ ) reductions by approximately 50% and 42%, respectively, as shown in Figure 4.5 and Table 4.5. The secant modulus,  $E_{50}$ , was calculated as the slope of the secant line connecting from the origin to the point on the stress-strain curve corresponding to 50% the UC strength. These reductions are also found in the field after microcracking of CMS layers. Therefore, the procedure of loading the UC specimen to failure and stopping loading soon after reaching the peak strength would create a similar behavior of a microcracked CMS layer in the field.



(a)



(b)

Figure 4.4: Stress-strain curves of CMS with 5.0% cement after 48-hour curing: (a) loaded to the preloading stress level, and (b) after preloading

**Table 4.4: The UC test results for the CMS specimens with 5.0% cement during and after preloading**

Trial No.	Specimen No.	Preloading level	Preloading stress (psi)	Average preloading (psi)	Compressive strength (psi)	Average strength (psi)
<b>Specimen age</b>		<b>48 hours</b>			<b>50 hours</b>	
Trial 1	1	50%	110	112	211	240
	2		113		251	
	3		112		258	
Trial 2	4	70%	155	155	232	240
	5		155		234	
	6		154		255	
Trial 3	7	90%	210	210	279	231
	8		208		192	
	9		211		222	

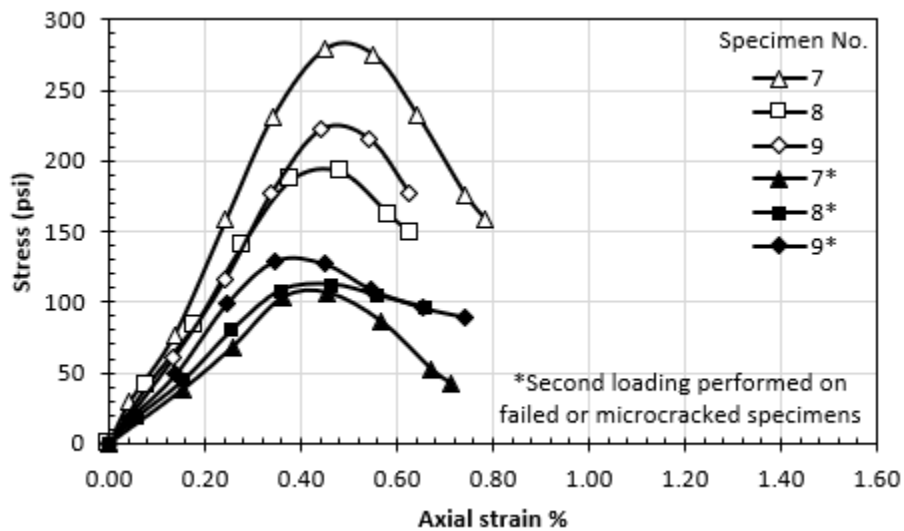


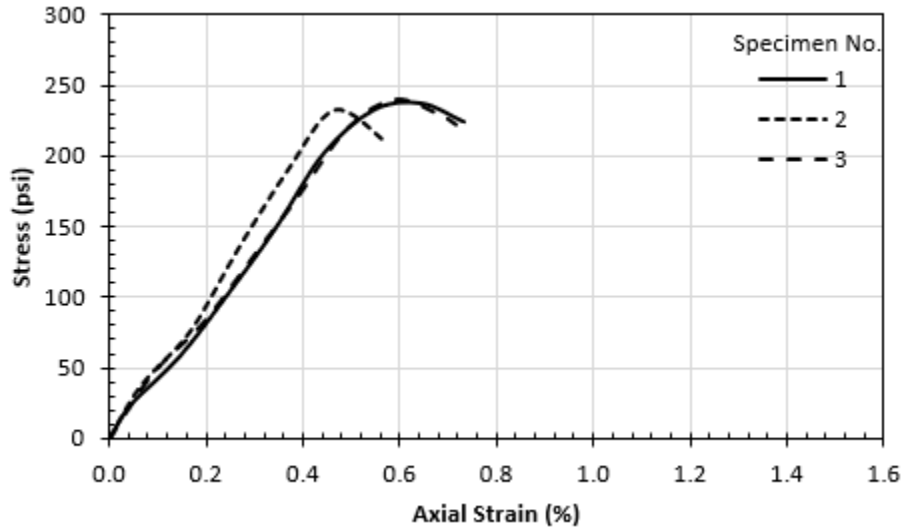
**Figure 4.5: Stress-strain curves before and after microcracking of CMS specimens in Trial 3 for the Marion County soil**

**Table 4.5: Unconfined compressive strengths and moduli of failed CMS specimens for the Marion County soil subjected to second loading**

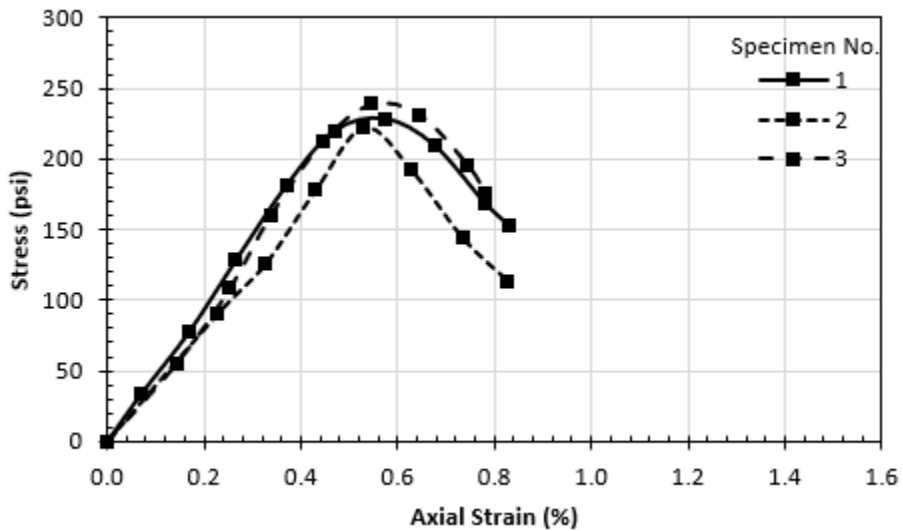
Trial No.	Specimen No.	Specimen age	Compressive strength (psi)	Average strength (psi)	Modulus, E <sub>50</sub> (ksi)	Average modulus, E <sub>50</sub> (ksi)	Strength reduction	Modulus, E <sub>50</sub> reduction
Trial 3	7	50 hours	279	231	65.8	54.0	50%	42%
	8		192		49.1			
	9		222		47.0			
Trial 3	7*	52 hours	106	116	26.0	31.3		
	8*		112		30.0			
	9*		129		37.9			

Note: \*Second loading performed on failed or microcracked specimens

In Trial 4, three additional CMS specimens were microcracked. Figure 4.6(a) presents their stress-strain curves. After the microcracking process, the specimens of Trial 4 were returned to the moisture room to continue the curing process and to allow the specimens to gain strength. After 7-day curing, the specimens of Trial 4 were tested for the UC strengths, and their stress-strain curves are presented in Figure 4.6(b). The average strength of these three CMS specimens was 230 psi. In other words, the 7-day UC strength of the microcracked specimens were the same as the ultimate UC strength at 2 days of un-cracked specimens. Moreover, the 7-day UC strength of the microcracked specimens was approximately 75% of the design strength of the CMS mix (i.e., 300 psi). This finding is similar to that for the strength of the CMS layer with microcracks in the field at the age of 7 days.



(a)



(b)

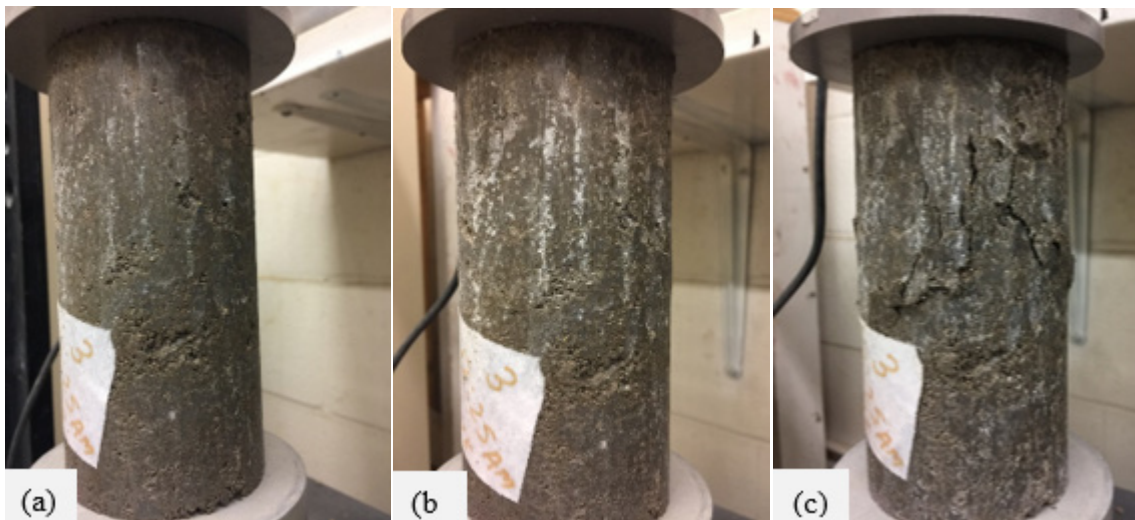
**Figure 4.6: Stress-strain curves of CMS specimens at 5% cement in Trial 4 for the Marion County soil: (a) during the microcracking process after 2-day curing, and (b) after the microcracking process after 7-day curing**

Table 4.6 summarizes the UC strengths of the CMS specimens before and after microcracking for Trial 4. Figure 4.7 shows the CMS specimen No. 3 of Trial 4 before microcracking, after microcracking at 48-hour curing, and after UC testing at 7-day curing. Microcracks were observed on the CMS specimens after the microcracking process. Based on the test procedure adopted and the test results obtained in this study, it is recommended that the

microcracking process in the laboratory should be controlled as loading of the CMS specimen passing the peak compressive strength by less than 0.1% axial strain and releasing the load soon after.

**Table 4.6: UC strengths of CMS specimens before and after microcracking for the Marion County soil**

Trial No.	Specimen No.	Compressive strength (psi)	Average strength (psi)	Compressive strength (psi)	Average strength (psi)
Specimen age		48 hours		7 days	
Specimen Condition		After initial compaction		After microcracked	
Trial 4	1	238	237	228	230
	2	233		223	
	3	240		239	



**Figure 4.7: CMS specimen No. 3 of Trial 4 for the Marion County soil: (a) before microcracking, (b) after microcracking at 48-hour curing, and (c) after UC testing at 7-day curing**

Table 4.7 shows the effects of the microcracks on the UC strength and modulus ( $E_{50}$ ) after the 7-day moist curing period. The un-cracked specimens of Mix No. 2 had a higher UC strength and a lower modulus (stiffness) than those of the microcracked specimens of Trial 4. The average UC strength of the microcracked specimens was approximately 75% that of the un-cracked specimens. However, the microcracked specimens had the moduli approximately 150% that of the un-cracked specimens since the specimens were preloaded during the microcracking process.



Furthermore, the modulus to strength ratio of the un-cracked specimens after 7-day curing was approximately 100, which is the same as suggested by Han (2015) for soil-cement. On the other hand, the ratio of modulus to strength for the microcracked specimens increased to approximately 200 since they were preloaded. These results indicate that the presence of the microcracks made the specimen weaker but stiffer.

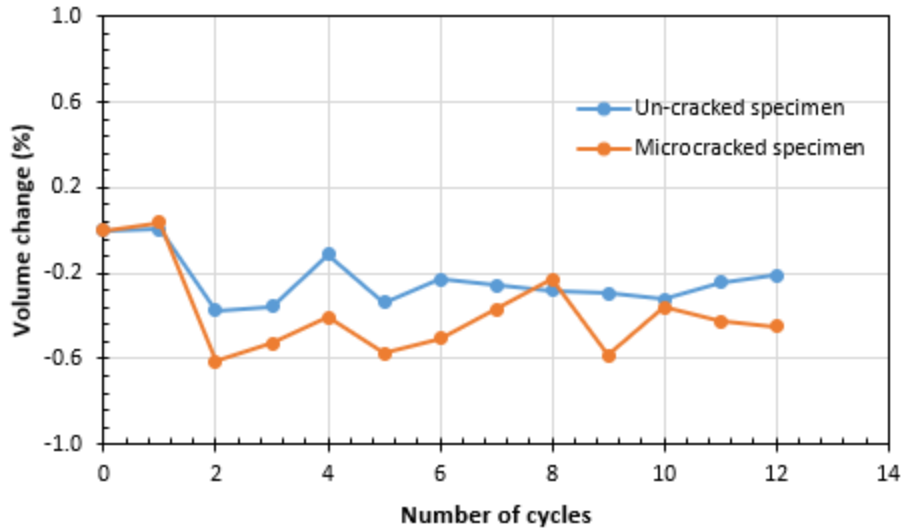
**Table 4.7: Effects of microcracks in CMS specimens on the UC strength and modulus ( $E_{50}$ ) at 7-day curing for the Marion County soil**

Specimen Condition	Specimen No.	Compressive strength (psi)	Average strength (psi)	Modulus, $E_{50}$ (ksi)	Average modulus, $E_{50}$ (ksi)	Modulus to strength ratio
Un-cracked specimens (Mix No. 2)	1	290	305	21.0	30.6	100
	2	306		32.1		
	3	349		40.0		
	4	337		27.2		
	5	242		32.5		
Microcracked specimens (Trial 4)	1	228	230	48.9	44.4	193
	2	223		39.6		
	3	239		44.6		

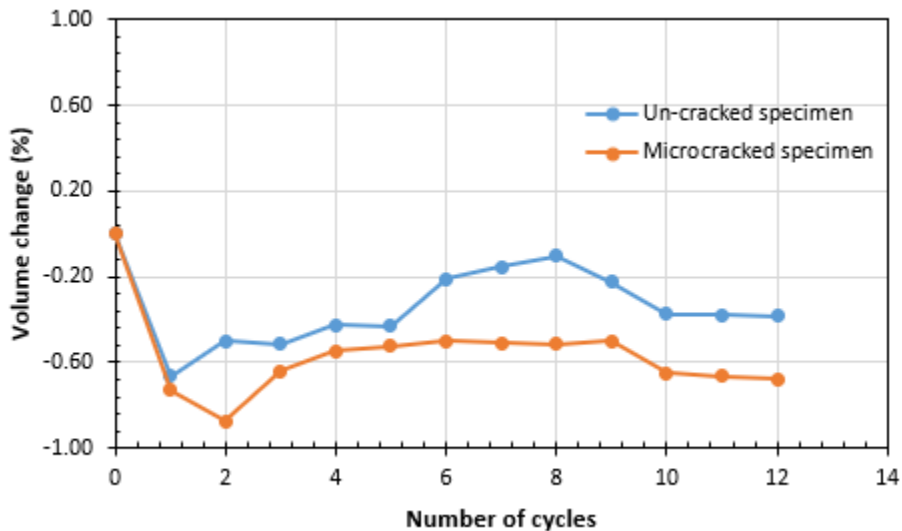
#### 4.2.1.1 Wet-Dry Cycle Test Results

The results of wet-dry cycle tests of CMS specimens for the Marion County soil are presented in this section. The procedure for the wet-dry cycle test was described earlier in Section 3.3.5. The wet-dry cycle test was conducted to evaluate the climatic effect on the properties of CMS with or without microcracking during its service life. Figure 4.8 shows the volumetric change of one un-cracked specimen and one microcracked specimen after 12 cycles of wetting and drying. In general, even though small maximum volumetric changes (-0.6% after wetting cycles and -0.9% after drying cycles) were measured, negative volumetric changes indicate a shrinkage behavior for both specimens. Also, the microcracked specimen had a slightly larger tendency for volumetric change due to easy infiltration and loss of water through microcracks. Considering the Marion County soil is a coarse-grained soil, its shrinkage potential is low. Figures B.3 and B.4 in Appendix B present the density and moisture content variations, respectively, during these cycles for both specimens. Figure 4.9 presents the mass loss results of an un-cracked specimen after 12 cycles of

wetting, drying, and brushing as recommended in ASTM D559. With increasing number of wet-dry cycles, the specimen mass loss increased to approximately 7% of the initial specimen mass after the 12th cycle. Since the specimens had small diameter and height, they could not simulate the shrinkage of CMS to form large cracks in field; therefore, this test may not be representative for a field condition and it should be cautioned to interpret the results from this test.



(a)



(b)

Figure 4.8: Volume change during the wet-dry test cycle based on: (a) wet condition and (b) dry condition

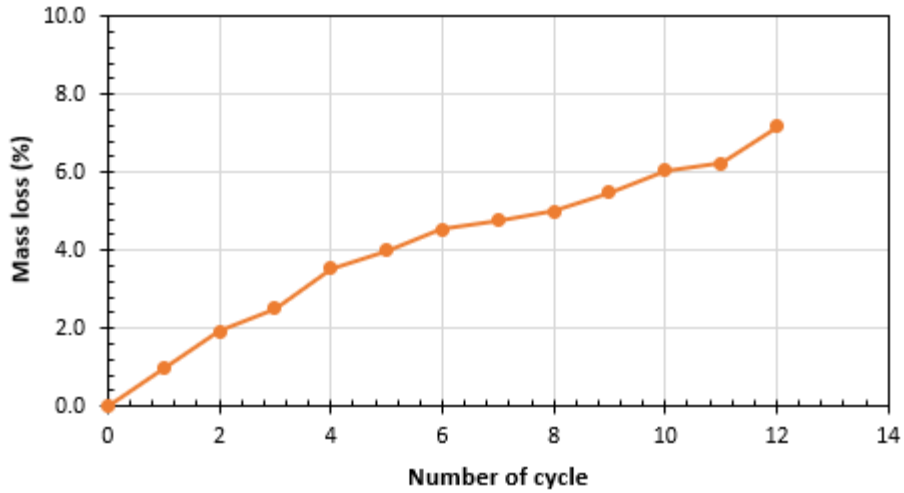


**Figure 4.9: Mass loss for the brushed specimen calculated after a complete wet-dry cycle for all cycles**

#### 4.2.1.2 Hydraulic and Electrical Conductivity Results

This section discusses the effects of microcracking on hydraulic and electrical conductivity of CMS specimens. Figure 4.10 shows the hydraulic conductivity (i.e., permeability) of one un-cracked specimen and one microcracked specimen at different effective stresses. These effective stresses represent different burial depths from the surface. In general, the un-cracked specimen had lower hydraulic conductivity than the microcracked specimen for all effective stresses. Also, the hydraulic conductivity for both un-cracked and microcracked specimens decreased as the effective stress increased because the specimen was compressed under higher confining pressure. The rate of decrease in the hydraulic conductivity for the microcracked specimen was higher than that for the un-cracked specimen, as the effective pressure tended to compress and close the microcracks in the specimen.

Figure 4.11 presents the electrical conductivity of one un-cracked specimen and one microcracked specimen in terms of their electrical resistivity at different degrees of saturation. The degree of saturation of the specimen changed as the specimen was cured for 7 days in the moisture room and placed in the hydraulic conductivity test chamber. Figure 4.11 shows that the microcracks increased the specimen electrical resistivity when the microcracked specimen was not fully saturated (<100%) as compared to the un-cracked specimen. However, at the degree of

saturation (i.e., 100%), the microcracked specimen had lower electrical resistivity than that for the un-cracked specimen. It should be noted that the saturation process of the reconstituted specimen prior to permeability testing lasted approximately 8 days. Therefore, the hydraulic conductivity testing on the microcracked and un-cracked specimens was initiated when the age of the specimens was 16 days after reconstitution.

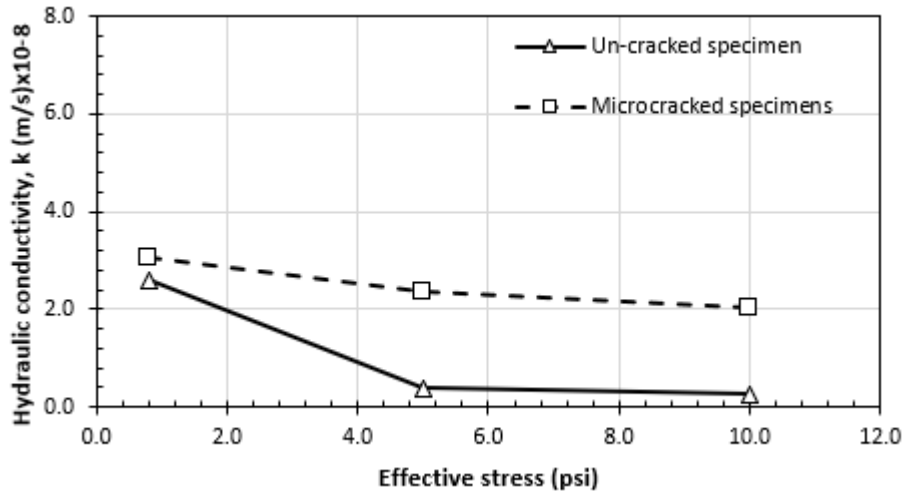


Figure 4.10: Hydraulic conductivity variation with different effective pressure

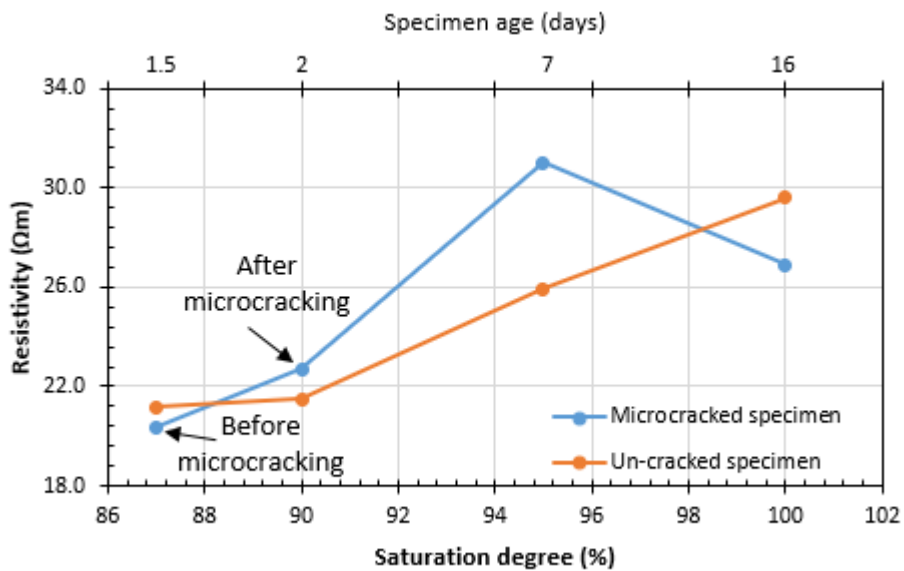


Figure 4.11: Resistivity variation with degree of saturation and age of CMS specimens for the Marion County soil

#### 4.2.2 Sedgwick County Soil

Following the recommendation for the microcracking procedure found based on the Marion County soil, six UC specimens of CMS at the desired cement content of 5.5% for the Sedgwick County soil were prepared and tested (or microcracked) after 48-hour moist curing. Table 4.8 provides the UC test results. The average UC strength of CMS after 48-hour curing was 155 psi, or 74% of the 7-day strength. Figure 4.12 presents the stress-strain curves of the UC tests of the CMS specimens at 5.5% cement content after 48-hour curing.

**Table 4.8: Unconfined compressive strength of CMS at 5.5% cement after 48-hour curing**

Group No.	Specimen No.	Compressive strength (psi)	Average strength (psi)
Group 1	1	154	155
	2	152	
	3	152	
Group 2	4	160	
	5	148	
	6	162	

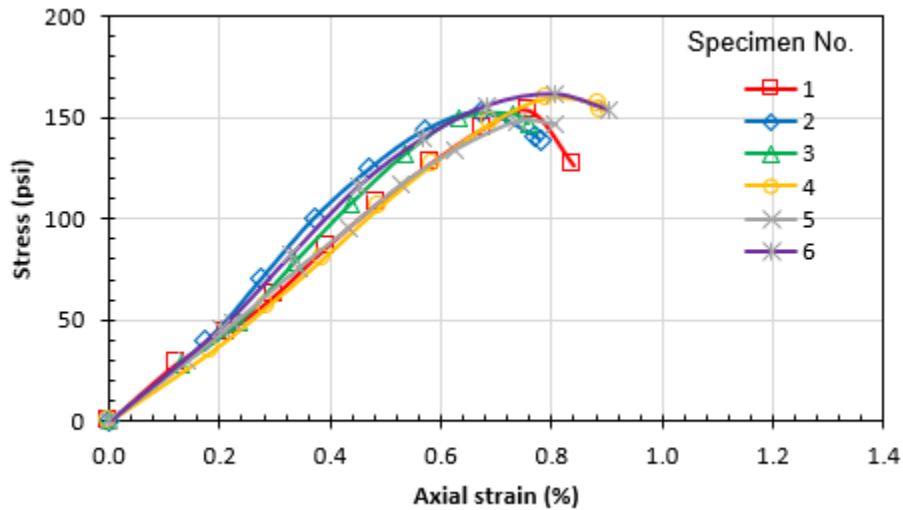


**Figure 4.12: Stress-strain curves of CMS at 5.5% cement after 48-hour curing for the Sedgwick County soil**

The specimens of Group 1 were microcracked by loading them to the ultimate UC strength after 48-hour curing time and then tested for the UC strength after a 2-hour waiting period. The UC tests of the second loading performed on failed or microcracked specimens from Group 1 showed the strength and modulus ( $E_{50}$ ) reductions by approximately 28% and 9%, respectively, as shown in Figure 4.13 and Table 4.9.

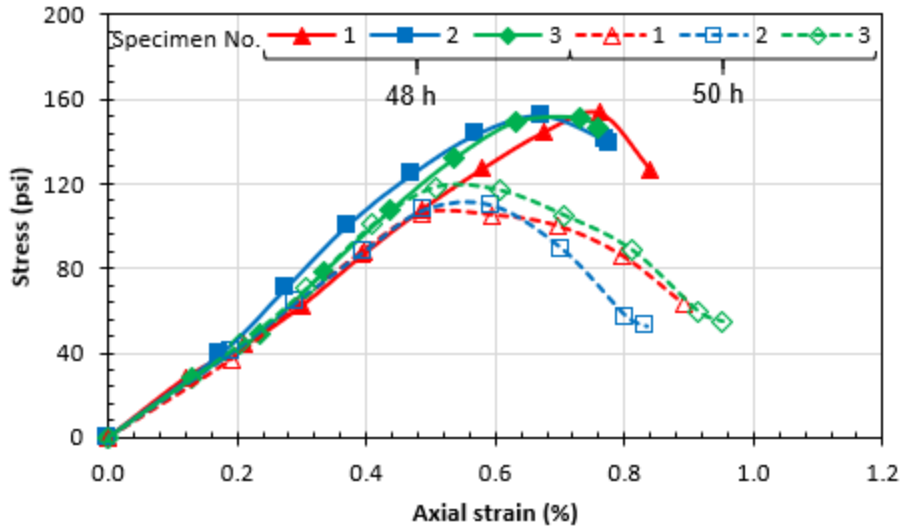


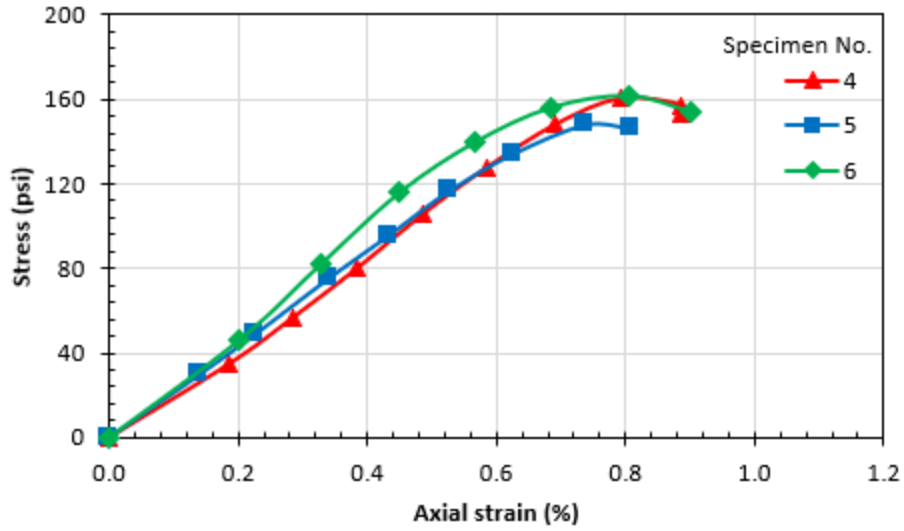
**Figure 4.13: Stress-strain curves before and after microcracking of CMS specimens in Group 1 for the Sedgwick County soil**

**Table 4.9: Unconfined compressive strengths and moduli of failed CMS specimens for the Sedgwick County soil subjected to second loading**

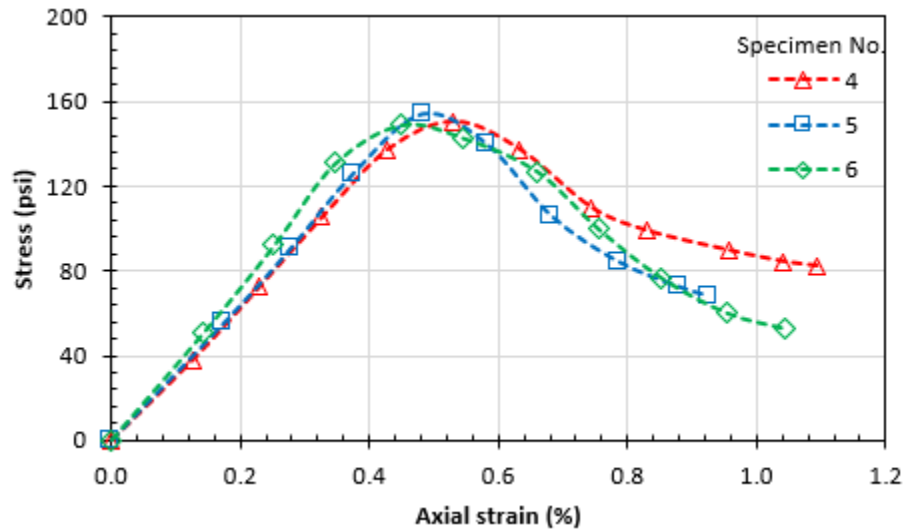
Group No.	Specimen No.	Specimen age	Compressive strength (psi)	Average strength (psi)	Modulus, $E_{50}$ (ksi)	Average modulus, $E_{50}$ (ksi)	Strength reduction	Modulus, $E_{50}$ reduction
Group 1	1	48 hours	154	153	21.7	23.4	28%	9%
	2		152		26.2			
	3		152		22.2			
Group 1	1	50 hours	106	111	20.4	21.3		
	2		110		21.2			
	3		118		22.5			

In Group 2, three UC specimens of the CMS were microcracked, and their stress-strain curves are shown in Figure 4.14(a). After the microcracking process, the specimens of Group 2 were returned to the moisture room to continue the curing process and to allow the specimens to gain strength. After 7-day curing, these specimens were tested for the UC strengths, and their stress-strain curves are presented in Figure 4.14(b). The average strength of these three CMS specimens was 151 psi. In other words, the 7-day UC strength of the microcracked specimens was approximately the same as the two-day UC strength of un-cracked specimens. Moreover, the 7-day UC strength of the microcracked specimens were 72% of the design strength of the CMS mix (i.e., 210 psi). Table 4.10 summarizes the UC strengths of the CMS specimens before and after microcracking for Group 2. Figure 4.15 shows the CMS specimen No. 4 of Group 2 before microcracking, after microcracking at 48-hour curing, and after UC testing at 7-day curing.

Table 4.11 shows the effects of the microcracks on the UC strength and modulus ( $E_{50}$ ) after the 7-day moist curing period. The un-cracked specimens of Mix No. 2 had a higher UC strength and a lower modulus (stiffness) than those of the microcracked specimens of Group 2. The average UC strength of the microcracked specimens was approximately 74% that of the un-cracked specimens. However, the microcracked specimens had moduli approximately the same as that of the un-cracked specimens even though the specimens were preloaded during the microcracking process. Furthermore, the modulus to strength ratio of the un-cracked specimens after 7-day curing was approximately 160, and that for the microcracked specimens increased to approximately 219. These results indicate that the presence of the microcracks made the specimen weaker but slightly stiffer.



(a)



(b)

**Figure 4.14: Stress-strain curves of CMS specimens at 5.5% cement in Group 2 for the Sedgwick County soil: (a) during the microcracking process after 2-day curing, and (b) after the microcracking process after 7-day curing**



**Table 4.10: UC strengths of CMS specimens before and after microcracking for the Sedgwick County soil**

Group No.	Specimen No.	Compressive strength (psi)	Average strength (psi)	Compressive strength (psi)	Average strength (psi)
Specimen age		48 hours		7 days	
Specimen Condition		After initial compaction		After microcracked	
Group 2	4	160	157	149	151
	5	148		154	
	6	162		150	

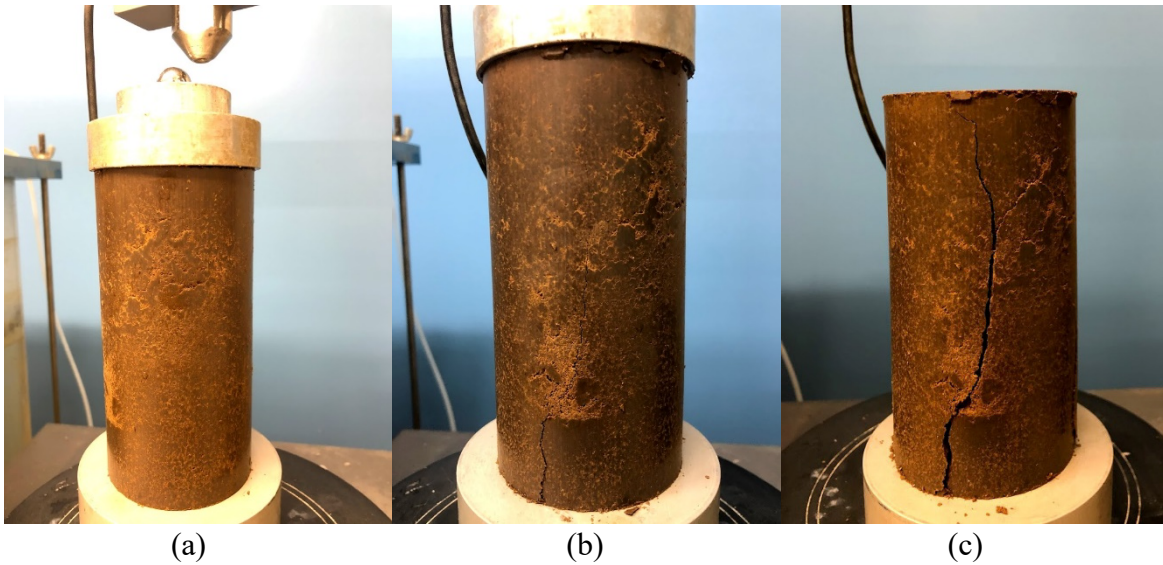


**Figure 4.15: CMS Specimen 4 of Group 2 for the Sedgwick County soil: (a) before microcracking, (b) after microcracking at 48-hour curing, and (c) after UC testing at 7-day curing**

**Table 4.11: Effects of microcracks in CMS specimens on the UC strength and modulus ( $E_{50}$ ) at 7-day curing for the Sedgwick County soil**

Specimen Condition	Specimen No.	Compressive strength (psi)	Average strength (psi)	Modulus, $E_{50}$ (ksi)	Average modulus, $E_{50}$ (ksi)	Modulus to strength ratio
Un-cracked specimens (Mix No. 2)	1	194	202	29.8	32.6	160
	2	200		32.7		
	3	211		35.0		
Microcracked specimens (Group 2)	4	149	151	35.8	33.1	219
	5	154		32.1		
	6	150		31.5		

# Chapter 5: Field Study

## 5.1 Electrical Resistivity

The effect of microcracking was evaluated in the field by measuring the in-situ resistivity before and after microcracking. The Wenner 4-pin method as described in ASTM Test Method G57 (2012) was used to evaluate the field electrical resistivity before and after microcracking along the South 87<sup>th</sup> Street site in Sedgwick County and another site located in Hutchinson, Kansas. The on-site soils stabilized at the Hutchinson site comprised of clayey sand with gravel, which is similar to the soil encountered along the Marion County site.

The 4-pin resistivity method developed by Wenner (1915), involves the use of 4 pins driven into the ground as shown in Figure 5.1. A current is applied to the outer pins, and the voltage between the inner pins is measured. The resistivity is a function of the current, voltage, and spacing of the electrodes (equal to the depth of the test).

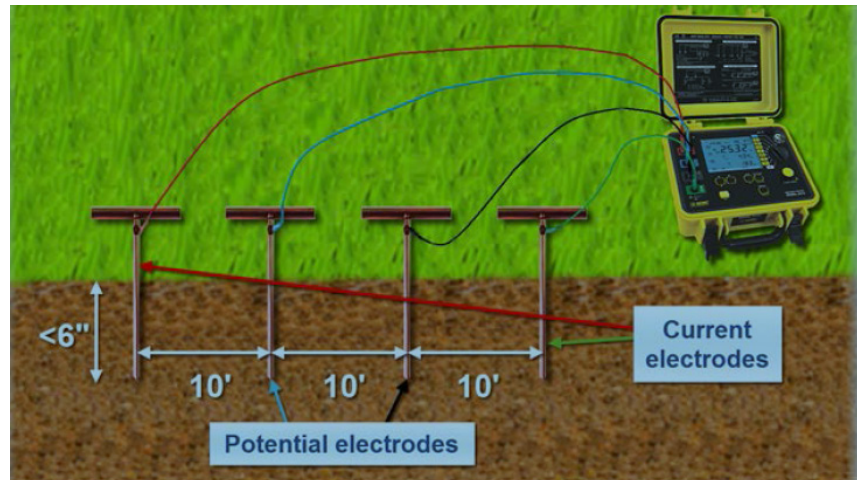


Figure 5.1: Typical Wenner 4-Pin Setup

The resulting equation is:

$$\rho = 2\pi \times a \times (\Delta\phi / I)$$

Equation 5.1

Where:

$\rho$  is the resistivity,

"a" is the spacing between the electrodes,

$\Delta\phi$  is the voltage, and

I is the applied current.

The current is usually applied using an instrument that supplies alternating current, otherwise polarization effects occur at the electrodes that can alter the reading. The field electrical resistivity results collected from S. 87<sup>th</sup> Street in Sedgwick County and the site in Hutchinson, KS, before and after microcracking are presented in Tables 5.1 and 5.2, respectively. The results presented in Tables 5.1 and 5.2 did not show a clear correlation between the electrical resistivity and the microcracking process. This result may indicate that the effect of microcracking on the electrical resistivity is within the accuracy of its measurement.

**Table 5.1: Field electrical resistivity before and after microcracking on the Sedgwick County site**

Site Location	GPS Coordinates (Latitude, Longitude)	Test Condition	Pin Spacing (cm)	Resistance (ohms)
S. 87 <sup>th</sup> Street Sedgwick County	37.533541, -97.210226	Before Microcracking	0.25	40.8
			0.5	19.3
			0.75	15.7
			1.0	11.1
		After Microcracking	0.25	4.5
			0.5	9.6
			0.75	8.6
			1.0	9.3
	37.533554, -97.212308	Before Microcracking	0.25	23.0
			0.5	19.1
			0.75	13.8
			1.0	10.2
After Microcracking		0.25	22.4	
		0.5	16.1	
		0.75	13.0	
		1.0	10.5	

**Table 5.2: Field electrical resistivity before and after microcracking on the Hutchinson site**

Site Location	GPS Coordinates (Latitude, Longitude)	Test Condition	Pin Spacing (cm)	Resistance (ohms)
Hutchinson, KS	Coordinates not available	Before Microcracking	0.25	17.63
			0.5	12.91
			0.75	8.48
			1.0	7.57
		After Microcracking	0.25	17.98
			0.5	12.89
			0.75	9.93
			1.0	8.14

## 5.2 Light Weight Deflectometer Test Results

The light weight deflectometer (LWD) test is a dynamic plate loading test that is typically used to determine the dynamic deformation modulus ( $E_{lwd}$ ) of soil. The test consists of the soil subjected to a pulse load applied via a disk-shaped steel plate or aluminum plate. The loading mechanism consists of a drop weight that falls along a rod and hits the top of the plate as shown in Figure 5.2. The LWD system is equivalent to a two degree of freedom (DOF) mass-spring-damper system during the loading and rebound until the moment that the impact load becomes zero, after which the system decouples. The LWD equipment used in this study is the Zorn ZFG 3.0 LWD. This test equipment does not have a load cell and assumes a constant applied load of 1.59 kips (7.07 kN) when the weight is dropped from a full height of 28.5 inches (0.724 m) on soils with different stiffness values. The rate of the movement at the center of the plate is recorded by a velocity sensor. The maximum displacement is calculated by means of single integrals of the velocity. The load history and peak load are estimated based on the mass and the drop height. The modulus determined by the LWD is calculated using Equation 5.2 based on the Bousinesq equation.

$$E = \frac{2k_s}{Ar_0} (1 - \nu^2)$$

Equation 5.2

Where:

$A$  is the stress distribution factor,

$\nu$  is the Poisson's ratio,

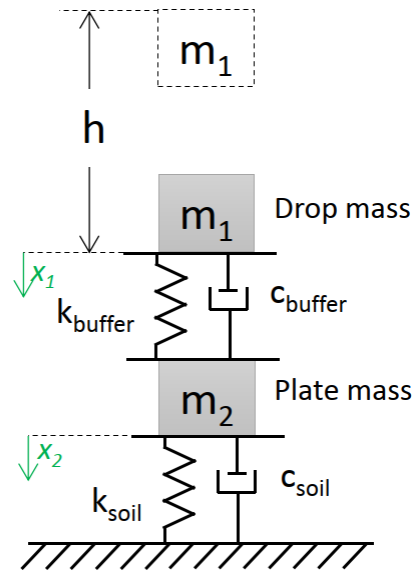
$k_s = \left| \frac{F_{peak}}{w_{peak}} \right|$ ,  $F_{peak}$  is the peak load,

$w_{peak}$  is the maximum displacement, and

$r_0$  is the plate radius.



(a)

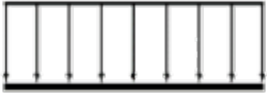
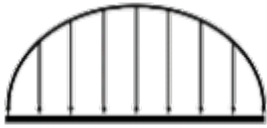



(b)

**Figure 5.2: The Zorn LWD device: (a) photo and (b) schematics of the LWD and subgrade system (two DOF)**

The previous equation assumes the subgrade to be isotropic, linearly elastic, and homogeneous semi-infinite continuum. Terzaghi, Peck, and Mesri (1996) defined the stress distribution under a plate as a function of plate rigidity and soil type. Table 5.3 denotes the stress distribution coefficients ( $A$ ) typical of different types of soils under the LWD plate.

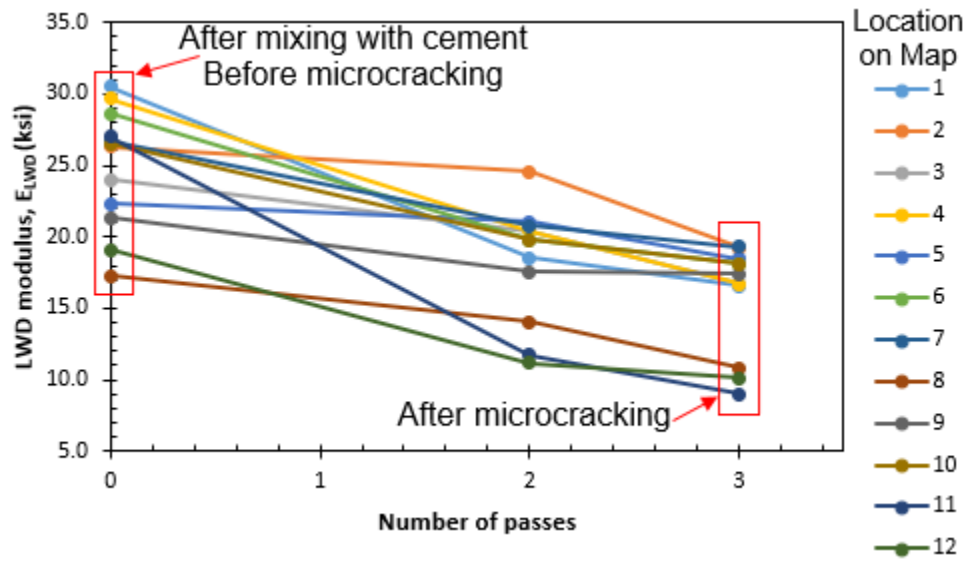
**Table 5.3: Stress distribution factors for different types of soil**

Soil Type	Factor ( $A$ )	Stress Distribution Shape
Uniform (mixed soil)	$\pi$	
Granular material (parabolic)	$3\pi/4$	
Cohesive (inverse parabolic)	4	

For both Marion County and Sedgwick County projects described earlier in Section 3.2.1, the LWD tests were performed along the test sections for these projects. Figure 5.3 shows the LWD test locations and results for Marion County. Figure 5.3(b) shows that the microcracking process, which was achieved by applying three passes of a roller compactor, reduced the dynamic modulus by approximately 17% to 67% as compared to that before microcracking. Figure 5.4 shows the LWD test locations and results for Sedgwick County. Figure 5.4(b) shows the effects of modifying the subgrade with 5.5% cement as the LWD modulus increased for all locations after mixing with cement. Also, Figure 5.4(c) demonstrates that microcracking reduced the dynamic moduli by approximately 22% to 56% as compared to those before microcracking.



(a)

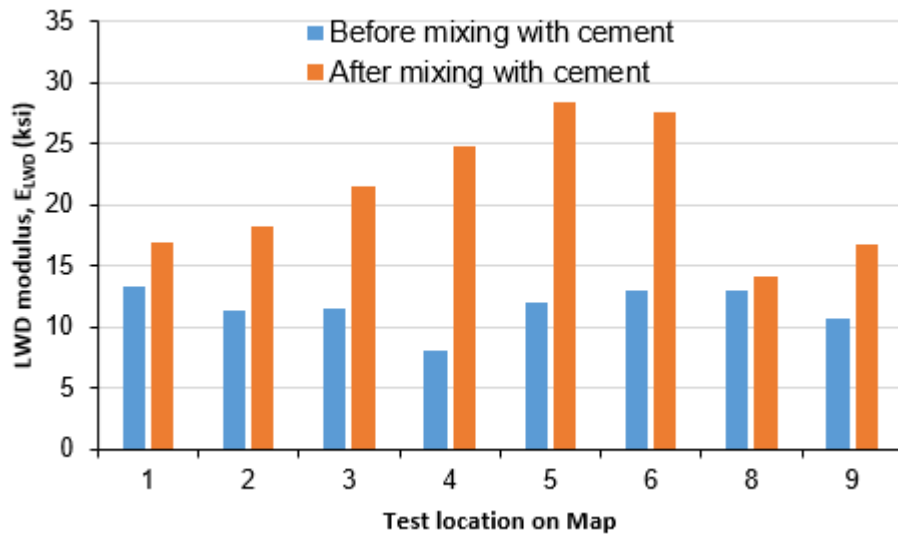


(b)

Figure 5.3: LWD tests conducted for the Marion County project: (a) testing locations and (b) effect of microcracking



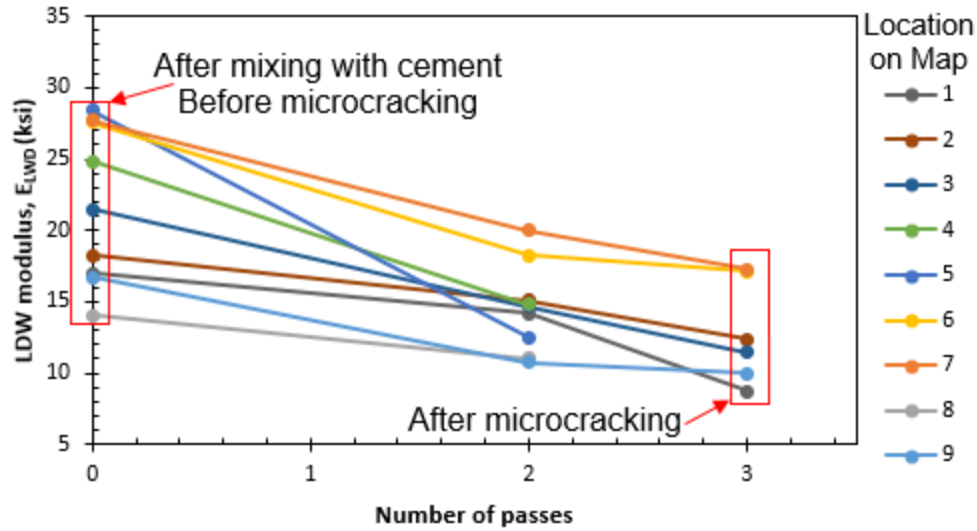
(a)



(b)

Figure 5.4: LWD tests conducted for the Sedgwick County project: (a) testing locations, (b) effect of cement, and (c) effect of microcracking





(c)

Figure 5.4: LWD tests conducted for the Sedgwick County project: (a) testing locations, (b) effect of cement, and (c) effect of microcracking (Continued)

### 5.3 Falling Weight Deflectometer (FWD) Field Testing

Flexible pavement performance is correlated with the pavement surface deflection, which can be measured by non-destructive test methods. The surface deflection and its corresponding nondestructive deflection testing equipment can be divided into three categories: steady-state deflection (Dynalect and Road Rater), static deflection (Benkelman Beam), and impact load deflection (Falling Weight Deflectometer). Recently, FWD testing is most commonly used to evaluate the pavement performance, identify potential problems, and calculate the pavement layer moduli and the subgrade resilient modulus, which can be used for estimating the pavement structural capacity. The components of an FWD system include: a hydraulic system, loading weight and plate, load cell, deflection sensors, and a control system.

The FWD test is conducted in the field by dropping a large weight onto a circular plate positioned on the pavement surface as shown in Figure 5.5. The plate diameter is 300 mm. This pulse load simulates the magnitude and duration of a rolling vehicle wheel and is measured with a load cell mounted on top of the loading plate. The pavement responses (surface deflections) due to the load are measured by a series of deflection sensors mounted at various distances from the

loading point. The sensor distances for the FWD tests conducted in this study were 0, 12, 18, 24, 36, 48, and 60 inches away from the center of the loading plate. The measured deflections at each sensor are called deflection basins.

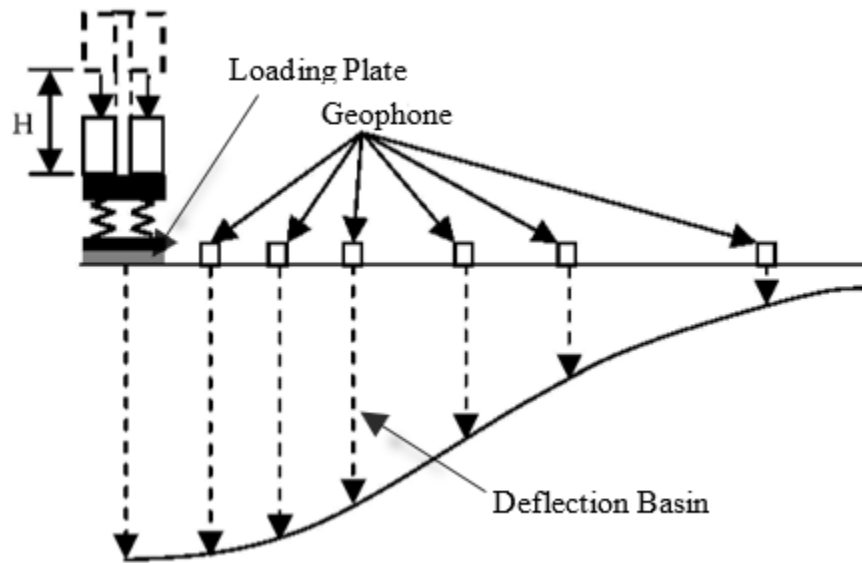


**Figure 5.5: Schematic of FWD and deflection basin**

The pavement surfaces along 87<sup>th</sup> Street in Sedgwick County and 330<sup>th</sup> Avenue in Marion County were tested using the FWD in the field by KDOT personnel on October 30<sup>th</sup> and October 31<sup>st</sup>, 2018, respectively. Jils FWD equipment was used at these two sites. The FWD testing was performed in accordance with the ASTM D4694-09 (2015), “Standard Test Method for Deflections with a Falling-Weight-Type Impulse Load Device,” and ASTM D4695-03 (2015), “Standard Guide for General Pavement Deflection Measurements.” The deflection tests consisted of one seating drop and three recording drops per test location. A test load of 9,000 pounds in accordance with the KDOT Specification was used. The FWD testing was performed at an interval of approximately 500 feet along each lane (eastbound and westbound) and approximately 100 feet in a staggered pattern for both lanes. The testing was divided into two sections, eastbound (EB) and westbound (WB) lanes. The testing length for each section was approximately 1 mile. Test locations were along the right wheel of the driving lane. A total of 103 testing points along the existing 87<sup>th</sup> Street (with 51 testing points at EB lane and 52 at WB lane) were performed. Also, a

total of 104 testing points along the existing 330<sup>th</sup> Avenue (with 52 testing points at EB lane and 52 at WB lane) were performed. The FWD test locations are shown in Table C.1 of Appendix C. Following the FWD testing survey, a total of eight pavement cores were obtained by KDOT personnel from each site. The thicknesses of the asphalt pavement identified from the collected pavement cores along 87<sup>th</sup> Street Sedgwick County and 330<sup>th</sup> Avenue Marion County were 2 and 3 inches, respectively. Note that the back-calculation procedure for FWD is sensitive and dependent on the thickness of the provided individual pavement layers. Subgrade visual classification was provided by Terracon.

### *5.3.1 FWD Analysis*

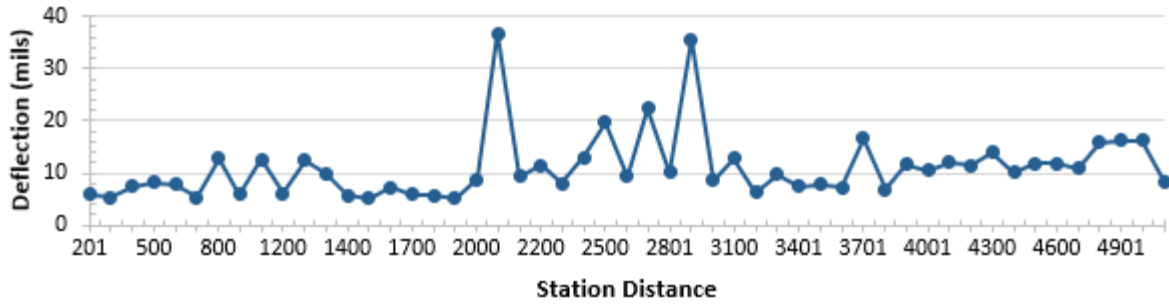
Back-calculation is an analysis method used for computing pavement layer moduli and the subgrade resilient modulus based on pavement deflection basins generated by FWD (Muench, Mahoney, & Pierce, 2003). The back-calculation process is started by assuming the initial moduli of pavement layers. The values are usually estimated based on the engineer's experience or equations. After assuming the initial layer moduli, pavement surface deflections can be calculated using pavement response models. The calculated deflections are then compared to the measured values. An iterative process is implemented by adjusting the pavement layer moduli to have a good match (within some tolerable error) between the measured and theoretical deflections. The back-calculation analyses were performed in this study using the AASHTO Back-Calculation Tool (BCT) to estimate the pavement layer moduli. This program was released on the AASHTOWare Pavement ME Design website ([www.me-design.com](http://www.me-design.com)) on July 2, 2018, and it utilizes the EVERCALC back-calculation engine.

A flexible pavement cross section was considered in the back-calculation BCT analyses including asphalt layer, cement-modified soil layer, and 2-ft compacted subgrade layer on top of an infinite half-space subgrade layer.

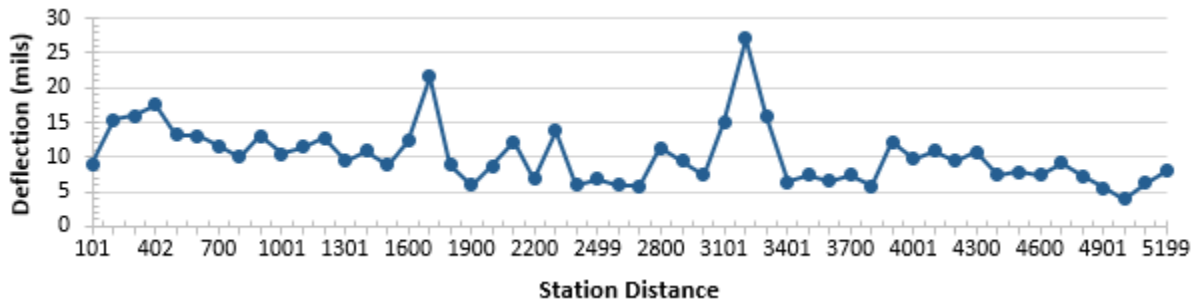
This approach is based on a recent publication by the Federal Highway Administration (FHWA) Publication No. FHWA-HRT-16-010 (Bruinsma, Vandenbossche, Chatti, & Smith, 2017). The study showed that a four-layer system with a 2-ft (0.6-m) compacted subgrade layer on top of an infinite half-space subgrade: (a) provided the lower root mean square (RMS) values

among other layer combinations considered, and (b) can be the most realistic design inputs for the MEPDG software.

Selected/typical seed, minimum, and maximum values for layer moduli as well as assumed Poisson's ratio values are presented in Figures 5.6 and 5.7 for 87<sup>th</sup> Street in Sedgwick County and 330<sup>th</sup> Avenue in Marion County, respectively. The back-calculated moduli with station locations for 87<sup>th</sup> Street in Sedgwick County and 330<sup>th</sup> Avenue in Marion County are presented in Figures 5.8 and 5.9, respectively. E(1), E(2), E(3), and E(4) in these two figures represent the moduli of the asphalt layer, the cement-modified soil layer, the compacted subgrade layer, and the native subgrade layer. The data for these figures for the EB lane and WB lane of 87<sup>th</sup> Street and 330<sup>th</sup> Avenue are summarized in Tables C.2 to C.3 and Tables C.4 to C.5, respectively, in Appendix C. Figures 5.8 and 5.9 show that there were some variations of the moduli at different stations for each layer, the asphalt layer had the moduli of approximately 10 times that of the cement-modified soil, and the compacted and native subgrade had similar moduli.



(a)



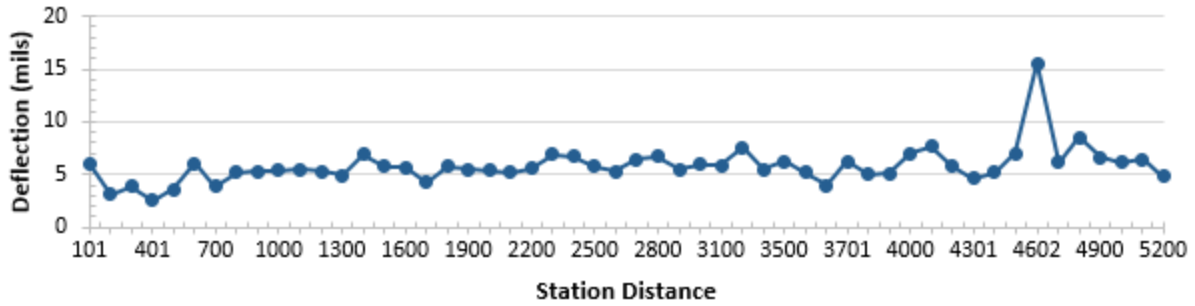
(b)

Number of Layers

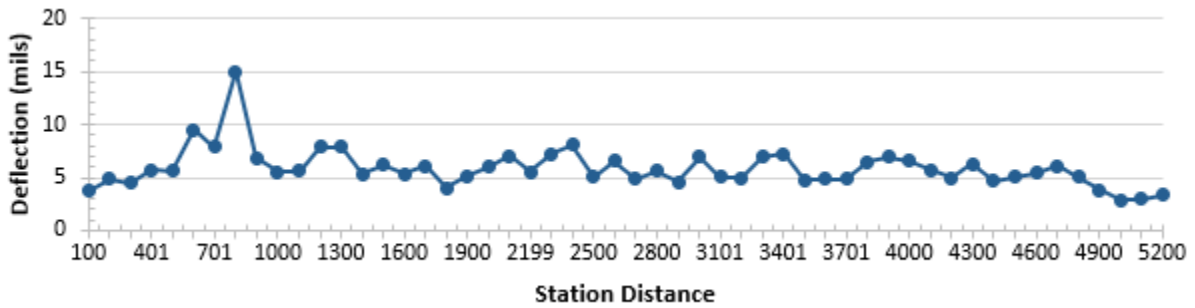
Layer	Layer Type	Layer Thickness (in)	Poisson's Ratio	Minimum Modulus (ksi)	Maximum Modulus (ksi)	Mean (Seed) Modulus (ksi)	Fixed
Layer 1	AC (AC)	2	0.35	400	4000	1000	<input type="checkbox"/>
Layer 2	Treated Base (Cement Treat)	10	0.35	20	500	100	<input type="checkbox"/>
Layer 3	Subgrade (Fine Grained)	24	0.45	1	50	15	<input type="checkbox"/>
Layer 4	Subgrade (Fine Grained)	0	0.45	1	100	15	<input type="checkbox"/>

(c)

**Figure 5.6: Measured deflections and inputs: (a) EB lane, (b) WB lane, and (c) input layer modulus and Poisson's ratio values for back-calculation of the 87<sup>th</sup> Street pavement in Sedgwick County**



(a)



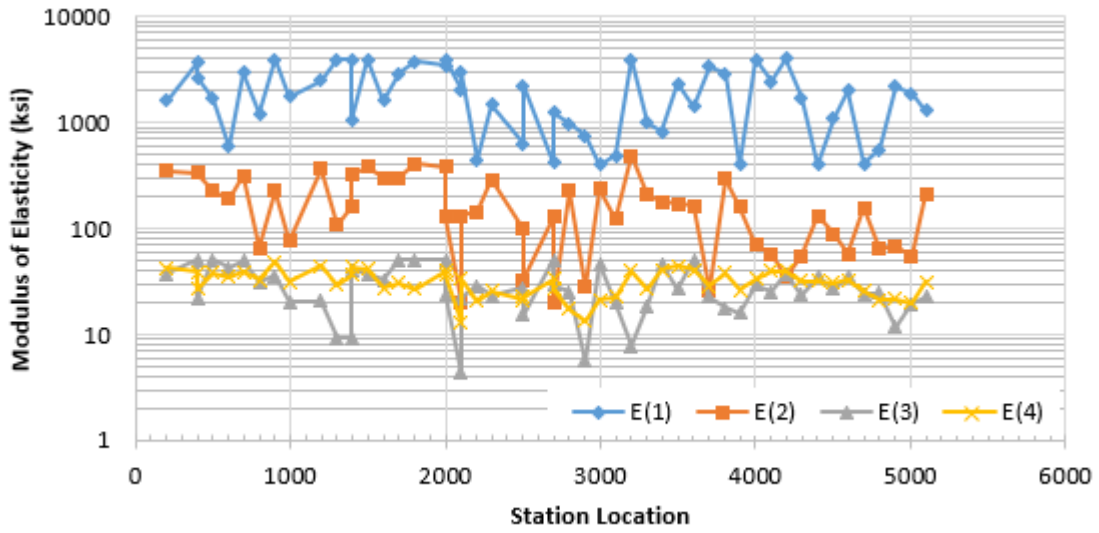
(b)

Number of Layers

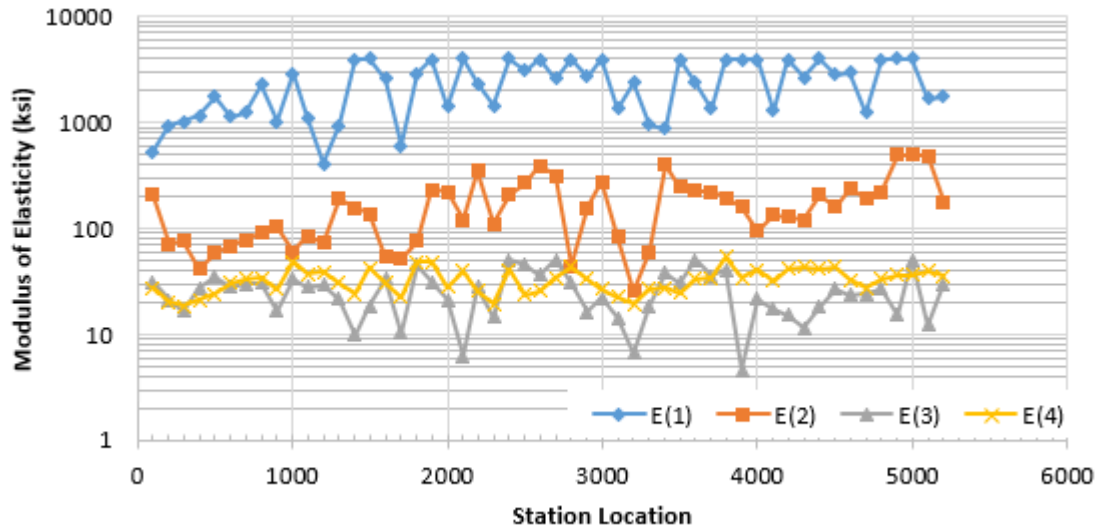
Layer	Layer Type	Layer Thickness (in)	Poisson's Ratio	Minimum Modulus (ksi)	Maximum Modulus (ksi)	Mean (Seed) Modulus (ksi)	Fixed
Layer 1	AC (AC)	3	0.35	200	4000	1000	<input type="checkbox"/>
Layer 2	Treated Base (Cement Treat	12	0.35	20	500	100	<input type="checkbox"/>
Layer 3	Subgrade (Fine Grained)	24	0.45	1	50	15	<input type="checkbox"/>
Layer 4	Subgrade (Fine Grained)	0	0.45	5	100	15	<input type="checkbox"/>

(c)

**Figure 5.7: Measured deflections and inputs: (a) EB lane, (b) WB lane, and (c) input layer modulus and Poisson's ratio values for back-calculation of the 330<sup>th</sup> Avenue pavement in Marion County**

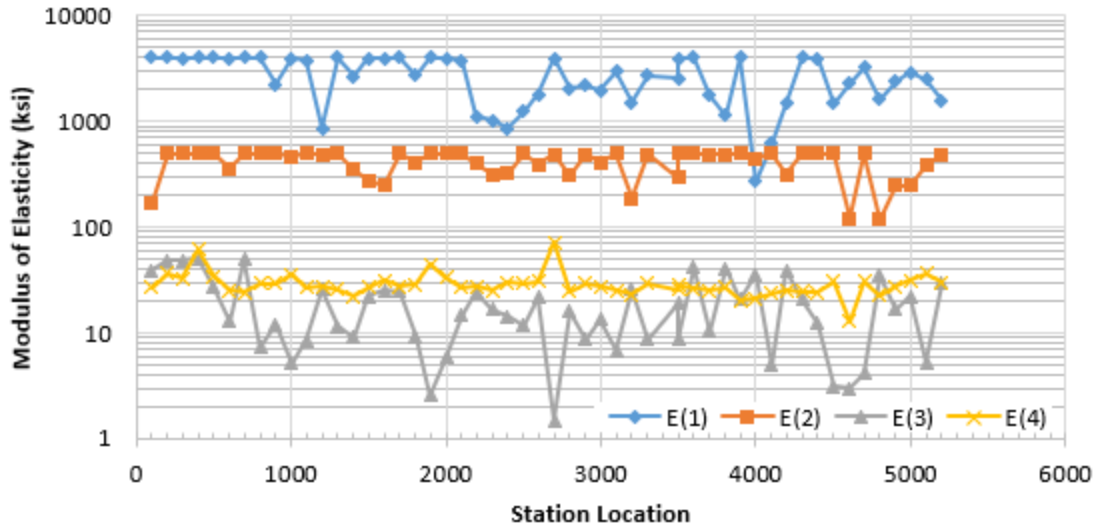


(a)

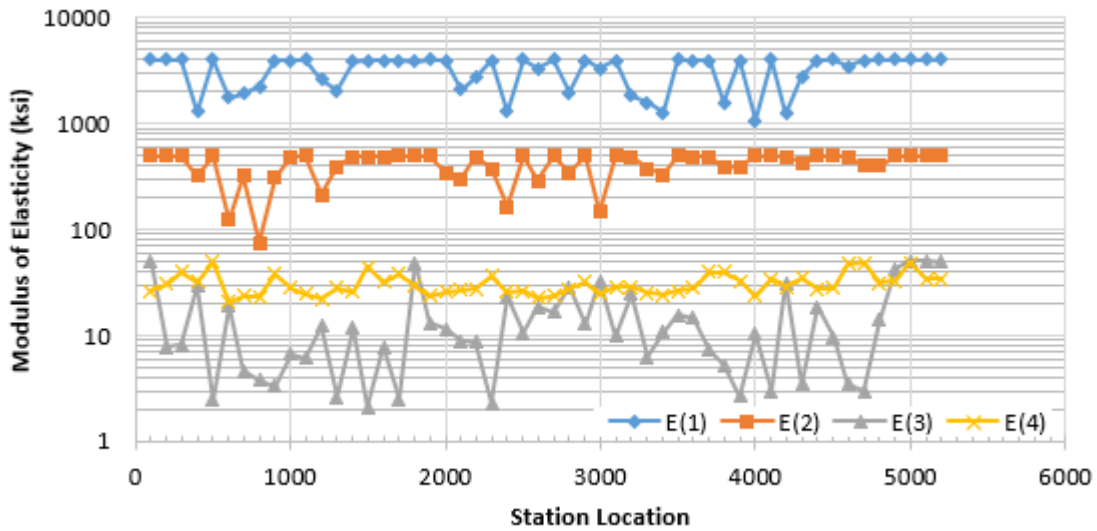


(b)

**Figure 5.8: Back-calculated modulus versus station locations along 87<sup>th</sup> Street in Sedgwick County: (a) EB lane and (b) WB lane**



(a)



(b)

Figure 5.9: Back-calculated modulus versus station locations along 330<sup>th</sup> Avenue (Marion County): (a) EB lane and (b) WB lane



## 5.4 Resilient Modulus Results

### 5.4.1 Laboratory Reconstituted Specimens

The resilient modulus results for the reconstituted specimens prepared in the lab at the desired cement contents are summarized in Tables C.6 through C.13. It is evident that the resilient modulus values increase with the confining pressure and the deviatoric stress. This result is consistent with that in Hanifa, Abu-Farsakh, and Gautreau (2015), i.e., higher confining stresses resulted in higher resilient moduli. The analysis of these test data will be presented later.

### 5.4.2 Field Core Specimens

Tables 5.4 through 5.7 summarize the resilient modulus data of the microcracked specimens cored from the field. The resilient modulus values,  $M_r$ , varied between 25 and 60 ksi. These  $M_r$  values fall within the range published by Hanifa et al. (2015). It is also obvious that the higher confining pressure resulted in the higher resilient modulus. The test data also show that the  $M_r$  values increased with the increase of the deviatoric stresses.

**Table 5.4: Resilient Modulus of Cracked CMS Specimen No. 1 Cored from Marion County**

Parameter	Chamber Confining Pressure	Actual Applied Cyclic Stress	Actual Applied Contact Stress	Resilient Modulus
Designation	S3	S <sub>cyclic</sub>	S <sub>contact</sub>	M <sub>r</sub>
Unit	psi	psi	psi	psi
Sequence 1	6	1.73	0.20	45,519
Sequence 2	6	3.50	0.40	49,939
Sequence 3	6	5.29	0.61	53,121
Sequence 4	6	7.10	0.81	55,842
Sequence 5	6	8.86	1.04	58,512
Sequence 6	4	1.73	0.19	35,901
Sequence 7	4	3.52	0.39	39,333
Sequence 8	4	5.30	0.60	42,490
Sequence 9	4	7.11	0.79	45,891
Sequence 10	4	8.88	1.00	49,619
Sequence 11	2	1.73	0.18	25,211
Sequence 12	2	3.53	0.37	28,097
Sequence 13	2	5.34	0.56	31,395
Sequence 14	2	7.13	0.77	34,843
Sequence 15	2	8.89	0.98	38,316

**Table 5.5: Resilient Modulus of Cracked CMS Specimen No. 2 Cored from Marion County**

Parameter	Chamber Confining Pressure	Actual Applied Cyclic Stress	Actual Applied Contact Stress	Resilient Modulus
Designation	S3	S <sub>cyclic</sub>	S <sub>contact</sub>	M <sub>r</sub>
Unit	psi	psi	psi	psi
Sequence 1	6	1.66	0.24	35,926
Sequence 2	6	3.38	0.44	39,188
Sequence 3	6	5.08	0.65	41,673
Sequence 4	6	6.77	0.87	44,381
Sequence 5	6	8.46	1.06	47,118
Sequence 6	4	1.67	0.20	33,680
Sequence 7	4	3.36	0.42	36,988
Sequence 8	4	5.08	0.63	39,414
Sequence 9	4	6.79	0.84	42,053
Sequence 10	4	8.51	1.04	44,891
Sequence 11	2	1.65	0.18	31,047
Sequence 12	2	3.36	0.39	33,824
Sequence 13	2	5.07	0.61	36,275
Sequence 14	2	6.81	0.81	38,811
Sequence 15	2	8.53	1.01	41,631

**Table 5.6: Resilient Modulus of Cracked CMS Specimen No. 4 Cored from Marion County**

Parameter	Chamber Confining Pressure	Actual Applied Cyclic Stress	Actual Applied Contact Stress	Resilient Modulus
Designation	S3	S <sub>cyclic</sub>	S <sub>contact</sub>	M <sub>r</sub>
Unit	psi	psi	psi	psi
Sequence 1	6	1.11	0.46	56,245
Sequence 2	6	2.69	0.69	57,179
Sequence 3	6	4.35	0.91	58,386
Sequence 4	6	6.02	1.14	60,316
Sequence 5	6	7.67	1.35	62,061
Sequence 6	4	1.25	0.43	45,306
Sequence 7	4	2.94	0.60	46,697
Sequence 8	4	4.65	0.78	48,346
Sequence 9	4	6.33	1.01	50,616
Sequence 10	4	8.00	1.22	52,780
Sequence 11	2	1.49	0.27	30,661
Sequence 12	2	3.17	0.47	33,788
Sequence 13	2	4.88	0.65	36,258
Sequence 14	2	6.54	0.88	39,021
Sequence 15	2	8.21	1.10	41,789

**Table 5.7: Resilient Modulus of Cracked CMS Specimen No. 6 Cored from Marion County**

Parameter	Chamber Confining Pressure	Actual Applied Cyclic Stress	Actual Applied Contact Stress	Resilient Modulus
<b>Designation</b>	<b>S3</b>	<b>S<sub>cyclic</sub></b>	<b>S<sub>contact</sub></b>	<b>M<sub>r</sub></b>
Unit	psi	psi	psi	psi
Sequence 1	6	1.73	0.21	48,821
Sequence 2	6	3.48	0.42	51,958
Sequence 3	6	5.24	0.63	52,523
Sequence 4	6	7.03	0.83	53,739
Sequence 5	6	8.80	1.03	55,144
Sequence 6	4	1.74	0.20	39,500
Sequence 7	4	3.52	0.40	42,085
Sequence 8	4	5.32	0.59	44,204
Sequence 9	4	7.07	0.81	46,185
Sequence 10	4	8.84	1.01	47,920
Sequence 11	2	1.71	0.20	28,768
Sequence 12	2	3.51	0.38	31,757
Sequence 13	2	5.33	0.58	34,143
Sequence 14	2	7.11	0.80	36,495
Sequence 15	2	8.88	1.00	38,737

#### 5.4.3 Effect of Microcracking on Resilient Modulus

This field study evaluated the effect of microcracking on the resilient modulus  $M_r$  values at a specific stress level: a bulk stress of approximately 10 psi and an octahedral shear stress of 1.89 psi as suggested by Christopher, Schwartz, and Boudreau (2019), using the MEPGD  $M_r$ -stress model presented in Equation 5.3:

$$M_r = k_1 P_a \left( \frac{\theta}{P_a} \right)^{k_2} \left( \frac{\tau_{oct}}{P_a} + 1 \right)^{k_3} \quad \text{Equation 5.3}$$

Where:

$M_r$  = resilient modulus,

$\theta$  = bulk stress,

$\sigma_1 + \sigma_2 + \sigma_3$ ,  $\sigma_1$  = major principal stress,

$\sigma_2$  = intermediate principal stress =  $\sigma_3$  for  $M_R$  tests on cylindrical specimens,

$\sigma_3$  = confining pressure,

$\tau_{oct}$  = octahedral shear stress =  $\frac{1}{3} \sqrt{(\sigma_1 - \sigma_2)^2 + (\sigma_1 - \sigma_3)^2 + (\sigma_2 - \sigma_3)^2}$ ,

$\sigma_1 - \sigma_3 = \sigma_d$  = deviator stress,

$P_a$  = normalizing stress (atmospheric pressure), and

$k_1, k_2, k_3$  = regression constants (obtained by fitting resilient modulus test data to the equation).

Model parameters and  $M_r$  values at the aforementioned stresses are summarized in Table 5.8 and plotted in Figures 5.10 through 5.12. The effect of microcracks on resilient modulus (at  $\theta = 10$  psi and  $\tau = 1.89$  psi) was observed on two selected specimens per soil. Figure 5.13 shows that the average  $M_r$  values of microcracked specimens were slightly higher than the corresponding  $M_r$  values of the uncracked specimens. This finding is consistent with the effect of microcracking on  $E_{50}$  as previously indicated based on the laboratory data. It should be noted that this finding is based on two replicates. Therefore, it is highly recommended that additional resilient modulus testing be conducted to better assess the effect of microcracking on the result of resilient modulus.

**Table 5.8: Resilient Modulus Test Characteristics**

Soil Samples No.	$k_1$	$k_2$	$k_3$	$R^2$	$M_r @ \theta = 10$ psi and $\tau = 1.89$ psi
Sedgwick Un-cracked 1	1,284	0.145	0.708	0.96	19,308
Sedgwick Un-cracked 4	1,360	0.126	1.271	0.94	22,055
Average	1,322	0.136	0.990	1	<b>20,681</b>
Sedgwick Cracked 2	1,579	0.259	0.805	0.93	22,991
Sedgwick Cracked 3	1,271	0.100	1.049	0.94	20,268
Average	1,425	0.180	0.927	1	<b>21,630</b>
Marion Un-cracked 1	1,539	0.064	1.319	0.98	25,712
Marion Un-cracked 2	1,580	0.238	0.884	0.89	23,422
Average	1,560	0.151	1.101	1	<b>24,567</b>
Marion Cracked 3	1,440	0.219	1.204	0.93	22,356
Marion Cracked 4	1,785	0.159	0.938	0.90	27,453
Average	1,612	0.189	1.071	1	<b>24,904</b>

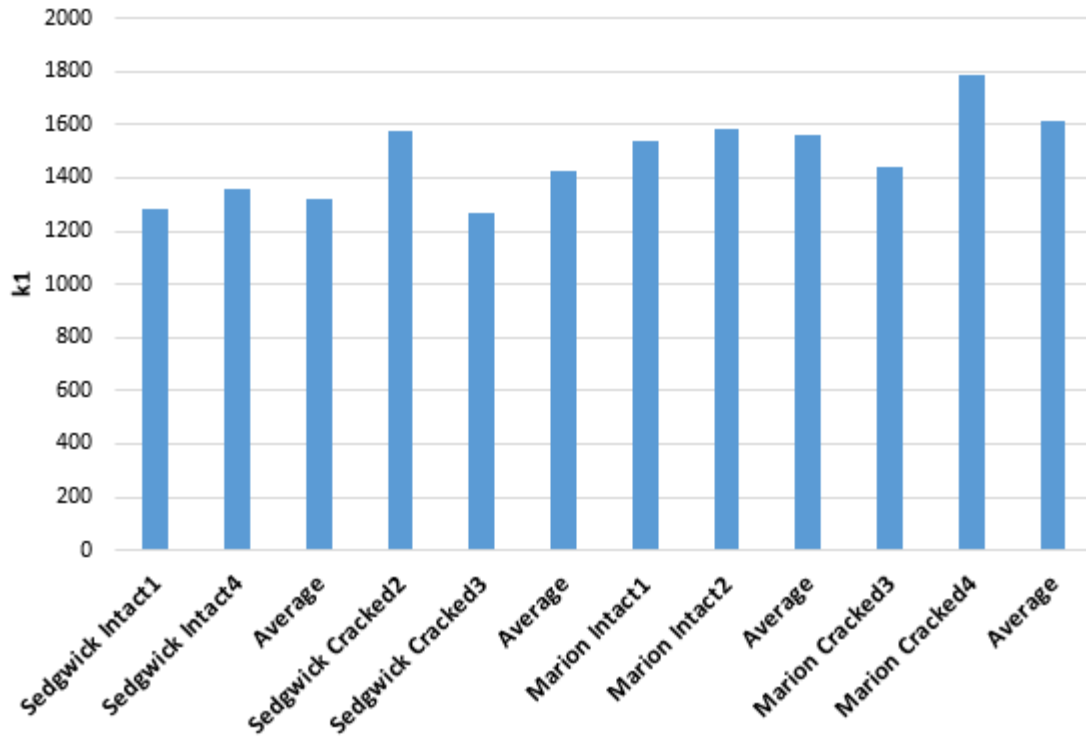


Figure 5.10:  $k_1$  Values

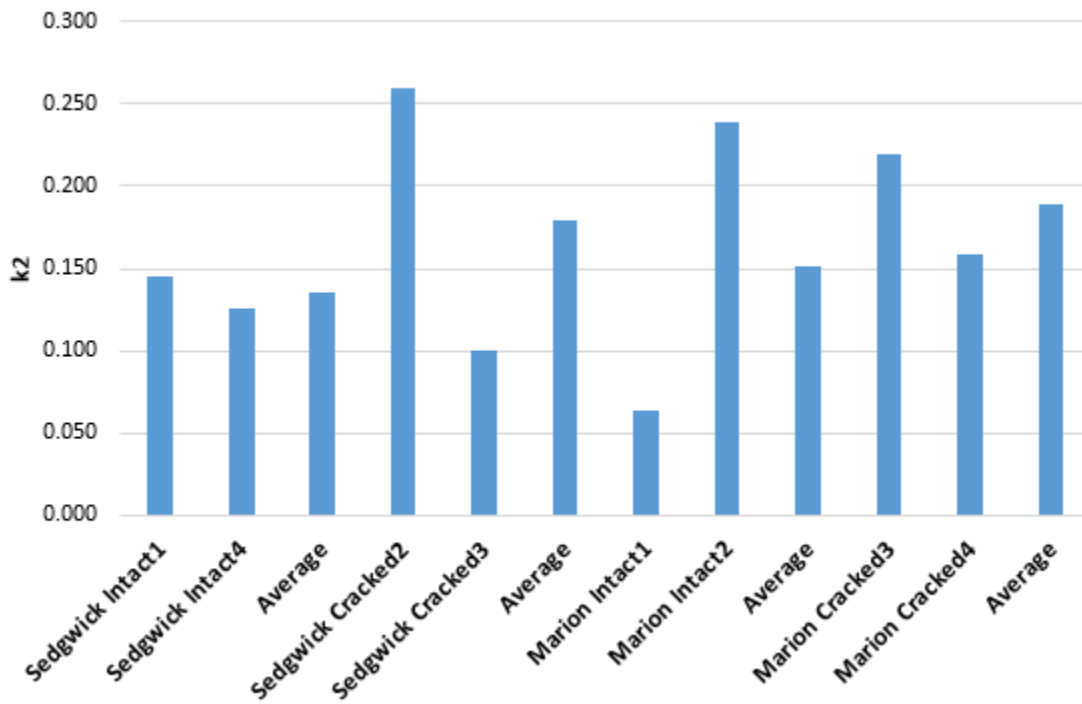


Figure 5.11:  $k_2$  Values

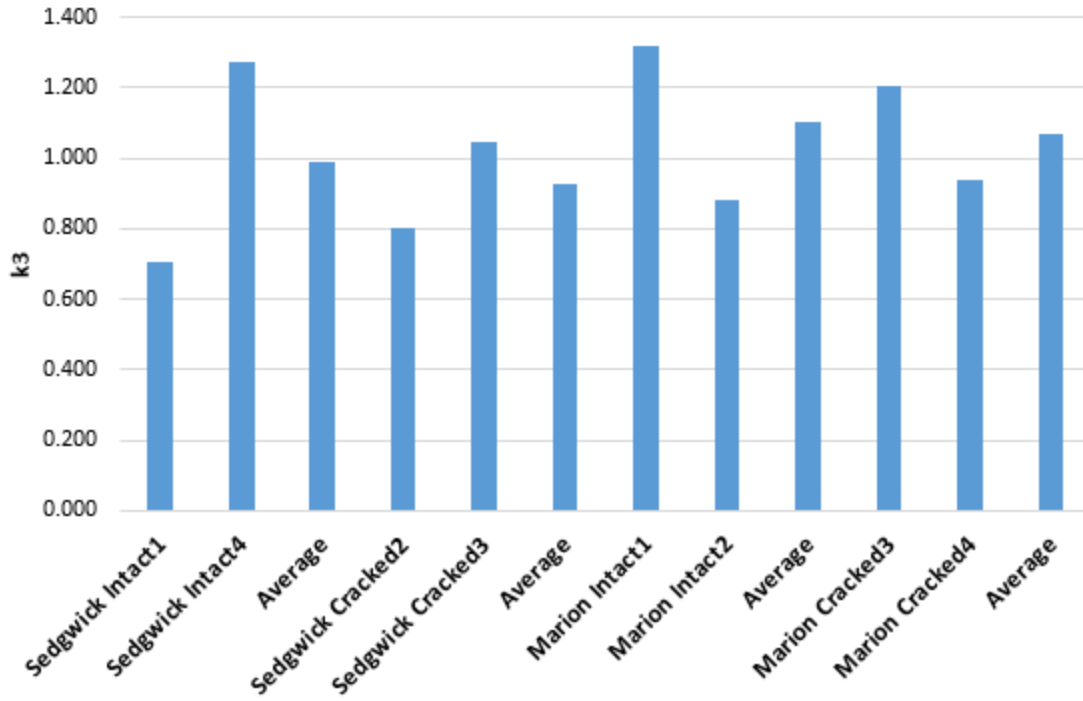


Figure 5.12:  $k_3$  Values

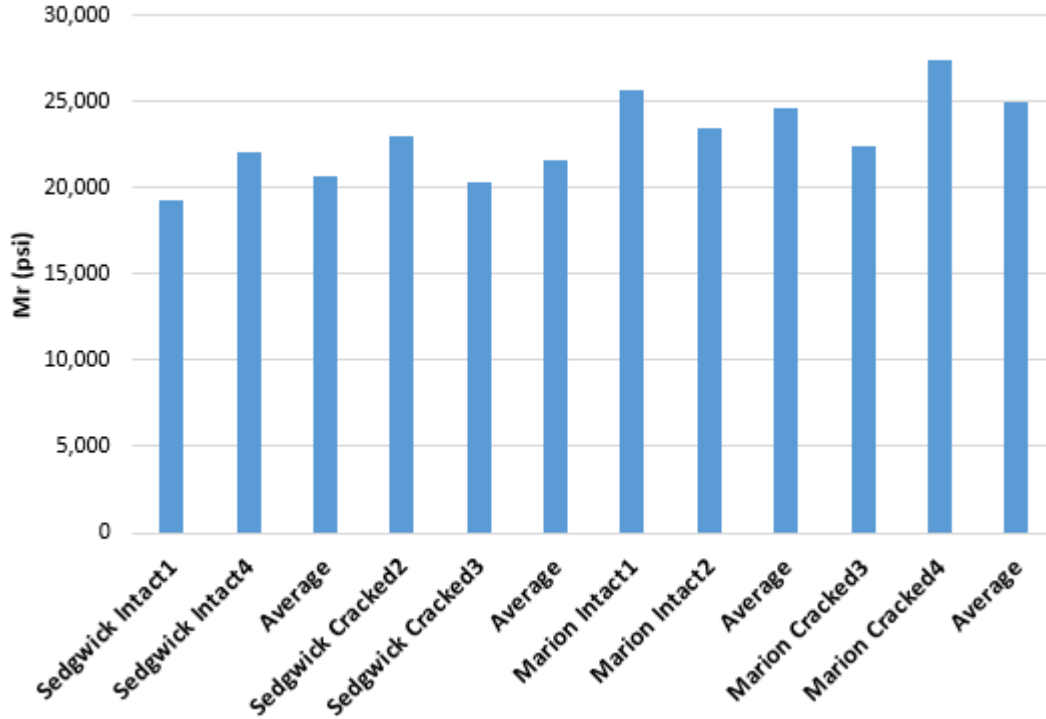


Figure 5.13: Resilient Moduli of the Remolded CMS Specimens for Sedgwick County and Marion County Soils

## Chapter 6: Conclusions and Recommendations

### 6.1 Conclusions

This study developed a laboratory procedure to simulate the microcracking process adopted in the field for cement-modified soil (CMS) subgrade. The developed procedure utilized unconfined compression (UC) test specimens, which were preloaded to different stress levels as compared with the unconfined compressive strength. It was found that when the preloading stress level was lower than the unconfined compressive strength, no microcrack was generated and their compressive strengths were not degraded. To generate microcracks, this study found that the preloading stress level must be equal to the unconfined compressive strength of the CMS specimen. The CMS specimens right after microcracking had UC strengths of approximately 50% of those before microcracking and moduli of approximately 42% of those before microcracking. However, the specimens microcracked after a 48-hour curing period had 70% of the strength of the un-cracked specimens at the same curing period and their moduli was approximately 150% of the moduli of the un-cracked specimens. The microcracked specimens had a modulus to strength ratio approximately two times the un-cracked specimens. Based on the finding from this research, it is recommended that to achieve a representative microcracking process in the laboratory, loading of a CMS specimen (cured for 48 hours) should continue past the peak compressive strength by less than 0.1% axial strain and then the load should be released to zero. The microcracked specimens should be returned to the curing room for further curing to a desired curing period. Furthermore, the microcracking effects on the hydraulic conductivity and electrical resistivity were evaluated. The laboratory results of the reconstituted specimen from Marion County showed that microcracking increased the hydraulic conductivity of the specimen and reduced its electrical resistivity when the specimen was saturated. However, at a saturation degree of less than 100, microcracking increased the specimen electrical resistivity. Light Weight Deflectometer (LWD) tests were conducted in the field before the subgrade mixed with cement, after mixed with cement, and after microcracking. The LWD results showed that adding cement increased the subgrade modulus. However, after applying three passes of roller compaction to generate the microcracks, the subgrade modulus dropped to approximately 40% its original value on average. In addition, resilient modulus ( $M_r$ ) tests were conducted on the reconstituted specimens with and without microcracks. Based on the average  $M_r$ , the  $M_r$  values of the microcracked specimens were slightly

higher than those of the uncracked specimens. This is consistent with the finding on the effect of microcracking on specimens moduli ( $E_{50}$ ) calculated from the UC tests (i.e., under static loading).

## 6.2 Recommendations

The following procedure is recommended to prepare and test a cement modified subgrade (CMS) specimen with microcracking:

1. Collect native soil from a project site.
2. Characterize the soil, such as gradation, soil type, maximum dry density, and optimum moisture content.
3. Based on the required unconfined compressive (UC) strength for the CMS for design, select a range of cement contents and prepare at least three UC specimens for each cement content to determine the desired cement content for the mix.
4. Using the desired cement content, prepare at least six UC specimens. Use half of the specimens for microcracking by following the procedure recommended in this study and use the rest of the specimens to determine the UC strength for uncracked CMS specimens.
5. To achieve a representative microcracking process in the laboratory, it is recommended that loading of the CMS specimen (cured for 48 hours) should continue past the peak compressive strength by less than 0.1% axial strain and then the load should be released to zero. The microcracked specimens should be returned to the moisture room for continuing curing.
6. Run UC tests on the uncracked and cracked CMS specimens after 7 days of moist curing. Determine the UC strengths and moduli ( $E_{50}$ ) for both uncracked and microcracked specimens and calculate the percentage reduction of the modulus and the modulus to strength ratio.
7. The estimated modulus reduction from the laboratory can be used as a reference for the light weight deflectometer (LWD) tests to evaluate the modulus reduction of the subgrade required to achieve microcracking in field.



## References

- AASHTO T 307. (1999). *Determining the resilient modulus of soils and aggregate materials*. Washington, DC: American Association of State Highway and Transportation Officials.
- ASTM D422-63(2007)e2. (2007). *Standard test method for particle-size analysis of soils* (Withdrawn 2016). West Conshohocken, PA: ASTM International. doi: 10.1520/D0422-63R07E02, [www.astm.org](http://www.astm.org)
- ASTM D559 / D559M-15. (2015). *Standard test methods for wetting and drying compacted soil-cement mixtures*. West Conshohocken, PA: ASTM International. doi: 10.1520/D0559\_D0559M-15, [www.astm.org](http://www.astm.org)
- ASTM D698-12e2. (2012). *Standard test methods for laboratory compaction characteristics of soil using standard effort (12 400 ft-lbf/ft<sup>3</sup> (600 kN-m/m<sup>3</sup>))*. West Conshohocken, PA: ASTM International. doi: 10.1520/D0698-12E02, [www.astm.org](http://www.astm.org)
- ASTM D1632-17. (2017). *Standard practice for making and curing soil-cement compression and flexure test specimens in the laboratory*. West Conshohocken, PA: ASTM International. doi: 10.1520/D1632-17, [www.astm.org](http://www.astm.org)
- ASTM D1633-17. (2017). *Standard test methods for compressive strength of molded soil-cement cylinders*. West Conshohocken, PA: ASTM International. doi: 10.1520/D1633-17, [www.astm.org](http://www.astm.org)
- ASTM D1883-16. (2016). *Standard test method for California Bearing Ratio (CBR) of laboratory-compacted soils*. West Conshohocken, PA: ASTM International. doi: 10.1520/D1883-16, [www.astm.org](http://www.astm.org)
- ASTM D2487-17. (2017). *Standard practice for classification of soils for engineering purposes (Unified Soil Classification System)*. West Conshohocken, PA: ASTM International. doi: 10.1520/D2487-17, [www.astm.org](http://www.astm.org)
- ASTM D4318-17e1. (2017). *Standard test methods for liquid limit, plastic limit, and plasticity index of soils*. West Conshohocken, PA: ASTM International. doi: 10.1520/D4318-17E01, [www.astm.org](http://www.astm.org)

- ASTM D4694-09. (2015). *Standard test method for deflections with a falling-weight-type impulse load device*. West Conshohocken, PA: ASTM International. doi: 10.1520/D4694-09R15, [www.astm.org](http://www.astm.org)
- ASTM D4695-03. (2015). *Standard guide for general pavement deflection measurements*. West Conshohocken: PA: ASTM International. doi: 10.1520/D4695-03R15, [www.astm.org](http://www.astm.org)
- ASTM D5084-16a. (2016). *Standard test methods for measurement of hydraulic conductivity of saturated porous materials using a flexible wall permeameter*. West Conshohocken, PA: ASTM International. doi: 10.1520/D5084-16A, [www.astm.org](http://www.astm.org)
- ASTM G57-06. (2012). *Standard test method for field measurement of soil resistivity using the Wenner four-electrode method*. West Conshohocken, PA: ASTM International. doi: 10.1520/G0057-06R12, [www.astm.org](http://www.astm.org)
- Bofinger, H. E. (1971). The behaviour of soil-cement pavements with special reference to the problem of cracking. In *Proceedings of the 4th Asian Regional Conference on Soil Mechanics and Foundation Engineering, July 1971, Bangkok, Thailand* (pp. 355–360).
- Bofinger, H. E., Hassan, H. O., & Williams, R. I. T. (1978). *The shrinkage of fine-grained soil-cement* (Supplementary Report 398). Crowthorne, Berkshire, England: Transport and Road Research Laboratory.
- Brandl, H. (1999). Mixed-in-place stabilization of pavement structures with cement and additives. In *Geotechnical engineering for transportation infrastructure: Theory and practice, planning and design, construction and maintenance: Proceedings of the Twelfth European Conference on Soil Mechanics and Geotechnical Engineering, Amsterdam, Netherlands, 7-10 June 1999* (pp. 1473–1481). Rotterdam, Netherlands: A.A. Balkema.
- Bruinsma, J. E., Vandenbossche, J. M., Chatti, K., & Smith, K. D. (2017). *Using falling weight deflectometer data with mechanistic-empirical design and analysis, Volume II: Case study reports* (Report No. FHWA-HRT-16-010). Washington, DC: Federal Highway Administration.
- Christopher, B. R., Schwartz, C., & Boudreau, R. (2006). *Geotechnical aspects of pavements reference manual* (Report No. FHWA-NHI-05-037). Retrieved from <https://www.fhwa.dot.gov/engineering/geotech/pubs/05037/05c.cfm>

- Das, B. M. (1990). *Principles of foundation engineering*. Boston, MA: PWS-Kent Publishing Company.
- George, K. P. (1968a). *Final report on the study of criteria for strength and shrinkage control of cement-treated bases*. University, MS: University of Mississippi.
- George, K. P. (1968b). Shrinkage characteristics of soil-cement mixtures. *Highway Research Record*, 255, 42–58.
- George, K. P. (1969). Cracking in pavements influenced by viscoelastic properties of soil-cement. *Highway Research Record*, 263, 47–59.
- George, K. P. (1973). Mechanism of shrinkage cracking of soil-cement bases. *Highway Research Record*, 442, 1–10.
- George, K. P. (2001). *Soil stabilization field trial, Interim Report I* (Report No. FHWA/MS-DOT-RD-01-133). University, MS: University of Mississippi.
- Han, J. (2015). *Principles and practice of ground improvement*. Hoboken, NJ: John Wiley and Sons.
- Hanifa, K., Abu-Farsakh, M. Y., & Gautreau, G. P. (2015). *Design values of resilient modulus for stabilized and non-stabilized base* (Report No. FHWA/LA.14/521). Baton Rouge, LA: Louisiana Transportation Research Center.
- Litzka, J. & Haslehner, W. (1995). Cold in-place recycling on low-volume roads in Austria. In *Sixth International Conference on Low-Volume Roads, Minneapolis, Minnesota, June 25-29, 1995, Conference Proceedings* (pp. 189–194). Washington, DC: Transportation Research Board.
- Muench, S. T., Mahoney, J. P., & Pierce, L. M. (2003). *WSDOT pavement guide interactive*. Olympia, WA: Washington State Department of Transportation.
- Muhunthan, B., & Sariosseiri, F. (2008). *Interpretation of geotechnical properties of cement treated soils* (Report No. WA-RD 715.1). Olympia, WA: Washington State Department of Transportation.
- National Cooperative Highway Research Program (NCHRP). (2004). *Guide for mechanistic-empirical design of new and rehabilitated pavement structures*. Washington, DC: Author.

- Portland Cement Association (PCA). (2003). *Reflective cracking in cement stabilized pavements* (Publication IS537). Skokie, IL: Author.
- Scullion, T. (2002). Precracking of soil-cement bases to reduce reflection cracking: Field investigation. *Transportation Research Record, 1787*, 22–30.
- Sebesta, S. (2005). Use of microcracking to reduce shrinkage cracking in cement-treated bases. *Transportation Research Record, 1936*, 2–11.
- Simpson, A. L., Schmalzer, P. N., & Rada, G. R. (2007). *Long term pavement performance project laboratory materials testing and handling guide* (Report No. FHWA-HRT-07-052). McLean, VA: Federal Highway Administration.
- Terzaghi, K., Peck, R. B., & Mesri, G. (1996). *Soil mechanics in engineering practice* (3rd ed.). New York, NY: John Wiley & Sons.
- US Department of the Army. (1992). Soil stabilization for roads and airfields. In *Military soils engineering*, Field Manual 5-410 (Chapter 9). Washington, DC: Headquarters, Department of the Army. Retrieved from [http://faculty.unlv.edu/mjnicho/military\\_soils\\_fm5\\_410.pdf](http://faculty.unlv.edu/mjnicho/military_soils_fm5_410.pdf)
- Vanapalli, S. K., Fredlund, D. G., & Pufahl, D. E. (1999). The influence of soil structure and stress history on the soil-water characteristics of a compacted till. *Géotechnique, 49*(2), 143–159.
- Wenner, F. (1915). *A method of measuring earth resistivity* (Scientific Paper 258). Washington, DC: National Bureau of Standards.

# Appendix A: Properties of Cement

<b>Cement Mill Test Report</b>	
Month of Issue:      April-19	
Plant:	Sugar Creek Plant
Product:	Portland Cement Type I-II (MH)
Shipped:	Mar-19
Manufactured:	Mar-19

The current version of ASTM C 150 and AASHTO M 85 Standard Requirements

CHEMICAL ANALYSIS			PHYSICAL ANALYSIS		
Item	Spec limit	Test Result	Item	Spec limit	Test Result
Rapid Method, X-Ray (C 114)			Air content of mortar (%) (C 185)		
SiO <sub>2</sub> (%)	—	20.3		12 max	8
Al <sub>2</sub> O <sub>3</sub> (%)	6.0 max	4.7	Blaine Fineness (m <sup>2</sup> /kg) (C 204)		
Fe <sub>2</sub> O <sub>3</sub> (%)	6.0 max	3.0		260 - 430	363
CaO (%)	—	63.6	-325 (%) (C 430)		
MgO (%)	6.0 max	1.5		—	97.3
SO <sub>3</sub> (%)	3.0 max *	3.2	Autoclave expansion (%) (C 151)		
Loss on Ignition (%)	3.5 max	2.4		0.80 max	-0.02
Insoluble residue (%)	1.5 max	0.38	Compressive strength (PSI) (C 109)		
CO <sub>2</sub> (%)	—	1.5			
Limestone (%)	5.0 max	3.7			
CaCO <sub>3</sub> in Limestone (%)	70 min	92			
Adjusted Potential Phase Composition (C 150)					
C <sub>3</sub> S (%)	—	53			
C <sub>2</sub> S (%)	—	18			
C <sub>3</sub> A (%)	8 max	7			
C <sub>4</sub> AF (%)	—	9			
C <sub>3</sub> S+4.75*C <sub>3</sub> A (%)	100 max	88			
Heat of hydration, 3 Day (C1702) Cal/g					
	—	68.9			
ASTM C 150-16 and AASHTO M 85-16 Optional Chemical Requirements:					
NaEq (%)	0.60 max	0.55			

\* May exceed 3.0% SO<sub>3</sub> maximum based on our C 1038 results of <0.02% expansion at 14 days.

We certify that the above described cement meets the chemical and physical requirements of Type I and Type II (MH) for the current version of ASTM C 150 & AASHTO M 85 STANDARD.

Sugar Creek Plant  
2200 N Courtney Rd.  
Sugar Creek, MO 64050  
816-257-3608

Certified By:

  
Paul Engel - Quality Coordinator

Figure A.1: Cement properties used in Marion County

# Cement Mill Test Report

Month of Issue: April-19

Plant: Sugar Creek Plant  
Product: Portland Cement Type I-II (MH)  
Shipped: Mar-19  
Manufactured: Mar-19

The current version of ASTM C 150 and AASHTO M 85 Standard Requirements

## Base Cement Phase Composition

Item	Test Result
C3S (%)	55
C2S (%)	19
C3A (%)	8
C4AF (%)	10

We certify that the above described cement meets the chemical and physical requirements of Type I and Type II (MH) for the current version of ASTM C 150 & AASHTO M 85 STANDARD.

Sugar Creek Plant  
2200 N Courtney Rd.  
Sugar Creek, MO 64050  
816-257-3608

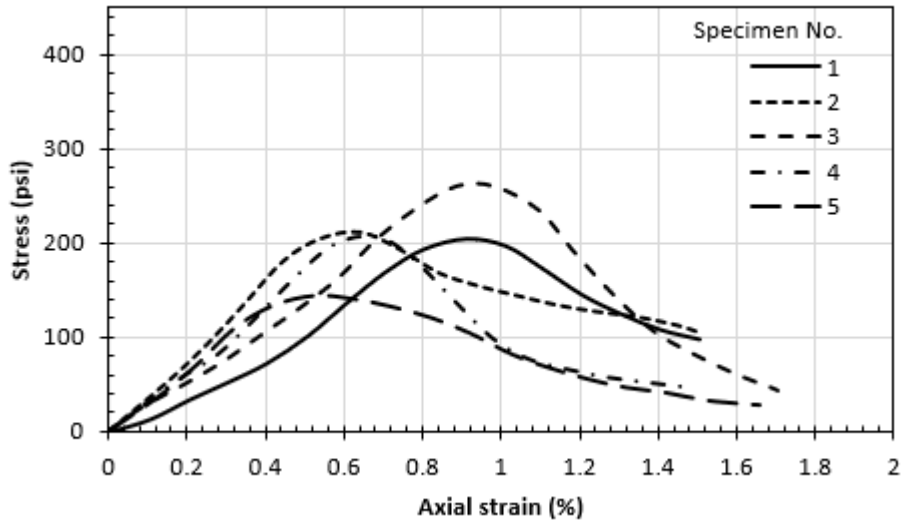
Certified By:



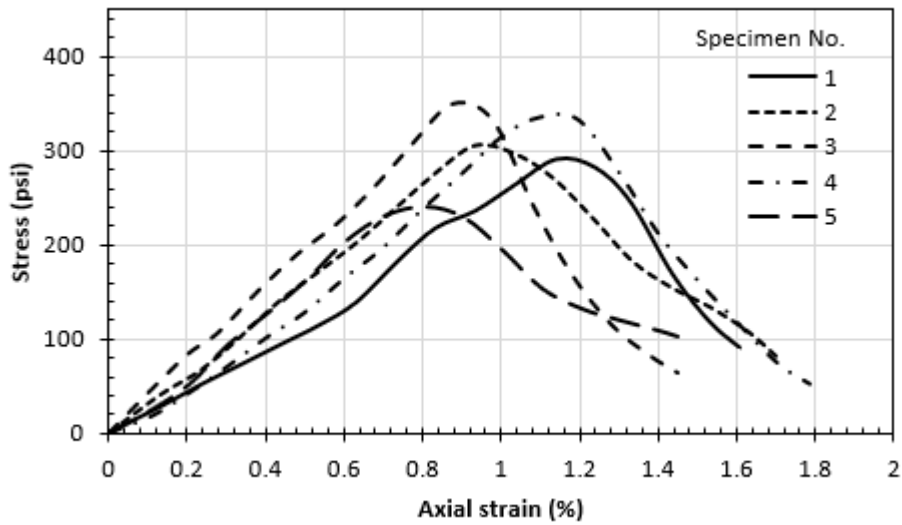
Paul Engel - Quality Coordinator

Figure A.1: Cement properties used in Marion County (Continued)

## Appendix B: Additional Figures Related to Chapter 4

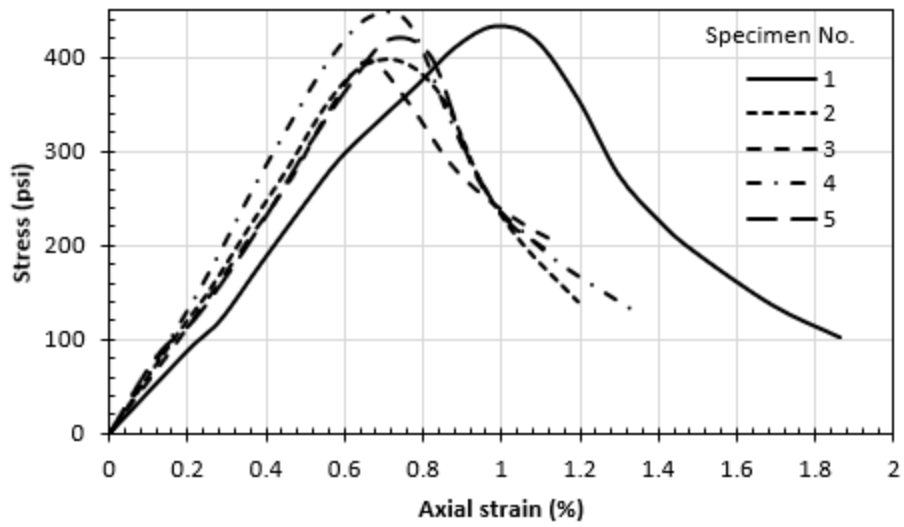


(a)



(b)

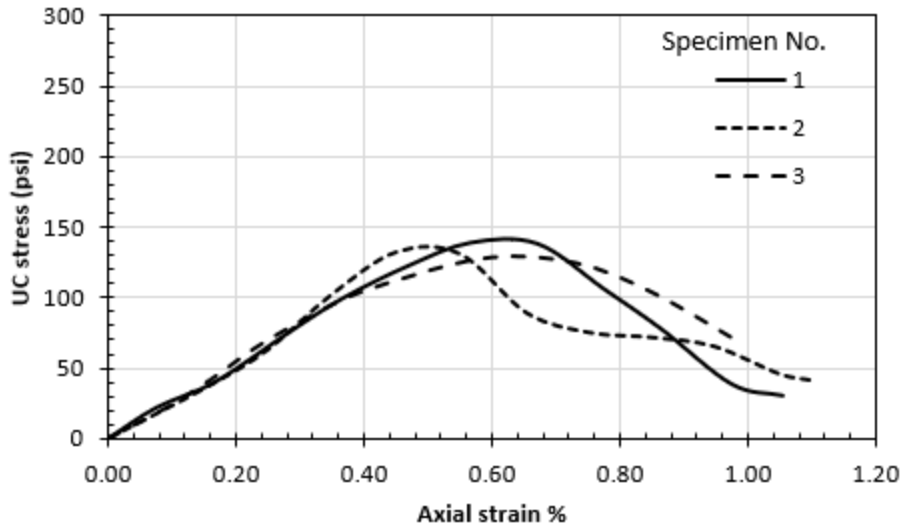
Figure B.1: Stress-strain curves of CMS specimens of Marion County after 7-day curing at cement contents: (a) 3.5%, (b) 5.0%, and (c) 6.5%



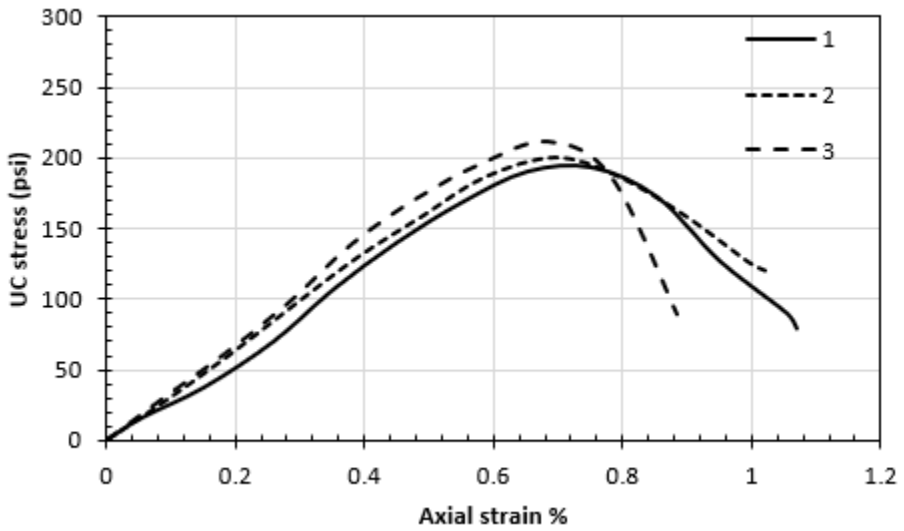
(c)

**Figure B.1: Stress-strain curves of CMS specimens of Marion County after 7-day curing at cement contents: (a) 3.5%, (b) 5.0%, and (c) 6.5% (Continued)**



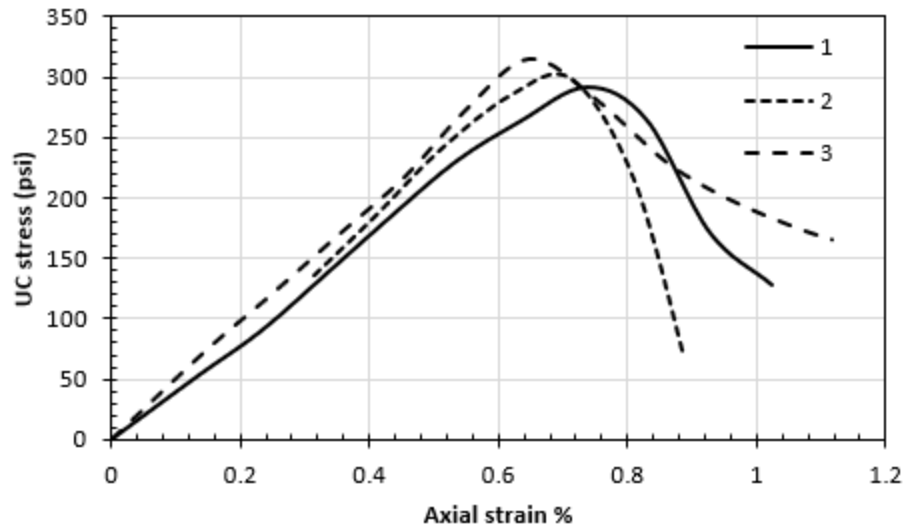


(a)



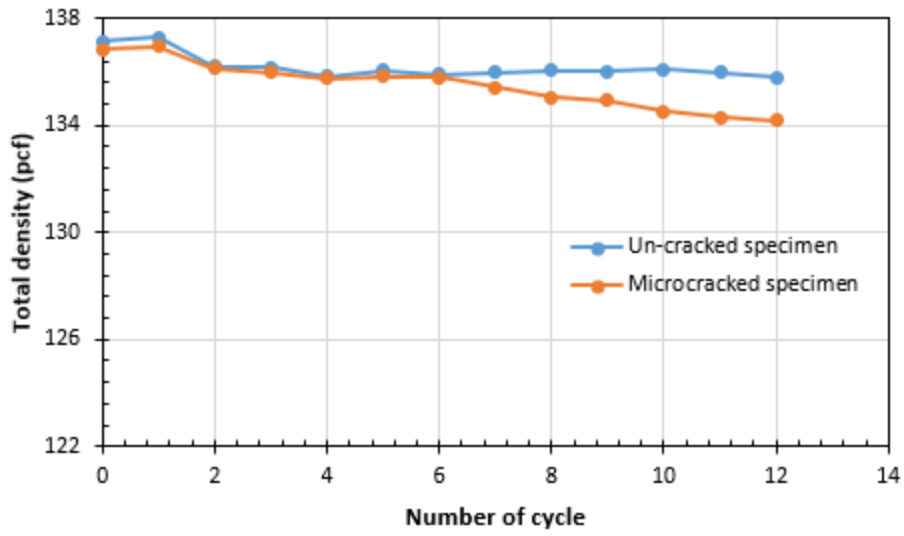
(b)

**Figure B.2: Stress-strain curves of CMS specimens of Sedgwick County after 7-day curing at cement contents: (a) 4.0%, (b) 5.5%, and (c) 7.0%**

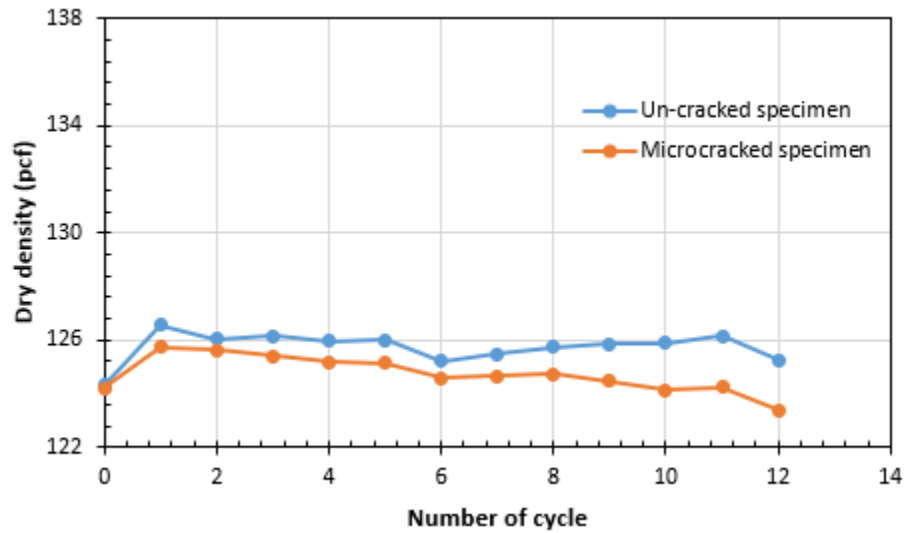


(c)

**Figure B.2: Stress-strain curves of CMS specimens of Sedgwick County after 7-day curing at cement contents: (a) 4.0%, (b) 5.5%, and (c) 7.0% (Continued)**



(a)



(b)

Figure B.3: Density variation during the wet-dry cycles (a) total density after wet cycles and (b) dry density after dry cycles

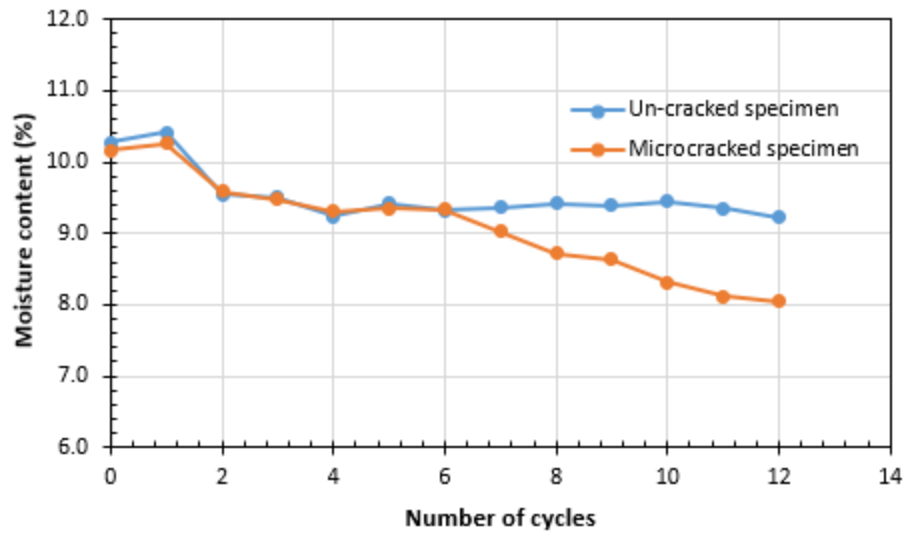


**Figure B.4: Moisture variation after wet cycles**

## Appendix C: Data Related to Chapter 5

**Table C.1: GPS coordinated for the FWD testing**

87 <sup>th</sup> Street, Sedgwick County				330 <sup>th</sup> Avenue, Marion County			
EB		WB		EB		WB	
Latitude	Longitude	Latitude	Longitude	Latitude	Longitude	Latitude	Longitude
37.320208	-97.135203	37.320208	-97.135203	38.330736	-97.200582	38.330778	-97.189935
37.320205	-97.134792	37.320133	-97.125116	38.330744	-97.200377	38.330768	-97.190142
37.320203	-97.134797	37.320141	-97.125322	38.330734	-97.200169	38.330777	-97.190350
37.320203	-97.134591	37.320131	-97.125525	38.330741	-97.199959	38.330764	-97.190558
37.320190	-97.134388	37.320140	-97.125728	38.330731	-97.199752	38.330772	-97.190764
37.320192	-97.134183	37.320131	-97.125935	38.330742	-97.199544	38.330759	-97.190971
37.320183	-97.133978	37.320140	-97.126137	38.330731	-97.199338	38.330769	-97.191180
37.320187	-97.133770	37.320140	-97.126137	38.330742	-97.199125	38.330758	-97.191388
37.320178	-97.133565	37.320140	-97.126137	38.330733	-97.198916	38.330769	-97.191597
37.320184	-97.133565	37.320140	-97.126137	38.330744	-97.198711	38.330759	-97.191804
37.320184	-97.133565	37.320140	-97.126756	38.330734	-97.198502	38.330770	-97.192013
37.320184	-97.133565	37.320140	-97.126756	38.330745	-97.198292	38.330760	-97.192221
37.320184	-97.133565	37.320140	-97.126756	38.330735	-97.198086	38.330768	-97.192427
37.320184	-97.133565	37.320140	-97.126756	38.330746	-97.197877	38.330760	-97.192637
37.320184	-97.133565	37.320140	-97.126756	38.330736	-97.197665	38.330769	-97.192847
37.320184	-97.133565	37.320140	-97.126756	38.330747	-97.197458	38.330758	-97.193056
37.320184	-97.133565	37.320140	-97.126756	38.330737	-97.197251	38.330768	-97.193264
37.320184	-97.133565	37.320140	-97.126756	38.330746	-97.197047	38.330758	-97.193470
37.320184	-97.133565	37.320140	-97.126756	38.330736	-97.196840	38.330768	-97.193679
37.320167	-97.131290	37.320140	-97.126756	38.330751	-97.196630	38.330756	-97.193889
37.320167	-97.131290	37.320140	-97.126756	38.330741	-97.196426	38.330756	-97.193889
37.320167	-97.131290	37.320161	-97.129015	38.330750	-97.196216	38.330756	-97.193889
37.320167	-97.131290	37.320161	-97.129015	38.330741	-97.196008	38.330756	-97.193889
37.320167	-97.131290	37.320161	-97.129015	38.330751	-97.195802	38.330756	-97.193889
37.320167	-97.131290	37.320161	-97.129015	38.330741	-97.195595	38.330756	-97.193889
37.320167	-97.131290	37.320161	-97.129015	38.330751	-97.195386	38.330756	-97.193889
37.320167	-97.131290	37.320161	-97.129015	38.330741	-97.195176	38.330756	-97.193889
37.320167	-97.131290	37.320169	-97.130256	38.330751	-97.194967	38.330756	-97.193889
37.320167	-97.131290	37.320169	-97.130256	38.330741	-97.194759	38.330763	-97.195767
37.320167	-97.131290	37.320168	-97.130874	38.330752	-97.194552	38.330763	-97.195767
37.320167	-97.131290	37.320182	-97.131080	38.330743	-97.194343	38.330763	-97.195767
37.320167	-97.131290	37.320176	-97.131284	38.330754	-97.194136	38.330763	-97.195767
37.320167	-97.131290	37.320188	-97.131488	38.330743	-97.193928	38.330763	-97.195767
37.320167	-97.131290	37.320180	-97.131696	38.330745	-97.193512	38.330763	-97.195767
37.320167	-97.131290	37.320192	-97.131899	38.330745	-97.193511	38.330763	-97.195767

87 <sup>th</sup> Street, Sedgwick County				330 <sup>th</sup> Avenue, Marion County			
EB		WB		EB		WB	
Latitude	Longitude	Latitude	Longitude	Latitude	Longitude	Latitude	Longitude
37.320167	-97.131290	37.320184	-97.132106	38.330756	-97.193303	38.330763	-97.195767
37.320167	-97.131290	37.320194	-97.132311	38.330745	-97.193094	38.330763	-97.195767
37.320167	-97.131290	37.320185	-97.132515	38.330757	-97.192881	38.330763	-97.195767
37.320167	-97.131290	37.320198	-97.132720	38.330746	-97.192677	38.330763	-97.195767
37.320167	-97.131290	37.320191	-97.132926	38.330757	-97.192471	38.330763	-97.195767
37.320167	-97.131290	37.320204	-97.133130	38.330746	-97.192263	38.330763	-97.195767
37.320167	-97.131290	37.320198	-97.133336	38.330756	-97.192053	38.330763	-97.195767
37.320112	-97.126565	37.320209	-97.133539	38.330745	-97.191843	38.330763	-97.195767
37.320112	-97.126564	37.320200	-97.133745	38.330753	-97.191635	38.330763	-97.195767
37.320108	-97.126157	37.320213	-97.133949	38.330744	-97.191425	38.330763	-97.195767
37.320117	-97.125931	37.320206	-97.134153	38.330755	-97.191216	38.330763	-97.195767
37.320117	-97.125931	37.320218	-97.134360	38.330745	-97.191009	38.330763	-97.195767
37.320120	-97.125602	37.320213	-97.134565	38.330757	-97.190802	38.330763	-97.195767
37.320109	-97.125330	37.320226	-97.134773	38.330747	-97.190592	38.330763	-97.195767
37.320119	-97.125126	37.320222	-97.134976	38.330760	-97.190384	38.330763	-97.195767
37.320119	-97.125126	37.320234	-97.135181	38.330750	-97.190177	38.330763	-97.195767
		37.320227	-97.135387	38.330762	-97.189968	38.330763	-97.195767

**Table C.2: Back-calculated modulus versus station location at 87<sup>th</sup> Street EB lane in Sedgwick County**

Station No.	HMA Thickness (in)	Treated Base Thickness (in)	Surface Temperature (°F)	Asphalt	Base	2-ft Subgrade	Infinite Subgrade
				E(1) (ksi)	E(2) (ksi)	E(3) (ksi)	E(4) (ksi)
201	2.0	10.0	69.4	1606	349	37	42
401	2.0	10.0	65.9	3658	333	50	39
401	2.0	10.0	66.2	2633	333	22	27
502	2.0	10.0	71	1687	224	50	38
602	2.0	10.0	66.8	586	191	42	35
702	2.0	10.0	69	2940	316	49	39
803	2.0	10.0	69.4	1222	66	32	32
898	2.0	10.0	70.6	3954	228	36	48
998	2.0	10.0	69.5	1742	77	20	32
1199	2.0	10.0	61.1	2492	366	21	44
1299	2.0	10.0	64.6	3896	108	9	29
1399	2.0	10.0	62.2	3954	159	9	36
1399	2.0	10.0	61	1038	325	41	44
1500	2.0	10.0	63.8	3909	379	38	42
1600	2.0	10.0	61.3	1604	298	33	28
1700	2.0	10.0	63	2876	302	50	31
1800	2.0	10.0	65.3	3727	411	50	27
2001	2.0	10.0	63.4	3460	383	50	40
2001	2.0	10.0	63.5	3909	129	24	36
2101	2.0	10.0	64.9	2051	20	4	13
2101	2.0	10.0	63.6	2938	131	22	34
2202	2.0	10.0	63.7	447	143	29	21
2302	2.0	10.0	63.9	1467	289	23	26
2497	2.0	10.0	63.7	633	100	28	21
2497	2.0	10.0	63.2	2223	33	15	23
2698	2.0	10.0	66.1	417	128	50	33
2698	2.0	10.0	65.9	1233	20	29	27

Station No.	HMA Thickness (in)	Treated Base Thickness (in)	Surface Temperature (°F)	Asphalt	Base	2-ft Subgrade	Infinite Subgrade
				E(1) (ksi)	E(2) (ksi)	E(3) (ksi)	E(4) (ksi)
2798	2.0	10.0	63.8	973	225	25	17
2899	2.0	10.0	65.5	743	28	6	13
2999	2.0	10.0	67.4	400	236	46	21
3099	2.0	10.0	66.2	487	124	20	23
3200	2.0	10.0	65.8	3909	489	8	39
3300	2.0	10.0	65.1	995	208	19	27
3400	2.0	10.0	66.7	828	180	47	41
3501	2.0	10.0	68	2330	171	27	44
3601	2.0	10.0	68.6	1412	164	50	41
3701	2.0	10.0	67	3385	26	23	29
3802	2.0	10.0	68.8	2892	292	18	38
3902	2.0	10.0	64.8	400	159	16	26
4002	2.0	10.0	68.2	3909	69	30	33
4103	2.0	10.0	67	2418	58	25	40
4198	2.0	10.0	67.1	4000	35	37	40
4298	2.0	10.0	67.7	1711	55	24	32
4404	2.0	10.0	68.2	401	132	35	32
4499	2.0	10.0	66.8	1092	88	27	30
4599	2.0	10.0	67.4	2007	57	35	33
4699	2.0	10.0	66.2	409	157	24	26
4800	2.0	10.0	66.1	549	65	25	21
4900	2.0	10.0	66.8	2195	69	12	22
5005	2.0	10.0	67.6	1895	55	19	20
5100	2.0	10.0	66.1	1294	212	23	31
2798	2.0	10.0	63.8	973	225	25	17
<b>Average</b>	<b>2.00</b>	<b>10.00</b>	<b>65.98</b>	<b>2018</b>	<b>180</b>	<b>29</b>	<b>31</b>
<b>St dev</b>	<b>0.00</b>	<b>0.00</b>	<b>2.39</b>	<b>1241</b>	<b>122</b>	<b>13</b>	<b>8</b>
<b>COV</b>	<b>0.00</b>	<b>0.00</b>	<b>3.62</b>	<b>61</b>	<b>68</b>	<b>46</b>	<b>27</b>



**Table C.3: Back-calculated modulus versus station location at 87<sup>th</sup> Street WB lane in Sedgwick County**

Station No.	HMA Thickness (in)	Treated Base Thickness (in)	Surface Temperature (°F)	Asphalt	Base	2-ft Subgrade	Infinite Subgrade
				E(1) (ksi)	E(2) (ksi)	E(3) (ksi)	E(4) (ksi)
101	2.0	10.0	64.8	527	208	31.5	27.3
201	2.0	10.0	67.4	939	72	21.4	20.1
301	2.0	10.0	67.2	1008	77	16.8	18.6
402	2.0	10.0	67.6	1159	41	27.2	21.0
500	2.0	10.0	67.8	1761	59	34.8	24.1
600	2.0	10.0	68.7	1140	69	28.1	30.9
700	2.0	10.0	67.2	1227	79	30.0	33.6
800	2.0	10.0	67.4	2280	91	30.4	34.4
900	2.0	10.0	70	1012	104	16.7	27.0
1001	2.0	10.0	69.7	2925	60	33.6	48.7
1101	2.0	10.0	67.7	1118	84	27.8	37.6
1200	2.0	10.0	68.5	408	73	29.2	39.2
1301	2.0	10.0	68.5	927	191	21.6	30.6
1400	2.0	10.0	70.3	3909	156	9.9	24.0
1501	2.0	10.0	69	4000	137	18.5	42.0
1600	2.0	10.0	71.5	2577	54	33.1	30.5
1700	2.0	10.0	69.6	609	51	10.3	22.6
1800	2.0	10.0	68.8	2909	76	45.4	48.3
1900	2.0	10.0	68.8	3909	231	31.2	48.4
2000	2.0	10.0	69.1	1414	222	21.3	27.9
2101	2.0	10.0	68.5	4000	121	6.2	40.0
2200	2.0	10.0	71.4	2333	351	28.1	25.9
2300	2.0	10.0	68.7	1441	110	14.8	19.3
2400	2.0	10.0	67.1	4000	208	50.0	40.6
2499	2.0	10.0	67.1	3077	270	45.1	23.7
2600	2.0	10.0	69	3954	395	36.4	25.7
2700	2.0	10.0	66.8	2582	316	50.0	34.3

Station No.	HMA Thickness (in)	Treated Base Thickness (in)	Surface Temperature (°F)	Asphalt	Base	2-ft Subgrade	Infinite Subgrade
				E(1) (ksi)	E(2) (ksi)	E(3) (ksi)	E(4) (ksi)
2800	2.0	10.0	68.4	3954	44	30.5	43.4
2900	2.0	10.0	67.4	2712	157	16.2	33.4
3000	2.0	10.0	68.4	3909	278	22.0	26.7
3101	2.0	10.0	66.6	1356	83	14.2	22.7
3201	2.0	10.0	68.6	2370	26	6.7	19.3
3300	2.0	10.0	68.2	964	60	18.4	26.8
3401	2.0	10.0	65	879	401	37.7	27.3
3500	2.0	10.0	70.3	3909	245	30.9	24.5
3600	2.0	10.0	68.1	2396	227	50.0	33.7
3700	2.0	10.0	66.6	1360	223	35.4	33.8
3800	2.0	10.0	68	3909	196	40.9	54.1
3900	2.0	10.0	66.9	3909	161	4.6	34.2
4001	2.0	10.0	69.2	3909	95	21.4	41.0
4100	2.0	10.0	67.7	1307	133	17.5	32.1
4200	2.0	10.0	64.6	3908	130	15.4	41.2
4300	2.0	10.0	67.2	2660	120	11.5	43.2
4401	2.0	10.0	67.4	4000	206	18.0	41.3
4501	2.0	10.0	67.1	2849	161	26.8	43.4
4600	2.0	10.0	68.9	2980	235	23.8	33.0
4700	2.0	10.0	67.6	1240	194	23.9	27.5
4800	2.0	10.0	67.5	3909	221	27.1	33.4
4901	2.0	10.0	66.8	4000	500	15.4	36.2
5000	2.0	10.0	68.7	4000	500	50.0	36.8
5100	2.0	10.0	68.6	1693	489	12.3	39.9
5199	2.0	10.0	68.9	1769	178	29.7	35.4
<b>Average</b>	<b>2.00</b>	<b>10.00</b>	<b>68.09</b>	<b>2442</b>	<b>176</b>	<b>26</b>	<b>33</b>
<b>St dev</b>	<b>0.00</b>	<b>0.00</b>	<b>1.40</b>	<b>1250</b>	<b>121</b>	<b>12</b>	<b>9</b>
<b>COV</b>	<b>0.00</b>	<b>0.00</b>	<b>2.05</b>	<b>51</b>	<b>69</b>	<b>46</b>	<b>26</b>

**Table C.4: Back-calculated modulus versus station location at 330<sup>th</sup> Avenue EB lane in Marion County**

Station No.	HMA Thickness (in)	Treated Base Thickness (in)	Surface Temperature (°F)	Asphalt	Base	2-ft Subgrade	Infinite Subgrade
				E(1) (ksi)	E(2) (ksi)	E(3) (ksi)	E(4) (ksi)
101	3.0	12.0	56.9	4000	167.5	38.6	26.7
200	3.0	12.0	56	4000	500.0	48.7	36.6
300	3.0	12.0	56.1	3906	494.3	48.3	32.7
401	3.0	12.0	55.4	4000	500.0	50.0	61.6
500	3.0	12.0	54.2	4000	500.0	26.7	33.8
600	3.0	12.0	56.2	3909	356.3	12.8	25.3
700	3.0	12.0	56.3	4000	500.0	49.2	24.2
800	3.0	12.0	55	4000	500.0	7.3	29.6
900	3.0	12.0	56.6	2211	494.3	12.0	29.0
1000	3.0	12.0	53.1	3954	467.5	5.1	35.8
1100	3.0	12.0	57.2	3758	500.0	8.4	26.6
1200	3.0	12.0	56.5	865	488.6	25.8	27.5
1300	3.0	12.0	55	4000	500.0	11.4	25.5
1400	3.0	12.0	57.5	2644	354.0	9.1	22.2
1501	3.0	12.0	56.6	3909	274.7	22.0	27.0
1600	3.0	12.0	55.7	3909	246.2	25.0	31.1
1700	3.0	12.0	57.2	4000	500.0	24.8	27.6
1803	3.0	12.0	56.4	2713	409.2	9.3	28.5
1900	3.0	12.0	55.1	4000	500.0	2.6	44.0
2000	3.0	12.0	55.6	3960	494.3	5.8	33.4
2100	3.0	12.0	54	3789	494.3	14.7	26.8
2200	3.0	12.0	56.1	1111	395.6	24.3	27.7
2300	3.0	12.0	55.5	1020	313.3	16.6	25.1
2400	3.0	12.0	57.7	862	324.6	14.4	29.7
2500	3.0	12.0	57.5	1252	494.3	11.7	29.3
2600	3.0	12.0	57.1	1807	394.4	21.6	30.3
2700	3.0	12.0	56	3909	488.6	1.5	72.0

Station No.	HMA Thickness (in)	Treated Base Thickness (in)	Surface Temperature (°F)	Asphalt	Base	2-ft Subgrade	Infinite Subgrade
				E(1) (ksi)	E(2) (ksi)	E(3) (ksi)	E(4) (ksi)
2800	3.0	12.0	57.1	2035	305.8	15.9	24.7
2900	3.0	12.0	56.8	2162	488.6	8.6	29.3
3000	3.0	12.0	57.2	1940	412.4	13.5	27.2
3100	3.0	12.0	57.2	2987	496.8	6.8	25.3
3200	3.0	12.0	57.3	1521	186.4	26.0	23.1
3300	3.0	12.0	56.7	2706	488.6	8.7	29.4
3500	3.0	12.0	57.7	2516	297.4	18.9	25.5
3500	3.0	12.0	56.1	3954	494.3	8.7	28.1
3600	3.0	12.0	55.9	4000	500.0	41.5	26.5
3701	3.0	12.0	56.6	1743	488.6	10.2	25.0
3802	3.0	12.0	56.8	1136	488.6	40.2	26.9
3901	3.0	12.0	56.3	4000	500.0	20.5	20.3
4000	3.0	12.0	57.7	268	450.0	35.3	21.2
4100	3.0	12.0	57	616	498.2	4.9	23.8
4200	3.0	12.0	56.7	1460	313.8	38.5	25.0
4301	3.0	12.0	57.1	4000	500.0	20.9	24.7
4401	3.0	12.0	58	3954	494.3	12.3	23.9
4501	3.0	12.0	58.6	1488	494.3	3.1	30.4
4602	3.0	12.0	58.3	2298	121.6	3.0	12.7
4700	3.0	12.0	58	3227	494.3	4.1	30.5
4800	3.0	12.0	57.7	1619	118.4	34.8	22.7
4900	3.0	12.0	55.7	2383	246.5	16.8	27.7
5000	3.0	12.0	58.3	2891	245.2	22.2	31.0
5100	3.0	12.0	58.2	2505	379.6	5.2	36.2
5200	3.0	12.0	56.9	1569	488.6	29.5	29.8
<b>Average</b>	<b>3.00</b>	<b>12.00</b>	<b>56.58</b>	<b>2778</b>	<b>416</b>	<b>19</b>	<b>29</b>
<b>St dev</b>	<b>0.00</b>	<b>0.00</b>	<b>1.13</b>	<b>1201</b>	<b>113</b>	<b>14</b>	<b>9</b>
<b>COV</b>	<b>0.00</b>	<b>0.00</b>	<b>2.00</b>	<b>43</b>	<b>27</b>	<b>72</b>	<b>31</b>

**Table C.5: Back-calculated modulus versus station location at 330<sup>th</sup> Avenue WB lane in Marion County**

Station No.	HMA Thickness (in)	Treated Base Thickness (in)	Surface Temperature (°F)	Asphalt	Base	2-ft Subgrade	Infinite Subgrade
				E(1) (ksi)	E(2) (ksi)	E(3) (ksi)	E(4) (ksi)
100	3.0	12.0	58.8	4000	500	50	26
200	3.0	12.0	60.1	4000	500	8	30
300	3.0	12.0	60.1	4000	500	8	40
401	3.0	12.0	61.5	1301	321	30	32
501	3.0	12.0	61.4	4000	495	2	49
600	3.0	12.0	61.8	1742	123	19	21
701	3.0	12.0	62.3	1919	321	5	24
800	3.0	12.0	61.9	2242	75	4	23
900	3.0	12.0	61.8	3954	310	3	38
1000	3.0	12.0	61.9	3909	489	7	28
1100	3.0	12.0	62.1	4000	495	6	25
1200	3.0	12.0	62.4	2612	214	12	22
1300	3.0	12.0	60.8	2050	394	3	28
1400	3.0	12.0	62.1	3822	489	12	26
1501	3.0	12.0	62.9	3909	489	2	44
1600	3.0	12.0	61.8	3909	489	8	32
1700	3.0	12.0	60.9	3909	497	3	38
1800	3.0	12.0	62.3	3818	500	48	29
1900	3.0	12.0	61.1	4000	500	13	24
2000	3.0	12.0	63.3	3909	341	12	26
2100	3.0	12.0	62.3	2093	300	9	27
2199	3.0	12.0	63.4	2688	484	9	28
2300	3.0	12.0	60.6	3909	371	2	37
2400	3.0	12.0	63.2	1293	164	23	26
2500	3.0	12.0	62.7	4000	500	11	26
2600	3.0	12.0	62.6	3272	288	19	23
2700	3.0	12.0	63.4	4000	500	17	24

Station No.	HMA Thickness (in)	Treated Base Thickness (in)	Surface Temperature (°F)	Asphalt	Base	2-ft Subgrade	Infinite Subgrade
				E(1) (ksi)	E(2) (ksi)	E(3) (ksi)	E(4) (ksi)
2800	3.0	12.0	61.9	1962	340	29	27
2900	3.0	12.0	62	3954	494	13	32
3000	3.0	12.0	61.8	3315	148	33	25
3101	3.0	12.0	60.2	3946	494	10	29
3200	3.0	12.0	63.2	1847	489	25	29
3300	3.0	12.0	61.1	1559	378	6	25
3401	3.0	12.0	63	1260	325	11	24
3500	3.0	12.0	61.6	4000	500	15	26
3600	3.0	12.0	62.5	3954	491	15	28
3701	3.0	12.0	61.1	3909	489	7	40
3800	3.0	12.0	61.4	1561	382	5	40
3900	3.0	12.0	59.7	3909	392	3	32
4000	3.0	12.0	62.4	1074	494	10	23
4100	3.0	12.0	61.5	4000	500	3	34
4200	3.0	12.0	63.2	1246	489	31	29
4300	3.0	12.0	62.4	2797	430	4	35
4400	3.0	12.0	61.8	3954	492	18	28
4501	3.0	12.0	61.9	4000	500	10	28
4600	3.0	12.0	64.1	3458	489	4	47
4701	3.0	12.0	62.4	3909	396	3	49
4800	3.0	12.0	63.5	4000	402	14	31
4900	3.0	12.0	62.4	4000	500	42	33
4999	3.0	12.0	62.5	4000	500	50	49
5100	3.0	12.0	64.1	4000	500	50	34
5200	3.0	12.0	64.2	4000	500	50	34
<b>Average</b>	<b>3.00</b>	<b>12.00</b>	<b>62.03</b>	<b>3228</b>	<b>418</b>	<b>15</b>	<b>31</b>
<b>St dev</b>	<b>0.00</b>	<b>0.00</b>	<b>1.13</b>	<b>1034</b>	<b>114</b>	<b>14</b>	<b>7</b>
<b>COV</b>	<b>0.00</b>	<b>0.00</b>	<b>1.82</b>	<b>32</b>	<b>27</b>	<b>93</b>	<b>24</b>

**Table C.6: Resilient Modulus of the Uncracked CMS Specimen No. 1 for the Sedgwick County Soil**

Parameter	Chamber Confining Pressure	Actual Applied Cyclic Stress	Actual Applied Contact Stress	Resilient Modulus
Designation	$S_3$	$S_{cyclic}$	$S_{contact}$	$M_r$
Unit	psi	psi	psi	psi
Sequence 1	6	1.84	0.21	20,684
Sequence 2	6	3.62	0.39	21,139
Sequence 3	6	5.42	0.61	23,735
Sequence 4	6	7.27	0.81	24,831
Sequence 5	6	9.10	1.02	25,375
Sequence 6	4	1.86	0.23	20,014
Sequence 7	4	3.68	0.45	20,705
Sequence 8	4	5.46	0.61	21,577
Sequence 9	4	7.27	0.79	22,563
Sequence 10	4	9.20	1.01	24,102
Sequence 11	2	1.80	0.19	18,011
Sequence 12	2	3.62	0.45	19,517
Sequence 13	2	5.45	0.59	20,894
Sequence 14	2	7.24	0.79	22,217
Sequence 15	2	9.14	1.03	23,614

**Table C.7: Resilient Modulus of the Uncracked CMS Specimen No. 4 for the Sedgwick County Soil**

Parameter	Chamber Confining Pressure	Actual Applied Cyclic Stress	Actual Applied Contact Stress	Resilient Modulus
Designation	$S_3$	$S_{cyclic}$	$S_{contact}$	$M_r$
Unit	psi	psi	psi	psi
Sequence 1	6	1.73	0.25	21,118
Sequence 2	6	3.89	0.44	25,945
Sequence 3	6	5.44	0.61	28,696
Sequence 4	6	7.43	0.82	28,487
Sequence 5	6	9.17	1.02	30,551
Sequence 6	4	1.72	0.23	20,756
Sequence 7	4	3.91	0.46	24,329
Sequence 8	4	5.42	0.63	25,952
Sequence 9	4	7.48	0.81	27,832
Sequence 10	4	9.12	0.99	29,612
Sequence 11	2	1.72	0.22	20,025
Sequence 12	2	3.78	0.44	22,712
Sequence 13	2	5.55	0.61	24,682
Sequence 14	2	7.48	0.82	27,571
Sequence 15	2	9.17	1.01	27,907

**Table C.8: Resilient Modulus of the Uncracked CMS Specimen No. 1 for the Marion County Soil**

Parameter	Chamber Confining Pressure	Actual Applied Cyclic Stress	Actual Applied Contact Stress	Resilient Modulus
Designation	$S_3$	$S_{cyclic}$	$S_{contact}$	$M_r$
Unit	psi	psi	psi	psi
Sequence 1	6	1.90	0.20	24,647
Sequence 2	6	3.56	0.41	27,068
Sequence 3	6	5.38	0.62	29,988
Sequence 4	6	7.23	0.82	32,558
Sequence 5	6	9.05	1.01	34,438
Sequence 6	4	1.97	0.22	24,422
Sequence 7	4	3.50	0.42	26,608
Sequence 8	4	5.33	0.59	28,877
Sequence 9	4	7.29	0.81	30,712
Sequence 10	4	9.07	0.99	33,268
Sequence 11	2	1.96	0.22	23,927
Sequence 12	2	3.60	0.44	26,161
Sequence 13	2	5.37	0.61	28,762
Sequence 14	2	7.21	0.78	30,449
Sequence 15	2	9.07	0.98	31,961

**Table C.9: Resilient Modulus of the Uncracked CMS Specimen No. 2 for the Marion County Soil**

Parameter	Chamber Confining Pressure	Actual Applied Cyclic Stress	Actual Applied Contact Stress	Resilient Modulus
Designation	$S_3$	$S_{cyclic}$	$S_{contact}$	$M_r$
Unit	psi	psi	psi	psi
Sequence 1	6	1.92	0.20	26,906
Sequence 2	6	3.74	0.43	30,863
Sequence 3	6	5.41	0.55	31,913
Sequence 4	6	7.24	0.81	33,197
Sequence 5	6	9.06	0.98	34,460
Sequence 6	4	1.90	0.21	22,279
Sequence 7	4	3.74	0.45	24,378
Sequence 8	4	5.47	0.56	27,861
Sequence 9	4	7.24	0.78	30,671
Sequence 10	4	9.10	0.99	31,203
Sequence 11	2	1.94	0.19	22,241
Sequence 12	2	3.76	0.45	24,299
Sequence 13	2	5.41	0.61	26,102
Sequence 14	2	7.27	0.82	29,429
Sequence 15	2	9.09	1.01	30,103



**Table C.10: Resilient Modulus of the Cracked CMS Specimen No. 2 for the Sedgwick County Soil**

Parameter	Chamber Confining Pressure	Actual Applied Cyclic Stress	Actual Applied Contact Stress	Resilient Modulus
Designation	$S_3$	$S_{cyclic}$	$S_{contact}$	$M_r$
Unit	psi	psi	psi	psi
Sequence 1	6	1.78	0.24	25,545
Sequence 2	6	3.71	0.44	28,224
Sequence 3	6	5.41	0.61	30,752
Sequence 4	6	7.25	0.80	32,882
Sequence 5	6	9.15	1.02	34,122
Sequence 6	4	1.79	0.23	23,124
Sequence 7	4	3.67	0.44	27,002
Sequence 8	4	5.46	0.62	28,454
Sequence 9	4	7.28	0.81	32,345
Sequence 10	4	9.14	0.99	33,657
Sequence 11	2	1.80	0.22	22,325
Sequence 12	2	3.69	0.44	23,221
Sequence 13	2	5.53	0.61	24,610
Sequence 14	2	7.28	0.78	26,194
Sequence 15	2	9.19	0.98	28,563

**Table C.11: Resilient Modulus of the Cracked CMS Specimen No. 3 for the Sedgwick County Soil**

Parameter	Chamber Confining Pressure	Actual Applied Cyclic Stress	Actual Applied Contact Stress	Resilient Modulus
Designation	$S_3$	$S_{cyclic}$	$S_{contact}$	$M_r$
Unit	psi	psi	psi	psi
Sequence 1	6	1.91	0.19	20,714
Sequence 2	6	3.75	0.44	23,146
Sequence 3	6	5.38	0.62	23,290
Sequence 4	6	7.22	0.81	24,347
Sequence 5	6	9.16	1.02	27,875
Sequence 6	4	1.89	0.23	20,223
Sequence 7	4	3.73	0.44	20,295
Sequence 8	4	5.35	0.62	22,790
Sequence 9	4	7.15	0.81	24,278
Sequence 10	4	9.18	1.02	26,141
Sequence 11	2	1.94	0.22	19,460
Sequence 12	2	3.72	0.44	19,901
Sequence 13	2	5.35	0.59	22,063
Sequence 14	2	7.25	0.79	24,141
Sequence 15	2	9.15	1.01	25,306

**Table C.12: Resilient Modulus of the Cracked CMS Specimen No. 3 for the Marion County Soil**

Parameter	Chamber Confining Pressure	Actual Applied Cyclic Stress	Actual Applied Contact Stress	Resilient Modulus
Designation	S <sub>3</sub>	S <sub>cyclic</sub>	S <sub>contact</sub>	M <sub>r</sub>
Unit	psi	psi	psi	psi
Sequence 1	6	1.72	0.21	25,614
Sequence 2	6	3.75	0.42	26,478
Sequence 3	6	5.43	0.61	27,400
Sequence 4	6	7.24	0.82	31,923
Sequence 5	6	9.03	1.01	34,702
Sequence 6	4	1.70	0.23	23,290
Sequence 7	4	3.72	0.44	25,778
Sequence 8	4	5.47	0.62	26,587
Sequence 9	4	7.22	0.83	28,061
Sequence 10	4	9.05	0.99	32,583
Sequence 11	2	1.73	0.22	18,376
Sequence 12	2	3.70	0.44	23,872
Sequence 13	2	5.47	0.61	25,373
Sequence 14	2	7.23	0.82	28,159
Sequence 15	2	9.02	1.01	31,239

**Table C.13: Resilient Modulus of the Cracked CMS Specimen No. 4 for the Marion County Soil**

Parameter	Chamber Confining Pressure	Actual Applied Cyclic Stress	Actual Applied Contact Stress	Resilient Modulus
Designation	S <sub>3</sub>	S <sub>cyclic</sub>	S <sub>contact</sub>	M <sub>r</sub>
Unit	psi	psi	psi	psi
Sequence 1	6	1.86	0.24	28,213
Sequence 2	6	3.75	0.43	32,785
Sequence 3	6	5.65	0.65	34,229
Sequence 4	6	7.26	0.83	33,347
Sequence 5	6	9.11	1.02	40,990
Sequence 6	4	1.84	0.25	27,310
Sequence 7	4	3.76	0.45	31,016
Sequence 8	4	5.66	0.64	33,052
Sequence 9	4	7.26	0.79	32,531
Sequence 10	4	9.11	1.03	35,696
Sequence 11	2	1.80	0.22	25,492
Sequence 12	2	3.74	0.45	28,573
Sequence 13	2	5.68	0.63	29,268
Sequence 14	2	7.27	0.81	32,375
Sequence 15	2	9.12	1.01	34,776

# K-TRAN

## KANSAS TRANSPORTATION RESEARCH AND NEW-DEVELOPMENT PROGRAM

